SKB

TECHNICAL REPORT 96-19

Application of space geodetic techniques for the determination of intraplate deformations and movements in relation with the postglacial rebound of Fennoscandia

Hans-Georg Scherneck, J M Johansson,
Gunnar Elgered

Chalmers University of Technology,
Onsala Space Observatory, Onsala, Sweden

April 1996

SVENSK KÄRNBRÄNSLEHANTERING AB
SWEDISH NUCLEAR FUEL AND WASTE MANAGEMENT CO

P.O.BOX 5864 S-102 40 STOCKHOLM SWEDEN
PHONE +46 8 665 28 00
FAX +46 8 661 57 19

APPLICATION OF SPACE GEODETIC TECHNIQUES FOR THE DETERMINATION OF INTRAPLATE DEFORMATIONS AND MOVEMENTS IN RELATION WITH THE POSTGLACIAL REBOUND OF FENNOSCANDIA

Hans-Georg Scherneck, J M Johansson, Gunnar Elgered

Chalmers University of Technology,
Onsala Space Observatory, Onsala, Sweden

April 1996

APPLICATION OF SPACE GEODETIC TECHNIQUES FOR THE DETERMINATION OF INTRAPLATE DEFORMATIONS AND MOVEMENTS IN RELATION WITH THE POSTGLACIAL REBOUND OF FENNOSCANDIA

Hans-Georg Scherneck, Jan M. Johansson,
Gunnar Elgered

Chalmers University of Technology
Onsala Space Observatory, Onsala, Sweden

April 1996

Keywords: Space Geodesy, Recent Crustal Movements, Postglacial Rebound, Tectonics

ABSTRACT

This report introduces into space geodetic measurements of relative positions over distances ranging from tens to thousands of kilometres. Such measurements can routinely be carried out with repeatabilities on the order of a few millimeters.

The basic techniques which are presented at detail are Very Long Baseline Interferometry (VLBI), employing observations of radioastronomical objects in the distant universe, and ranging measurements to satellites of the GPS, the Global Positioning System.

We report that these techniques have helped to trace plate tectonic motions. More recently deformation within continents, i.e. strain patterns of more regional character have been detected.

We present the SWEPOS system of permanently operating GPS stations as one of the major geoscience investments starting in 1993. This system has been designed, devised and furnished as a joint effort between the National Land Survey of Sweden and ourselves, the geoscience group at Onsala Space Observatory, Chalmers University of Technology, using funds provided by Knut and Alice Wallenberg's Foundation and the Swedish Council for Planning and Coordination of Research (FRN).

We describe the operations within SWEPOS with the main purpose to detect crustal motions in Fennoscandia. For this purpose a project named BIFROST was created; BIFROST stands for Baseline Inferences for Fennoscandian Rebound Observations, Sea-level and Tectonics. It combines the efforts of a number of investigators at different sites and contributes to a number of international research programs in geophysics and geodesy. We foresee observing operations within BIFROST of at least ten years if deformation rates of 0.1 mm/yr are to be concluded at a 95 percent confidence level.

First results are presented, indicating movements which generally support the notion of a dominating displacement pattern due to the postglacial rebound of Fennoscandia. However, deviations exist. In order to discern regional movements of a presumably tectonic origin the coverage of the region must be extended, both concerning the areas that neighbour Sweden and array densification within the country. Densification is indicated in those areas which are notable for an increased seismicity. These are an area of 200 km radius encircling lake Vänern and the coastland of upper Norrland and its extension into northern Bothnia.

SAMMANFATTNING

Denna report ger en detaljerad beskrivning av geodetisk mätteknik med avseende på relativ positionering över långa distanser, från ett tiotal till flera tusen kilometer. Positionernas repeterbarhet är därvid på en nivå av ett fåtal millimeter.

De tekniker som används är VLBI, *Very Long Baseline Interferometry*, radioastronomiska observationer av objekt i utkanten av universum, och distansmätning mot satelliter i GPS, *Global Positioning System*.

I en tillbakablick beskriver vi hur dessa metoder har bidragit till att de tektoniska plattornas rörelser kunnat bestämmas. Under de senaste åren har man även kunnat mäta förskjutningar i skorpan av mer regional karaktär.

Vi kommer att presentera SWEPOS, det svenska stationsnätet för satellitbaserad precisionsgeodesi. Detta system kom till stånd 1993 som en gemensam insats av Lantmäteriverket och oss på Chalmers genom en stor finansiell satsning från FRNs sida och ytterligare anslag från Knut och Alice Wallenbergs Stiftelse.

Processering och analys av kontinuerliga observationer från SWEPOS sker i ett samarbetsprogram med namnet BIFROST, *Baseline Inferences for Fennoscandian Rebound Observations, Sea-level and Tectonics*, ung. baslinjemätningar i Fennoskandien för bestämning av den postglaciala landhöjningen, havsytans långsiktiga variationer och tektoniska rörelser. I BIFROST deltar ett antal svenska och internationella forskargrupper med bidrag till ett flertal internationella projekt inom geofysik och geodesi. Den totala löptiden för observationsverksamheten i samband med BIFROST kommer att vara på minst tio år om relativrörelser på en 99 % konfidensnivå av 0.1 mm/år skall skunna fastställas.

Vi presenterar första resultat från 2.5 års observationer. Ett förhärskande rörelsemönster med landhöjningens karakteristik är skönjbar, men för första gången kan även horisontella rörelser detekteras. Avvikelser från teoretiska modeller finns dock. För att kunna dra säkrare slutsater i avseende på eventuella konsekvenser av regional tektonik behövs dock en breddning av stationsnätet till grannländerna (är redan på gång), en förtätning i de intressanta regionerna (Väneområdet; övre Norrlands kustland samt i dess nordliga förlängning).

CONTENTS

Page

ABSTRACT ii

SAMMANFATTNING iii

SPACE GEODETIC TECHNIQUES FOR THE MONITORING OF DEFORMATIONS 1

1 PRINCIPLES 3
1.1 DISTANCE DETERMINATION, POINT POSITIONING 5
1.2 VLBI 7
1.2.1 Correlator facilities 11
1.2.2 Analysis 11
1.2.3 VLBI networks for geodesy 12
1.2.4 VLBI centres and campaigns 13
1.3 GPS 19
1.3.1 Codes and carriers 20
1.3.2 International GPS Service for Geodynamics: IGS 23
1.3.3 Data processing tools and analysis methods 24
1.4 PERTURBATIONS AND ERROR SOURCES 26
1.4.1 Ionosphere 27
1.4.2 Neutral atmosphere 28
1.4.3 Local site displacements 32

2 GEOPHYSICAL APPLICATIONS 39
2.1 TECTONIC DEFORMATION 39
2.2 EARTH ROTATION 42
2.3 GLOBAL CHANGE 43
2.4 POSTGLACIAL ISOSTATIC ADJUSTMENT 44
2.4.1 Inferring strain 51
2.4.2 Postglacial contra tectonic movement 52
2.4.3 Potential contribution of GPS 54
2.4.4 VLBI AND GPS TOGETHER 56

3 HISTORICAL REVIEW: ONSALA 57

3.1 VLBI—Technical developments at Onsala 1980–date 57
3.1.1 The telescopes and the feeds 57
3.1.2 The Mark–III data acquisition system 59
3.1.3 The water vapour radiometer (WVR) 59
3.1.4 Observations 60
3.1.5 VLBI results 64
3.2 GPS—1986 to 1993 66
3.2.1 Gravity measurements 68
3.3 FUNDING 68

4 GPS NETWORKS 70
4.1 TECHNICAL REQUIREMENTS FOR PERMANENT OBSERVING SITES 71
4.1.1 Antenna support structures 72
4.1.2 Antennas 75
4.1.3 Receivers 76
4.1.4 Other station equipment 76
4.2 THE SWEPOS SITES 76
4.2.1 SWEPOS sites design and equipment 77
4.3 DATA FLOW, PROCESSING, ARCHIVING 86
4.3.1 Data from the satellite receivers 86
4.3.2 Data flow in SWEPOS 87
4.3.3 Solving geodetic parameters 88
4.3.4 Differential GPS 89

5 RESULTS FROM TWO YEARS OF OPERATION 90
5.1 Baselines from SWEPOS/BIFROST 90
5.1.1 Adjustment of reference frame motion 90
5.1.2 Individual baseline results Sep. 1993–Nov. 1995 92
5.2 Discussion 93

6 FUTURE 108

7 ACKNOWLEDGMENTS 109

REFERENCES 110

APPENDIX 124

A INTERNET ADDRESSES 124

SPACE GEODETIC TECHNIQUES FOR THE MONITORING OF DEFORMATIONS

Without doubt the face of the earth has been reshaped over the geological eras considerably. Mountain chains have formed and collapsed, ocean basins have opened up and others closed again. The oldest part of the Atlantic ocean has been created between 120 and 60 million years, and the Norwegian Sea, now 2000 km wide, opened only 30 million years ago.

Remarkably though, some parts of the interior of continents have been left intact since billion of years, like the Archaen province in the northern part of the Fennoscandian shield. Judging from the shapes of the sutures between accreated masses of different but old age and contrasting it with the rapid deformation occuring at actively spreading or converging plates the proposition of the plate tectonic hypothesis that the interior of plates act as rigid is evident at a first glance.

We may ask ourselves to what limit this proposition is valid, and what observational evidence and what techniques would be needed to place a qualified specification as to the order of magnitude of deformation actually occurence in the central parts of plate units.

Claims exist, many are debatable (Muir Wood, 1993), much owing to the lack of hard data.

Over the last one million years, shield glaciers have repeatedly formed and disintegrated over the northern continents, prominently on the Fennoscandian shield and in the Hudson Bay area; they have scraped the surface, moved and removed sediments, but also loaded the earth with their weight, depressing the surface by as much as eight hundred metres.

Geodesy offers techniques for the study of movements. The concept devises repeated remeasurement of distances and orientations (intersite vectors or baselines) to detect the changes and suggest a model, in the simplest case to fit constant rates of change. To interprete the concluded rates they may be compared with tectonic models or evidence from seismological studies.

One such set of comparative data which has been widely used comes from a combination of age dating methods, paleomagnetism, and geochemical and petrological results to determine the evolution of in the first case the oceanic lithosphere. The problem is much more complex when dealing with continental lithosphere. Clearly there are areas where movements are conclusive and models relatively clear cut. But still it its difficult to

exclude movement in the 0.01–0.1 mm/yr range over distances of 100–200 km in the interior of plates where seismicity and other indicators of active tectonism (deviatoric stress, lateral variations of heat flow, coordinated systems of faults) are low.

If we speak in the plate tectonic picture of rigid plates that deform at their boundaries, a certain level of deformation indicators in plate interiors, low as it might be, still motivates the question How rigid ?, and if indirect evidence may exclude motions that are similarly steady as in an oceanic setting, there is still the possiblity of an episodic character to continental deformation. All in all, no evidence can match direct evidence, and geodesy has the capabilty to come up with qualified estimates of movement and thus can contribute uniquely.

The reson why few such definitive results are available, and moreover, why resolving the problem of possible localization of the deformation is so much more difficult is in part related to the limited level of accuracy so far achieved.

For localization the technique must be economically efficient, making networks with many observing stations feasible. Satellite observation will therefore be the monitoring method of choice. But also the technique is relatively young, and a certain time span, perhaps 10 yearsr, is required for detectable displacement to accumulate.

1 PRINCIPLES

The following presentation will in a short form introduce to geodetic measurement techniques which have evolved during the last 20 years, and which have been used successfully in application to the precise measurement of long distances, the geometric position of points fixed to the earth surface, and the kinematics of the coordinate frame to which these points refer. These techniques have in common that they are space-based. They have demonstrated long-term repeatabilities on the order of millimetres to a few centimetres for distances up to thousands of kilometres. Thus, methods are at hand which are capable to monitor motion as it might occur in conjunction with tectonics (millimetres per year) or other processes that deform the earth on geological time scales.

All what is needed are sufficiently stable reference marks which are representative for a geological unit and to which the measurements relate; to which the instruments are repeatedly brought or at which they are permanently installed. Owing to in particular the development of the Global Positioning System (GPS), satellite observation apparatus today is easy to transport and install despite high instrumental quality.

Terrestrial measurements using radar or laser equipment ("Geodolite") still have some potential on distances shorter than 10 to 40 km (e.g. Savage and Liesowski, 1995). Beyond 40 km the errors will almost inevitably exceed one centimetre even if intensive ancillary observations of perturbing parameters (mostly concerning the refractivity of air) are made. Since the beginning of this century terrestrial optical measurements have been sufficiently accurate to obtain regional deformation rates when the old data is combined with recent survey results, much owing to the long time base. Regional strain estimates may be based on remeasurements of angles in triangulation networks. An analysis of 60 years of triangulation involving 1 to 5 remeasurements by Donnellan et al. (1993) for the Ventura Basin in Southern California shows comparable accuracy with strain derived from satellite observations carried out in 2 to 3 campaigns spanning 4 years with standard deviations of typically 0.02 to 0.2 μstrain/yr.

The most severe limitation that is overcome by space methods concerns site intervisibility. Terrestrial measurements can circumvent this only by creating networks or transects involving secondary, intermediate observation points. Solutions gain strength by the number of network points. Thus, trilateration or levelling campaigns develop into large projects that require logistics and support to an extent that repeat surveys are only carried out at several decades interval.

A general source of limitation already mentioned is the refractive prop-

erty of air, especially of its water vapour ("wet") component. Whereas nitrogene and oxygene refract and delay electromagnetic waves largely proportional to the gas density which can be inferred from pressure observations ("dry" or hydrostatic component) the variation of wet component in time and space is particularly complicated. Surface measurements of humidity variations with hygrometers are not useful for modelling the higher atmospheric layers. Along long horizontal propagation paths local variations can be severe and the modelling of the perturbations becomes too complicated.

Space methods for positioning and baseline determination yield approximately equal precision in all three spatial components. All three cartesian vector components are determined in the same reference system. (Terrestrial methods usually determine either angles, distances, or height differences in horizontal or in height reference systems, respectively.) Along the vertical precision is slightly degraded in all these methods, including the terrestrial, as an inevitable consequence of the signals having to pass through a refracting atmosphere. (In effect it is the observation geometry which causes the dilution of precision, since targets are visible above but never below the horizon; horizontal components gain from the availability of observations at all azimuths.) However, the repeatability of determinations that involve a space component is unsurpassed by terrestrial methods at distances of more than ten kilometres, much owing to the fact that a horizontally travelling wave then passes through the same or through a greater air mass than a vertically travelling one.

Albeit the atmospheric error perturbes both terrestrial and space techniques, it is in the latter that the error level saturates and becomes largely independent of intersite distance. Considerable effort is spent today to reduce this error level, and several methods have become available. Chapter 1.4.2 below will resume the problem at more detail.

With space geodesy all components of a three-dimensional distance vectors can be determined simultaneously. This is unlike in classical geodesy where horizontal and vertical networks are treated separately using different types of instruments. In space geodesy, the problems relating to the vertical and thus to the geoid (equipotential surface of the gravity potential coinciding with mean sea level) are kept apart from the purely geometric problems of distance determinations in three dimensions.

Sloppy speaking, the earth must be viewed from space in order to relate to the position of points on its surface by means of a global geocentric coordinate system.

Thus we can identify a group of problems, each of which have their own technical approaches, for solutions in a clear setting of modern geodesy aiming to apply the respectively most adequate of space and terrestrial techniques:

- Vectorial **distances** up to 12.000 km, indicative of solid earth deformations – Very Long Baseline Interferometry, Satellite Ranging (by laser, by radio frequencies; particularly: GPS)

- **Origin and orientation of the coordinate frames** indicative of large-scale mass flow in earth interior, oceans, and atmosphere – VLBI and satellite ranging.

- Changes of **sea level** indicative of changes in climate, in global water budget.

- perturbations of the **gravity field,** indicative of mass redistribution inside and on the surface of the earth – Orbit dynamics of satellites, Altimetric sensing of the sea surface, gravimeters (portable, fixed site, ship-borne, air-borne), gradiometers on-board satellites.

The scope of this report will focus on deformations of the solid earth, specifically crustal motion on a regional scale. Thus, we emphasize the geometric techniques.

1.1 DISTANCE DETERMINATION, POINT POSITIONING

In a very general sense, the methods for relative point positioning which are the basis for the determination of baseline vectors are so-called **ranging** methods. They determine spatial distance components from timing operations on sending/receiving instances of electromagnetic waves. The geometric configuration of transmitters and receivers during an experiment is responsible to reduce the degrees of freedom with respect to the orientation of the baseline. Thus, ranging relates to the now classical clock-synchronisation problem of special relativity.

Ranging/timing in space geodesy employs radio waves which are modulated in one way or the other, natural or artificial. The modulating signals (the wave groups) serve as the timing marks. We mention

- **Very Long Baseline Interferometry (VLBI),** a method that has evolved from radio astronomy, using naturally emitted radiation from sources far out in the universe,

- the US DoD **Global Positioning System (GPS),** consisting of broadcasting satellites for navigation,

- the french **DORIS** system, provided by CNES, Toulouse, on-board a number of satellites, primarily used for precise orbit determination,

- a similar **Precise Range and Range Rate (PRARE)** system provided by the German DLR, and
- **Satellite Laser Ranging (SLR)**, where the satellites usually carry passive laser reflectors.

In the case of SLR, only high-orbit satellites provide the required low sensitivity for the earth's gravity field. Ranging to low-orbit satellites is one of the techniques most sensitive to the low-degree (long-wavelength) gravity field components. However, this report will only discuss SLR in passing since the technique depends on clear sky conditions, which makes it difficult to use in Scandinavia. Also, we have little practical experience with this system. The technique will be mentioned for its contributions, also potential ones.

Similarly, DORIS and PRARE are not further discussed. Both techniques employ actively emitting ground stations. Especially PRARE has not been available until recently (on-board ESA's ERS-2 and on a Russian satellite), and its precision needs to be assessed. DORIS has been available for several years now (Soudarin and Cazenave, 1995). Since satellites with DORIS capabilities have predominantly had low orbits, the precision of position determinations has been lower compared to GPS (typically several centimetres).

The space-borne component of GPS consists of high-orbit satellites. Thus, ranging techniques using GPS are only weakly dependent on the gravity field compared to low-orbit satellites. The satellite orbits do not suffer from atmospheric drag; among dissipative processes solar radiation pressure provides the most significant breaking force.

Satellite orbits revolve around the centre of gravity of the earth. With some limitiation in the accuracy, satellite ranging is capable of resolving the degree of freedom with respect to coordinate translation inherent in VLBI. As we shall see, this notion is important in perspective of changes in the volumes of ice and water.

We notice the complementary nature of the interrelations of the techniques

- VLBI provides the realisation of a non-rotating origin, and
- satellite methods resolve a rigid translation of the coordinate system that ties together points on the **solid** earth.

When both types of techniques arrive at compatible results, being equal within the error limits, we may have increased confidence in each of them. A key method to validate compatibility is **colocation of sites**,

meaning that different techniques operate at closely spaced points. the ties between which can safely be measured in situ.

We give here the ranging equation which is basic in these techniques (generalisation to VLBI by assuming the source at infinite distance cf below)

$$\mathbf{X} = \mathcal{P}\mathcal{N}\Omega\mathcal{X}\mathcal{Y}(\mathrm{x} + \Delta\mathrm{x}) \quad (1\text{-}1)$$

$$\Delta t = \tfrac{1}{c}|\mathbf{S} - \mathbf{X}| \quad (1\text{-}2)$$

where $\Delta\mathbf{x}$ is local site motion, $\mathbf{x}$ a geocentric site position vector, and $\mathbf{X}$ the same vector in a quasi-inertial system, the sequence of rotation matrices denotes from left to right: Precession, Nutation, Rotation around the conventional origin (UT1), and Polar motion. The matrix elements relate to the Earth Orientation Parameters (EOP). Local site motion includes a wide range of processes and associated parameters (solid earth tides, deformations due to loading of the crust by tides and air pressure, postglacial rebound, plate tectonics). The source position $\mathbf{S}$ may for instance be given in terms of the celestial coordinates of a radio source (VLBI) or through the ephemerides of a satellite. In the latter case this indirectly involves a gravity field model of the earth, planetary motion and various perturbations, including again the EOP's.

The ensemble of site position vectors and their rates together with their individual uncertainties constitute the International Terrerstrial Reference Frame (ITRF).

1.2 VLBI

Very Long Baseline Interferometry utilizes the microwave radiation that is emitted by distant astronomical objects. We will give a simplified description of the technique. More extensive descriptions are found in Shapiro (1976), Clark et al. (1985) and Rogers et al. (1993). As the sources are faint, high-gain antennas and low-noise receivers are needed. A minimum experiment configuration requires two participating radio telescopes. At each site two frequency bands are observed, one in the X-band around 8.4 GHz and the other in the S-band at 2.3 GHz.

The radiated signal consists of noise-like fluctuations. When the same source is simultaneously observed at two sites, the received signals correlate with each other (c.f. Fig. 1-1). Signal features (wave-groups) arrive a site A τ seconds before site B. If $\mathbf{b}$ denotes the vectorial distance between the sites, $\hat{\mathbf{n}}$ the direction to the radio source, and c the speed of light, then

$$\tau = \frac{1}{c}\,\mathbf{b}\cdot\hat{\mathbf{n}} \quad 1\text{-}3$$

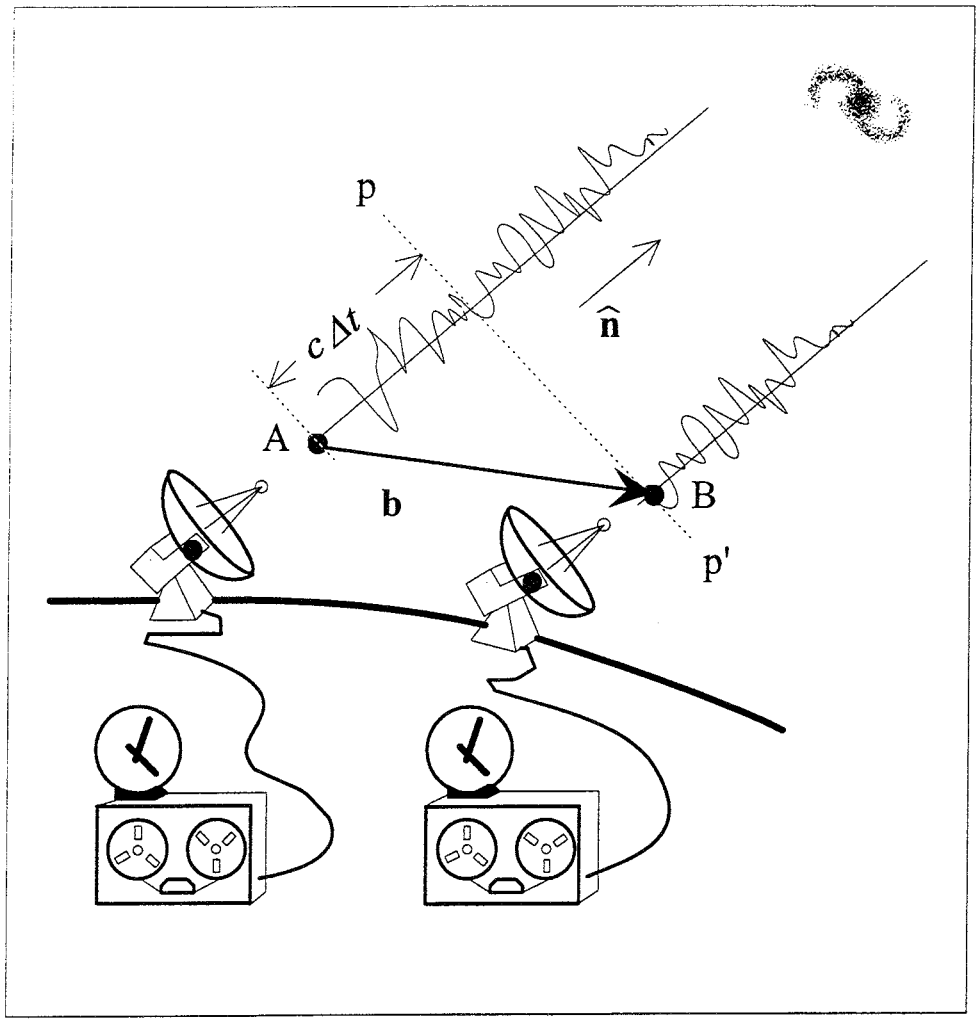

Figure 1-1. *Baseline geometry in VLBI. Two sites A and B being located* $\mathbf{b}$ *apart and observing the same radio-astronomical object at direction* $\hat{\mathbf{n}}$ *receive the same wave phase p–p' at different times; at station A it is delayed by* Δt*, the excess path being* $c\Delta t$ *where c is the speed of light, thus* $c\Delta t = \hat{\mathbf{n}} \cdot \mathbf{b}$ *which is the basic VLBI observation equation. In geodesy, the baseline vector* $\mathbf{b}$ *is the variable to be determined. This vector connects the reference points of the antennas indicated by the thick dark blobs.*

From a suite of observations of τ in a network of sites observing a catalogue of sources, the baseline vectors $\mathbf{b}$ can be solved. Observing at two frequencies (X- and S-band) allows to cancel at first order the wavegroup delays due to dispersion in the ionosphere.

The size of the antenna is a trade-off between mechanical stability, stiffness, low thermal and insolation susceptibility, and quick pointing mobility, all of which favour small instruments, and antenna gain to achieve high signal-to-noise ratio, being the virtue of large-diameter dishes. Near the optimum are 15 to 30 m diameter dishes. The particular technical design of the front-end receiver can compensate a specific antenna's gain

limition.

The technical realisation of the interferometric process, the determination of τ, involves separate stages as the observatories are located at large distances. Each site records the received signals on magnetic tape. For that purpose the high-frequency bands are downconverted and split into a number of channels (presently 14) of 4 MHz width each. In addition, an accurate clock signal, usually generated with a hydrogen maser (atomic frequency standard) at each site, is added to the signal at the input of the first amplifier of the receiver. From there it follows with the data stream onto the tape.

These tapes are shipped to a central facility where they are processed together in a correlator. The correlator determines the amount of shift of one tape with respect to the other that is necessary to obtain maximum alignment between the waveforms. Comparison with the clock records yields the group delay τ, the fundamental observable. (In addition, also the rate of the phase delay is determined in the correlation process as a secondary observable.) The timing offset between a pair of clocks can be eliminated owing to the fact that the delay changes quickly as the source-baseline angle (between $\hat{\mathbf{n}}$ and $\mathbf{b}$) varies due to the rotation of the earth.

The participating observatories need to comply with the technical standards for compatible equipment. This is particularly critical for the tapes that are recorded, since the tape bandwidth is limited and hence the high-frequency bands must be split and scanned in a band synthesis scheme with hard- and software components. The standards regulate the primary frequency allocations and signal bandwidths, the way they are split and down-converted, first into a number of intermediate bands and finally in a stage to fit the recorder bandwidth. This splitting of the basic band into narrower bands is the essence of the bandwidth synthesis technique. The standards regulate further the formats for writing of the tapes, the clock signal, etc. Different technical stages and realisations in the form of receiving terminals are signified with the successive generations of Mark–I, Mark–II etc. Mark–I was replaced by Mark-III by the end of the 1970's. The Mark–II system is exclusively designed for astronomy VLBI.

In Mark–I the recorded bandwidth of 360 kHz was switched sequentially in order to span a total bandwidth of up to 300 MHz. The fundamental improvement of Mark–III is that instead of one window 360 kHz wide, many windows of 2 MHz can be recorded simultaneously—also using the wide bandwidth synthesis technique—from both X– and S–band (center frequencies at approximately 8.4 and 2.3 GHz, respectively).

Currently a shift of technical standards is taking place, from Mark–III to Mark–IV, as a development primarily thrusted by astrophysics users. Specifically, this is the standard for the primary new array of ten VLBI

observatories for astrophysics and geodesy in the US. NRAO's Very Long Baseline Array (VLBA: cf. Kellermann and Thompson, 1985). The upgrade affects RF-IF converter units and the heads of the tape recorder. Mark-IV employs e.g. a doubled bandwidth (720 MHz) in the X-band, higher recording density, two bit coding of the received signals, achieving a wider tape bandwidth (up to 16 MHz) and thus an improved bandwidth coverage of the 720 MHz spanned band.

A Mark-IIIa mode for geodetic VLBI has been defined to achieve compatibility with the Mark-IV tape format, providing 4 MHz recorded bandwidth and 720 MHz spanned X-Band, thus coverad more sparsely. The expected benefit is a roughly doubled precision of the delay estimates (Rogers et al., 1993). Strict conformity with the VLBA standard also requires the use of a standardized 25 m telescope incl. feeds and amplifiers. For astronomy many more frequency bands are observed (10 bands between 0.3 and 45 GHz (even a 90 GHz band is discussed). But the dual-frequency observation mode in the S- and X-bands is specific for geodesy and astrometry since correction of ionospheric wave dispersion is essential, and is stipulated in Mark-IV/VLBA.

Mark-IIIA mode can be achieved also under Mark-IV/VLBA. Currently and for several years in the future it is staying as a standard in geodetic VLBI. Thus, the different networks that can be discerned on the basis of their purposes and their technical standards (NAVNET, R&D, VLBA, EURO-VLBI, see below) have Mark-IIIA and geodetic capabilities as a common denominator. Excluded will be those—primarily astronomical—sites which are not upgraded from Mark-II (a single-frequency system) and/or have weak receiving conditions for X- and S-bands or have unsuitable dishes.

For each observing campaign a schedule is devised which assigns observation intervals (typically some minutes) for the selected radio sources. It is the art (and science) of the schedule to provide the geometrical strength in the analysis headed for, given the geographical distribution of the participating sites. The selection of sources favours those which currently have low structural anomalies and variability. These properties can vary from year to year. However, in general low-structure objects are faint. Further criteria concern a reasonable elevation cutoff while the sources must be distributed over each observatory's sky as wide and homogeneous as possible. Telescope movements covering wide angular distances from one source to the other must proceed rapidly, so that the variable atmosphere at each observatory is scanned efficiently in many directions during as short time as possible. The purpose of the campaign will affect the schedule; e.g. for baseline variations a larger number of site parameters must be solved which calls for a larger set and wider spread of sources.

For these reasons, high telescope slewing speeds and high signal to noise

ratios are essential in geodetic VLBI.

Provided a feasible schedule, carrying out an experiment successfully requires a high degree of coordination between the sites, reliable staff and equipment at each observatory.

1.2.1 Correlator facilities

Correlator facilities that can be used for geodetic VLBI exist at the Haystack Observatory of Massachussetts Institute of Technology (MIT) near Boston, MA., at the USNO (US Naval Observatory, Washington, D.C.), and at MPI, Bonn (Max-Planck-Institute for Radioastronomy). Upgrades to Mark-IV are envisaged or under way at the US sites and at MPI. A new Mark-IV correlator is under progress at Westerbork, Holland, operated by the Netherlands Foundation for Research in Astronomy at Dwingeloo, Netherlands, for the JIVE consortium (Joint Institute for VLBI in Europe).

1.2.2 Analysis

In the analysis of VLBI networks a large number of parameters can be estimated. Thematically they can be grouped into

- Astronomical – Source positions
- Space-time – three parameters of general relativity
- Earth rotation – precession and nutation; rotation angle (=UT1) and polar motion
- Solid earth tides – vertical and horizontal response amplitude coefficients
- Solid earth deformation – site positions and rates
- Site environment – tropospheric zenith delay and rate
- Site equipment – clock offset and rate

to mention the most important.

We describe in short the principles behind the most common VLBI data analysis packages, particularly CALC-SOLVE (Ma et al., 1990; Herring et al., 1986). After correlation, CALC-SOLVE generates for every source observation and for every baseline the predictions of the fundamental

observables, delay and delay rate, using standard values of the parameters. The software also generates and stores in the data base the partial derivatives of the observables with respect to the model parameters. The observations are formatted accordingly in order to set up the (weighted) least-squares set of normal equations. These stages are termed DBASE and CALC. The solution of the least-squares system is the subject of the SOLVE-phase. The CALC data base is stored on file servers (e.g. at CDDIS) from where it can be transferred to sites which are equipped with SOLVE. Two major variants of SOLVE exist. The one at GSFC assumes piecewise linear sections (biases and constant rates) as a model for clocks and troposphere, whereas these parameters are modelled as random processes and determined by Kalman filtering in the SOLVE version (SOLVK) at CfA (Harvard-Smithsonian Center for Astrophysics).

SOLVE solutions spanning many years in which baseline rates and tectonic motion (but also long-term variations of earth rotation) can be determined in combined solutions using post-processing software GLOBL or GLOBK (the latter involves a Kalman filter model, conceiving the position parameters etc. as a state vector undergoing stochastic evolution).

1.2.3 VLBI networks for geodesy

A VLBI network consists of a number of observatories which participate in observation campaigs on a regular basis. The association is somewhat loose, and observatories usually join in two or three of the networks. Mark-III capabilities are the standard of most sites. Mark-IV is introduced within the next couple of years. We will summarize some of the more important applicationss in the next section. Here we give examples of the following recent networks,

- R&D – Research and Development, the NASA-coordinated network for the Crustal Dynamics Project and its follow-up missions in the 1990's. Since the summer of 1995 these monthly experiments have been replaced by longer sessions of one week or more, concentrating on studies of the Earth Rotation Parameters.
- NEOS (National Earth Orientation Service) – A joint venture of the US Naval Observatory (USNO) and the Geosciences Laboratory of the National Oceanic and Atmospheric Administration (NOAA). NEOS VLBI continues the core activities of IRIS (International Radio Interferometric Survey) with international participation in the NEOS-A network.
- IRIS – A subcommission of the IAG promoting the use of VLBI for earth orientation since 1981. Several IRIS subnets continue to operate also after the creation of NEOS.

- Europe – A network of European observatories for crustal deformations.
- NAVNET – A solely US Navy network for earth orientation.
- VLBA – As a joint effort between NASA and NRAO, facilities of the Very Long Baseline Array are used for crustal dynamics and earth orientation.

1.2.4 VLBI centres and campaigns

Geodetic applications of VLBI can roughly be grouped into three categories. Astrometric projects deal with the location and internal structure of radio sources. These studies are needed mainly as a support for the two central application areas, determining deformations in the global network, and monitoring earth rotation (Feissel et al., 1993). The latter task comprises not only the speed of rotation but also the movement of the axes in inertial space.

The distinction in application areas conforms with the notion of the changes of the baseline vectors, which naturally split into a deformation mode and a rigid mode, the latter of which comprises three orthogonal translations (which VLBI as a stricly differencing technique cannot observe) and three orthogonal rotations. Translation, orientation, and scale are global properties to which any subnet must conform.

The International Earth Rotation Service (IERS), a distributed organisation with its central bureau at Paris Observatory, has the task to provide the information necessary to define a Conventional Terrestrial Reference System and Conventional Celestial Reference System and to provide their interrelations as well as relations to other reference systems for the determination of earth orientation parameters. For this purpose, various coordinating centres and contributing centres submit observations, analysis results, ancillary information like atmospheric angular momentum, and their work on the development of the IERS standards. VLBI processing centres contribute primarily their solutions for site positions and earth rotation parameters. The IERS then prepares weighted combined solutions (cf. Annual Reports, e.g. IERS 1995) and distributes bulletines. The IERS also decides on the insertion of leap seconds between Atomic Time and Universal Coordinated Time.

The monitoring of crustal motion as the primary area of application of VLBI is conducted in coordinated, international projects of varying constellations of participating observatories and processing and analysis centres. The IERS holds these projects together, stating unambiguous standards and hence allowing intercomparison within and between techniques.

The contributing institutes are provided access to the data base and are free to analyze the results, highlighting individual problems and special issues.

Contributing analysis centres exist at NASA–GSFC, NASA–JPL, USNO, University of Bonn, Mizusawa Observatory (Japan), Ukraine Astronomical Observatory, Shanghai Observatory. Many more sites exist with full VLBI analysis capabilities (possessing observation data bases) but not contributing own solutions to the IERS. We mention two with which we have a record of colaboration, the Center for Astrophysics at Harward–Smithsonian Center for Astrophysics, and the Norwegian Defence Research Establishment (Andersen, 1995).

The research group at Onsala has SOLVE-facilities for VLBI-analysis in the form of both the Kalman-filter and the linear-section variants. This is feasible for the problems we are studying, which concern primarily atmosphere and clocks. The associated CALC data bases are acquired from GSFC and CfA over the Internet using the File Transfer Protocol.

Global crustal movements

We present first the two crustal motion surveys and the earth rotation survey in which OSO has been active. NASA has been the promotor of the Crustal Dynamics Project (CDP) throughout the 1980's (Bosworth et al., 1993; Coates et al., 1985). With redefinded goals, Dynamics of the Solid Earth can be seen as the on-going continuation of these efforts. NASA-GSFC (Goddard Space Flight Center) has been processing and analyzing the majority of global solutions, has been the processing, distribution and archiving centre for a large number of campaigns, and will continue these activities. During 1994/95 many NASA observing facilities, however, had to be closed and efforts be reduced in order to cope with budget restraints. Successor campaigns to CDP run under the Research and Development (R&D) title, additional experiments focus on circumpolar plate motion (POLAR). NASA observational activities in VLBI concentrate on the VLBA (in cooperation with NRAO). Development of the Mark-IV system continues at NASA, also using the mobile MV-3 system.

Longest possible baselines are observed in the GTRF (Global Terrestrial Reference Frame) experiments. This is a new network, starting in 1995. Here, a comparatively large number of sites (10–11) join with emphasis on consistency of the global plate tectonic model and the closure problem of relative plate motions. Onsala has participated in two campaigns during 1995, together with Madrid, Medicina, Fortaleza (Brazil), Fairbanks (Alaska), Hartebeesthoek (South Africa), Hobart (Tasmania), Kokee Park (Hawaii), Santiago de Chile, Seshan (China), Westford, and Yellowknife (Canada).

European crustal movements

European VLBI has its own user group (although CDDIS at NASA GSFC acts as a support and archiving centre). Experiments under this heading involve Mark-III capable observatories in Europe, which are located in Italy (Matera, Noto, Medicina), Spain (Madrid), Germany (Wettzell), Ukraine (Crimea), Norway (Ny Ålesund), not to forget our own site at Onsala. The Geodetic Institute at the University of Bonn (FRG) acts as a coordinating and processing centre.

Mobile VLBI activities used the NASA MV-2 and MV-3 units. A new transportable facility, TIGO, which integrates practically all techniques (VLBI, GPS, SLR, PRARE) is near completion at the German Institut für angewandte Geodäsie (IfAG).

The sites in southern Italy (Noto on Sicily, Matera in Apulia) came into operation comparatively recently (1989, 1990). Still later, in 1993, Crimea obtained Mark-III capability. Finally, the latest addition is Statens Kartverk's site in Ny Ålesund, operational since 1994.

Monitoring earth rotation

The monitoring of earth rotation calls for standard networks with a small number of sites regularly participating. These are strategically distributed as to obtain good geometry for the three possible rotation angles. The regularity of the campaigns concerns the set of sites as well as the periodicity of the schedule, usually one experiment in five days. During the 1980's an experimental phase, in which the space techniques quickly replaced the methods of optical astronomy, led over into quite routineous and tightly organized experiments.

As a joint effort NOAA's Geosciences Laboratory (NOAA-GL) and the US Naval Observatory (USNO) have been responsible for a group of experiments focussing on earth orientation (IRIS, now NEOS). Whereas IRIS was created as a subcommission of the International Association of Geodesy, NEOS is a program with US national support. The VLBI operations of IRIS continue into NEOS as the routines and participating sites are historically connected. However, IRIS was reorganized at the IAG General Assembly 1995. It will continue to perform the IRIS intensive campaigns for continuous daily solutions of UT1 from one-hour duration experiments each day at Greenbank and Wettzell.

NEOS comprises more techniques in addition to VLBI. The NEOS VLBI scheduling, operation and analysis centre is now solely at USNO, implying that these functions have been relocated from NOAA-GL. But NOAA's support for observational activities and active participation is

still granted. Sponsored projects concern e.g. most of the southern hemisphere sites, particularly Fortaleza in Brazil, which became operational in April 1993.

In the history of IRIS NOAA-GL has been acting as a processing and analysis centre, contributing the results from their POLARIS network to the IERS. In these networks radio telecopes at sites in stable crust cooperate emphasizing site geometry with respect resolvabilty of coordinate frame rotations in all components, UT1, Polar Motion, and Nutations. During its history starting in 1985 several extensions of the core network have been devised, e.g. IRIS-S (South) to test configurations with the southern hemisphere, IRIS-P (Pacific), and POLAR northern high-latitude observatories. Regular sessions at five day intervals and intensive sessions involving a smaller number of stations, were the basis of the standard VLBI analyses as the backbone of the IERS bulletin and combined solution services.

From 1990 on, the IRIS-S southern network experiments have been coordinated by IfAG Frankfurt/M. and the Geodetic Institute at the University of Bonn, more than 80 sessions, however no longer at regular interval. IRIS-P continues under the leadership of Mizusawa Observatory (Japan).

NEOS solutions, particularly regular high-rate EOP's are now based on a weighted combination of techniques (IERS Annual Report, 1994), with increasing input from GPS especially concerning high-rate variations. VLBI remains a strong contributor to these products; the responsibility for all regular VLBI activities within NEOS has been moved to the USNO from January 1, 1995. Despite of the N in NEOS spelling National, these activities rely not only on the NAVNET telescopes; the NEOS-A network consists of the radio telescopes at Wettzell, Fortaleza, Greenbank, Kokee Park, and Gilmore Creek. The NEOS-B network with monthly observations has been discontinued, however. There, Onsala was joining.

Extended intensive campaigns with 14 days duration have been conducted in 1994 and 1995 (CONT-94, CONT-95) for the purpose of monitoring earth orientation at the highest attainable accuracy in an intercomparison of the three different VLBI networks, NAVNET, VLBA, and the Crustal Dynamics R&D network.

Other VLBI networks

The Jet Propulsion Laboratory of NASA at Pasadena, Calif., is responsable for the tracking of spacecraft. Primarily the operation of sensors in deep space, like Voyager and Pioneer, requires large radio telescopes. A total of three of such instruments, located at Owens Valley (Calif.), Madrid (Spain) and Tidbinbilla (Australia), constitutes the Deep Space Network (DSN). The distribution of the instruments is sufficient for un-

interrupted visibility. The DSN is also used for geodetic VLBI. However, due to special technical requirements for satellite tracking the DSN has become compatible with Mark-III only after 1988. Some VLBI observations are made in the wide-band TEMPO format.

A group of radio telescopes in Russia/Siberia (QUASAR network) serves as the russian equivalent of the Deep Space Network. A Mark-III capability exists at Ussurisk, a 70-m-diameter antenna operated by the Russian Space Agency in the Russian Maritime Province. Parallel facilities exist under the Russian Academy of Science, however hitherto not up to Mark-III cooperative standards.

Mobile VLBI

The majority of VLBI observatories use relatively large antennas. These structures remain fixed at the sites. NASA has also three transportable radio telescope and accompanying instrument vans carrying a Mark-III terminal. The MV-2 and MV-3 instruments with their 3.6-m and 5-m dishes, respectively, have been repeatedly used at roughly 100 locations, 14 of them in Europe. Also, the mobile Mark-III terminal has been connected to permanent dishes, like the one at Algionquin Park, Canada. The larger 9-m MV-1 telescope was permanently placed at Vandenberg, Calif. until 1990.

Results from the campaigns in California (1983–1987), substantiating the notion of a San Andreas deformation zone and Basin-and-Range extension, have been reported in Clark et al. (1987). In the Alaska campaigns (Ma et al. 1990; Sauber et al., 1993), the site offset induced in the course of an intervening earthquake was detected. But most importantly this campaign probed the Alaska-Aleutian area of subduction tectonics, revealing large, steady deformation in the front zone, impying baseline shortening with respect to inland Alaska of 2–4 cm/yr.

The campaigns in Europe 1989 and 1992 were quite successful as far as the observations with the MV's are concerned. We shortly relate the report of Zarraoa et al. (1995). According the their analysis the major setback in the campaigns that involved Scandinavian sites was the low level of participation of fixed sites, resulting in weak geometries. At Trysil, Norway, the MV-2 system was semi-permanently observing in 15 experiments during 1992–1993. While the majority of the 1992 experiments gave results fully in line with the precision that can be expected at permanent sites, the 1993 results were seen to scatter, again probably an effect of a weak network configuration.

In the light of a steadly increasing accuracy that GPS can provide, mobile VLBI has lost much of the attraction it had gained around the mid 1980's. The small dish implies lower gain and thus lower accuracy. Although this

can be compensated if at least one high-gain low-noise antenna operates in the same survey, the advantage over GPS today is at best marginal. The instrument requires highly specialized and well-trained personell to operate under oftentimes demanding field conditions. Frequent repetition and long duration of site occupations as would be preferred in crustal dynamics meets an instrumental bottle neck in the few mobile instruments that are available. Davidson and Trask (1985) detail the system and the hardship.

Currently, the MV-3 system is used by NASA at Greenbelt as a Mark-IV development unit. MV-1 is at Yellow Knife, Canada.

VLBI final remarks and outlook

Within these projects repeated VLBI experiments have involved 41 fixed and 45 mobile radio telescope sites.

Due to budget constraints NASA has been forced to limit its VLBI involvement in observations to mainly the VLBA sites and to the Deep Space Network at JPL. That is, crustal dynamics will predominantly hinge on VLBA and on the international contributions. NASA GSFC continues to operate the coordinating, data service, and analysis work. However, both USNO NAVNET and NEOS observations can be used for crustal motion surveys; the data is available and compatible, although the campaigns are not always tailered for the purpose.

Continuing VLBI activities and combination of other techniques for earth rotation are concentrated under the roof of to the US Naval Observatory (USNO), running the NEOS and NAVNET VLBI networks.

An on-going trend sees network densification as the domain of GPS, where more and more permanent sites are being created. The role of VLBI will primarily address the global long-term stability of the reference systems. A network of VLBI core sites for crustal motion will operate with a few sites on each of the important tectonic plates. Hence there are interests to add sites in Asia, South America, and Africa. The number of experiments will decrease somewhat, but we will also see more long-duration experiments like CONT-94, CONT-95 Sites will be selected on criteria which emphasize the network configuration geometry and the stability of the point preferably in a well-defined geological environment. In some cases baselines with a long and lively history need to be continued in order to maintain a benchmark experiment. Examples: Westford–Onsala which is one from the very beginning, and Wettzell–Onsala as an important probe for intraplate deformation. In other cases, high latitude will favour VLBI for GPS, like in the case of Ny Ålesund, where GPS satellites always remain far from the zenith. Trying to look into the future, the expected level of activity will probably comprise 20 to 30

telescopes participating in 30 to 50 sessions each year.

The European network has been expanding during 1986 to 1994. With VLBI stations at Onsala, Wettzell, Ny Ålesund, and—prospectively—Svetloe being located in the perifery of the pleistocene glaciation area and in the same tectonic plate, these stations form an observation geometry suitable to resolve expected horizontal displacements due to postglacial rebound or eventual tectonic intraplate deformations.

1.3 GPS

Originally planned by the US Department of Defense (US DoD) already in the sixties and developed by the US Air Force during 1978–95, the Global Positioning System has become a widely used system for navigation, timing and precise positioning with a wide range of applications. The system has been officially declared Fully operational in 1995. The core of the GPS is the space segment, a set of 21 (+3) satellites which revolve around the earth on high orbits (12 h period, 20,200 km altitude, 55° inclination). Provided the local horizon so permits there are always at least four, at maximum 11 satellites visible at any place on the earth simultaneously.

During the stages of building up the system, the technical specifications of the satellites has been changing and the number of spacecrafts been increasing. Despite performance limitations and heterogeneity in geographic coverage in the initial phase, first use of the GPS for geodetic purposes has been announced already by Counselman and Shapiro (1979), MacDoran (1979), and Bossler et al. (1980).

The satellites broadcast coded messages on two carrier frequencies in the L-band (1.2, 1.6 GHz) that report spacecraft position and time of transmission. A user receives the signals and utilizes the codes in a timing/ranging operation or tracks the phase of the carrier in an integrated Doppler type of measurement. Ideally, the range to four satellites is sufficient for the determination of four parameters, three spatial parameters—the three co-ordinates of the receiver position—and one for the receiver time.

Being primarily devised as a military system, the access to the full real-time positioning capability of the GPS is restricted. Civil users may unrestrictedly use the Coarse Acquisition (C/A) service, which permits instantaneous positioning accuracy on the order of 100 m, or off-line post-process the observations from a number of receivers in order to obtain relative positions (baseline vectors, baselines) of any precision.

In practice some of the restrictions originally intended could be set aside.

For instance any user may put up a stationary receiver at a position known to him/her. Centering on such a base station, the relative position of a roving receiver can be determined with considerable accuracy (typically 3 m) can be achieved in near-real time, and this information might just be as valuable as one determined directly from the GPS, rendering an academic notion to the precision limit intention. To achieve the improvement the stationary receiver reports the difference between the predetermined and the current GPS-C/A position. This difference applies nearly exactly also at the roving receiver eventhough they may be hundreds of kilometres apart. Current developments consider more sophisticated methods which probably will push the limits by two orders of magnitude (cf. Chapter 4.3.4; see also Herring, 1996).

The following short description draws mostly from Dixon (1991) and Johansson (1992). We will keep a narrow scope with focus on precise relative positioning and mention applications which emphasize on rapidity, on real-time or navigation aspects only in passing.

1.3.1 Codes and carriers

In addition to the Coarse Acquisition code, GPS satellites broadcast a Precise Code (P) message. They phase-modulate the two carriers (L1 at 1.57542 GHz = 154×10.23 MHz, L2 at 1.22760 GHz = 120×10.23 MHz) to produce the following two signals

$$S_1 = A_{P_1} P(t) D(t) \cos \omega_1 t + A_{CA} CA(t) D(t) \sin \omega_1 t \quad (1\text{-}4)$$

$$S_2 = A_{P_2} P(t) D(t) \cos \omega_2 t \quad (1\text{-}5)$$

where the codes $P(t)$ and $CA(t)$ represent square waveforms of amplitude ± 1 with chip rates of 10.23 and 1.023 MHz, respectively. The actual amplitudes are denoted by A with the respective subscript, and $D(t)$ is a 50 Hz low-bitrate data message reporting about the satellite status and the almanach of the system.

The presence of two frequencies allows a first order compensation for the propagation delay created by the ionosphere. The total delay is inferred from the dispersion effect, c.f. Chapter 1.4.1.

The wavelengths corresponding with the codes are ~300 m (C/A) and ~30 m (P). The wavelengths corresponding with the carriers are ~19 cm (L_1) and ~24 cm (L_2). (As a rule of thumb, a positioning technique with a low degree of sophistication based on codes or carriers can achieve a precision of 1/100 of a wavelength.)

The codes are the result of an encryption process involving large prime numbers. The C/A message repeats after 1 ms, the P message only after 37 days. Both are perceived by an uninitiated user as if consisting

of a completely random bit stream (pseudo-random number, PRN), a property which also makes the signal robust against interference. Each satellite obtains one week worth of the P-code. Together with the spread-spectrum technique used in the modulation this allows that the same frequencies can be used on all satellites. (However, due to the relative motion of the satellites the signals received at ground are slightly Doppler shifted with respect to each other.) The receiver will identify each satellite by the identifying label of the PRN.

Although originally intended to be classified, the P-code information has already early been made available to civil manufacturers of instruments. Thus, receivers with P-code capability have been on the market since the mid eighties (e.g. Texas Instruments TI 4100). Proprietary measures for exclusively military use have instead been implemented in two ways:

- **SA - Selective Availability** primarily to prevent enhanced C/A technique to underrun the imposed 20 m accuracy threshold. For this purpose, the satellite oscillators are dithered and the clock epoch information is diluted.
- **AS - Antispoofing** a shorter, completely classified pseudo-random encryption of the P-code (Y-code).

Measurement of distance, determination of positions

A GPS receiver correlates the received code with a locally generated one. The time difference between the transmission and reception instances, Δt_s and Δt_r is converted into range ρ by multiplication with the speed of light. Delays Δt_p in the signal path and oscillator offsets in satellite Δt^j and receiver Δt_k introduce a range bias, presenting a pseudo-range R

$$R = \rho + c(\Delta t_r - \Delta t_s + \Delta t_p + \Delta t_k - \Delta t^j) \qquad 1\text{-}6$$

A set of difference operations can be performed on the simultaneous ranges: When more than one receiver observe the same satellite all but one oscillator clock offsets cancel; similarly, when one receiver observes more than one satellites, all but one satellite clock offsets cancel. The latter operation, basic as it might appear, is not necessarily the optimum strategy; a clock model for each satellite (as in GIPSY/OASIS-II, Lichten and Border, 1987) has also proven to be useful.

The range residual will consist of that fraction of Δt_p of the signal delay which is different for each satellite-receiver pair, which is predominantly an effect of different wave paths through the atmosphere and the ionosphere.

Reconstruction of the carrier signal, in the most direct way by squaring the signal or as a side-product of code extraction, allows to track its phase against the local oscillator (the code can be used to control the oscillator, which relaxes the demand on stability). The change in distance between satellite and receiver can be tracked accurately by tracking the evolution of the carrier phase

$$\rho = n\lambda + \phi\lambda \tag{1-7}$$

$$= \frac{v_\phi}{f}(n + \phi) \tag{1-8}$$

where v_ϕ is the phase velocity (unlike code, which propagates with the group velocity). The integration of phase ϕ starts at an initially unknown integer n, the so-called phase ambiguity. These integers can be determined in a (computationally intensive) process. A good starting position is required. Alternatively, code observations and carrier phase can be analysed in a simultaneous equation system. The code observations are given relatively low weight, generally enough to fix the solution near the actual phase ambiguities.

The range observations, the approximate (initially predicted) satellite and receiver positions and a large number of model parameters together form a set of overdetermined normal equations which can be solved in the sense of a least-squares error criterion. Mentioning the most relevant in the present context, solved-for parameters comprise (see e.g. Sovers and Border, 1990)

- improvements to either site or satellite positions
- earth orientation parameters (precession, nutation, UT1, polar motion)
- earth deformation parameters (tides)
- wave propagation parameters of the troposphere

During Anti Spoofing (AS), the P-code cannot directly be observed. Use of the codes on L1 and L2 can still be made.

In the presence of AS the P-code is encrypted. This code, normally refered to as Y-code, is unknown but the same on both frequencies. This fact could be used by cross-correlation of both frequencies to get an ionospheric estimate. The cross- correlation product and the C/A-code are used for initial editing of the carrier phase data at the preproccesing stage (see e.g. Melbourne, 1985; Wübbena, 1985; Blewitt, 1993).

The software features the possibility to enter the characteristics for each individual antenna into the solution.

1.3.2 International GPS Service for Geodynamics: IGS

In order to achieve high precision in position determination, the satellite measurements are processed off-line. The International Association of Geodesy has appointed a service organisation for GPS, IGS, for the purpose of providing ancillary data and other services for GPS users. The service comprises

- keeping archives and making data available of satellite observations at tracking sites, precise satellite orbits, earth orientation parameters (the latter disseminated in a technical bulletin);
- coordinating GPS tracking sites, including a set of technical and scientific standards;
- keeping a data bank with the descriptions of the sites, monuments, local ties, receiver types, technical specifications of antennas etc.

The IGS tracking network comprises currently more than 120 sites.

Under a central bureau a number of organisations contribute as either **analysis, data** or **operational centres**. Typically an operational centre would maintain a GPS station, continuously operate a receiver, sample ancillary (e.g. weather) data and contribute these to a data centre. In order to develop the technique the IGS arranges meetings and an electronic mail service for the exchange of ideas and experience.

Presently there exist three **global data centres** (NASA/CDDIS, IGN (France), SIO (San Diego)) and five **regional data centres** which supply tracking data from subsets of IGS sites.

The analysis centres compute site positions, EOP's and/or satellite orbit, typically from a certain subset of sites. The subset is selected on the basis of different criteria, some emphasizing global, some regional coverage. The growth of the global IGS network and the increasing number of regional networks (the analysis which may include non-IGS sites) calls for devising a level of **regional analysis centres**, which is presently in progress.

Regular processing of the operating centre's contributed data in overlapping networks is important for obtaining quality indicators for the users of the IGS data. As the number of IGS sites and the data batches are still growing a great deal of structure and administration in conjunction with these tasks are necessary.

A core network of roughly 100 sites is identified for which precise consistent global frame parameters are maintained, and from which precise

orbits are computed. Membership in core network requires good observation stability and rapid data delivery.

Several IGS processing centres provide after-the-fact orbit solutions. Rapid products can be obtained at a lag of only a few days over the Internet, e.g. from Scripps or NOAA/NGS. Final precise orbits are available at considerably longer delay, sometimes up to two months. The different processing centres use different site combinations of the IGS network and thus optimize the orbit solutions over a geographical area for which the subnet is most representative. The EMR Geodetic Survey Division in Ottawa, Canada, produces weighted combined global orbits, supplying an official IGS orbit solution. In these solutions the satellite position is determined typically with a precision of 0.1 to 0.15 metres. This translates to ground position errors in proportion of baseline length to satellite distance, i.e. typically a ratio of 1:100.

Details of the IGS structure can be obtained electronically, c.f. Appendix A.

1.3.3 Data processing tools and analysis methods

A number of computer program packages with two-frequency code and phase analysis and optional ambiguity resolution are available. We mention three, which have found wide spread: The Jet Propulsion Laboratory's GIPSY-OASIS-II (Webb and Zumberge, 1993); Bernese Software (Beutler et al., 1987) from the Astronomical Institute at the University of Bern, Switzerland; GAMIT from Scripps Institute of Oceanography, La Jolla, Cal. (Dong and Bock, 1989).

Regularly the software contains modules to model satellite orbits. The parameter estimation part is typically split up into a module that sets up the equation systems, providing partial derivatives of the target parameters with respect to observations, and the solving part that actually processes ("filters") the observations. To this end a number of perturbing processes must be taken care of. More details follow in Chapter 1.4.

Modules for the preparation of the observation data comprise procedures for editing code observations, fixing cycle slips (when receivers have lost lock of the carrier phase tracking) and providing two-frequency data combinations that are insensitive for ionospheric dispersion effects.

Orbit modelling

Precise position of a satellite in its orbit is needed in order to solve the pseudo-range equations of station pairs or networks. The onboard

generated satellite message contains rough preliminary ephemerides. The exact along-orbit position can only be inferred after correction of clock errors. If all of these parameters are solved. and this can actually be done to a precision of 10 cm. the position of a single receiver on the ground can be determined at ~1 centimetre precision from observations of four or more satellites.

Orbit modelling is time consuming, and data from a wide spread network of sites has to be acquired to serve as satellite tracking data. On the other hand, dealing with high-orbit satellites, the orbit dynamics are rather straightforward. The single largest complication in orbital dynamics concerns the satellite's passage through the earth shadow. The drop in radiation pressure creates a transient force and thus perturbations in the orbital motion. Several processing modifications can be applied, ranging from rejecting the respective satellite's ground observation data to sophisticated dynamic modelling which takes the radiation reflectance properties and geometry of individual surface elements of the satellite into account.

Mathematical solution procedures for orbit integration are included in the GIPSY/OASIS-II package of JPL (Lichten and Border, 1987; Webb and Zumberge, 1993).

Earth orientation

The use of precise orbits has a profound impact on the accuracy of the network solution. These orbits are given in a coordinate system that uniformly co-rotates with the earth. Deviations from this frame rotation are described by the earth orientation parameters (EOP, cf. Chapter 1.2.4). Actual data consistent with orbit solutions can be obtained from the IERS, available also from IGS or NASA/CDDIS.

Provided the network has sufficient global coverage, GPS based inference of EOP can be achieved (Dickey and Feissel, 1994). Increasing success with especially the short-term (up to 10 days) resolution capability places GPS at current only slightly short of VLBI.

Global reference frames

Site position solutions from GPS can be obtained in mainly three different ways. In the extreme case where only intersite distance vectors are required the network solutions can be retained as is. However, for most purposes requiring position estimates in a conventional reference frame, the data from regional (global) service stations are included in the analysis.

In the following description we will distinguish between the user stations in the target area on the one hand and the service sites on the other. and suppose that the latter contribute to precise. post-processed orbit solutions.

The confidence and stability of the solution at the sites of either type will differ. A gain in the over-all consistency is always achieved as the service sites are incorporated in the orbit solutions. Thus. the orbits convey the motion of the reference system which in turn is constructed on the basis of the service sites.[1]

Tying together the two types of sites the ambition is now to preserve the precision of the baselines of the target area and the long-term consistency of the service sites.

In the so-called nonfiducial approach the network includes data from a number of sites of the IGS network. The initial solution starts with the service site coordinates losely constrained (Heflin et al., 1992). Using the internationally adopted frame of reference positions and velocities of these service sites (e.g. obtained from the IERS) the solution—internally kept rigid—is rotated and translated into the global frame of date. Typically ten constraining sites are needed. A larger number may be required if the global solution shows weeknesses and/or the quality of satellite observations shows signs of degradation.

1.4 PERTURBATIONS AND ERROR SOURCES

In the following we review the a priori models which formulate known source-receiver range variations. The majority parameters of these models can be subject to estimation on the basis of the observations. We have already covered Earth Orientation parameters in Equation 1-2. A number of fundamental parameters which relate to special and general relativity are omitted as not interesting in the present context [2].

On way to characterize perturbations (e.g. of an instantaneous site position from its expected mean) is whether the process is predominantly deterministic (e.g. tides, precession, nutation) or predominantly stochastic. In the latter case, the random walk may be fast or slow with respect to a typical observation window. For polar motion, e.g., it is practical to

[1] More specifically, it is that part of the motion which is not included in the Earth Orientation Parameters, viz. deviations from a rigid rotation and translation of the global ensemble. N.B. the regional subset may very well comprise a motion component which can be represented by rigid body translations-rotations.

[2] They are important in orbit modelling and timing/ranging because of large differences between source and receiver gravity potentials, because of large distances and large relative velocities.

infer one daily average value with or without fixing the starting position at the previous estimate. Fast innovations, on the other hand, like in the clock behaviour or atmospheric delays, must be traced in some way. In practice there are three ways, (1) ancillary observations, (2) quasi-deterministically parametrized approximations like low-order polynomials, (3) stochastic processes. Option (2) in the form of linear sections is frequently used. Option (3) is conveniently adopted in Kalman filter versions of the parameter inversion process; software with a Kalman filter approach has become more abundant during the recent ten years.

The nature of the perturbing processes in relation to the accuracy ambition of space geodetic projects has favoured the creation of permanent networks in which observations can frequently be carried out campaign-wise or even permanently. Long time spans are needed so that perturbations can average out or that their temporal characteristics become evident. Dense sampling increases the capability to resolve transients and episodic evolutions. In this perspective, the regular sampling intervals and the homogeneous observing conditions that a permanent installation can achieve are highly favourable. The sacrifice is on the number of stations that can be handled. In GPS e.g., one day worth of data from typically 50 stations [3] can be handled in one simultaneous equation system; careful subnetting techniques can increase the number of solved station parameters in nonsimultaneous solutions without disturbing loss of consistency.

1.4.1 Ionosphere

In the context of perturbations and parameter estimation the ionosphere is special: Although its effect on range is great it poses relatively little problems in two-frequency measurements. The temporally variable abundance of free electrons in the ionosphere causes variable dispersion of passing radio signals. The effect thus introduces a signal group delay

$$\tau = \frac{\rho}{c} + \frac{A}{f^2} + \frac{B}{f^3} + ...$$

which in its leading dispersive term is inversely proportional to the square of the frequency. Parameter A is due to the total electron content along the path I (e^-/m^2),

$$A = 40.3 \times I$$

The differential delay between simultaneous measurements at two frequencies thus can be estimated by

$$\Delta\tau = \tau_1[(\frac{f_1}{f_2})^2 - 1]$$

[3] this figure is valid for GIPSY/OASIS-II; Bernese and GAMIT can handle up to 80 stations

to good precision. An equivalent relation holds for carrier phase. Expressed as path length variation, typical ionospheric delay variations may amount to tens of metres. At high latitudes the ionosphere has a generally lower electron content, but the variability is much greater than at low latitudes.

An ionosphere-free phase observable L_c is obtained by

$$L_c = \left(\frac{f_1^2 L_1 - f_2^2 L_2}{f_1^2 - f_2^2} \right) \qquad 1\text{-}9$$

where each phase range L_j relates to observed phase Φ_j as

$$L_j = -c\frac{\Phi_j}{f_j}, j = 1, 2$$

individually for each source-receiver pair.

In GPS the two frequencies are relatively close to each other. Yet the precision of the ionosphere correction is equivalent with the VLBI case since the latter has a lower signal to noise ratio.

A global system of permanent sites can be used to routinously map the ionosphere. Such a ionosphere service is currently in devised under IGS for applications in satellite orbit prediction and as a support for independent single-frequency surveys, including the precision-demanding VLBI in cases when the two-frequency option is not feasible (Sardon et al., 1994).

Presently the sunspot number is low. The ionospheric activity is going to increase to a maximum in the year 2001. This will affect the precision of GPS based measurements, and solving for second order dispersion terms will become actual.

1.4.2 Neutral atmosphere

An important source of measurement error in timing/ranging measurements (but also observations of angle) is induced in the neutral atmosphere, specifically effects associated with optical refraction. For these effects, gas density is the leading parameter, and it is in the troposphere where the largest part of the atmosphere's mass exists. In this section we are concerned with wave refraction and delay affecting electromagnetic radiation at centimetre to decimetre wavelengths as used in VLBI and GPS. A more detailed overview is found in Elgered (1993).

The un-ionized atmospheric gasses (like the free electrons in the ionosphere) perturb wave propagation in two ways, first by slowing down the propagation speed, and second owing to the vertical pressure gradient by offsetting and bending the ray path. Thus, the arrival time of a

wave group is delayed with respect to vacuum. The "path delay" signifies the slowness effect, whereas the bending effect is termed "geometric delay". However, in the neutral atmosphere the delays are practically independent of frequency.

Nitrogen and Oxygen remain in rather constant proportions. Thus, their effect is largely proportional on the air density integrated along the ray path, which can be inferred from surface barometric pressure. This rather uncomplicated effect amounts to typically 2.3 mm excess ray path per hPa surface pressure variation when observing in zenith direction.

On a plane earth with vertically homogeneous atmosphere, the excess path inceases with a factor of $1/\cos(\alpha)$ where α is the zenith angle ("mapping function"). More realistic mapping functions contain additional terms relating to the sphericity of the earth and to the vertical structure of the atmosphere, which contains geographic as well as thermodynamic parameters.

The variation of water vapour in the troposphere, spatial as well as temporal, however, implies a much more serious and complicated problem. Since water is involved, the corresponding terms are frequently called "wet" (wet delay, wet mapping function). Since no equilibrium conditions rule between partial water vapour pressure at the surface and the height-integrated density the propagation effects due to water vapour cannot be inferred from pressure as in the dry case. Surface measurements are not representative for the bulk of the troposphere, thus direct observations of the water vapour content is to employ profiles using balloon-borne radiosondes.

The relation between the water vapour partial pressure e and the wet delay in zenith direction ΔL_w measured in metres is

$$\Delta L_w = [1 + (6 \pm 3) \times 10^{-5} T_m](0.3754 \pm 0.0030) \int_S \frac{e}{T^2} Z_w^{-1} ds \qquad \text{1-10}$$

where T is the absolute temperature, T_m an effective mean temperature along the path through the troposphere, and Z_w^{-1} is the inverse compressibility factor of water vapour (the deviation from an ideal gas). Typically in Scandinavia ΔL_w in zenith direction may be as large as 20 cm, changing at rates of 1 to 2 cm/h. In the cold troposphere of the arctic regions water vapour effects are generally much smaller.

Experience from comparisons of GPS-derived vertical positions and observations of water vapour suggests that vertical estimation biases correlate with periods of high water vapour variability (Dodson et al. 1994; Jarlemark, 1994).

There are basically three ways to attack the problem. We have already mentioned radiosondes, which are usually launched at important airports

at 6 or 12 h intervals. For routine observations in large networks the data provided by weather balloons is too sparse in time and space. Then there is the possibility to estimate the delay parameter within the analysis of the geodetic data. Third, special independent measurement techniques have been developed to extract wave propagation parameters from microwave radiometric observations.

Wet delay from geodetic data

Here one utilizes the distribution of observation angles to the sources (satellites, radiogalaxies) in order to efficiently sample the total range of delays. Using a realistic mapping function as a model, the zenith delay at each site can be estimated as a linear parameter. The temporal evolution of the water vapour content and thus the zenith delay can be described most adequately in statistical terms as a random walk process. Hence the delay parameter can be estimated in a way similar to clock drift parameters. In a Kalman filter version of the observation equations the temporal random-walk like property of the process can be modelled with a good degree of realism. This is an approach taken in the GIPSY/OASIS-II program (Webb and Zumberge, 1993; Lichten, 1990) and in the SOLV-K version of the VLBI analysis package (Herring, 1986).

The accuracy of the mapping function at low elevation angles is crucial since these observations contribute most strongly in the parameter estimation owing to the long atmospheric path and large delay. Research on refining their formulation while keeping the number of characterizing parameters managably low is expected to lead to major improvements in the observation and analysis methods (Rogers et al., 1993). This must be matched with a trade-off of the elevation limit below which observations will have to be discarded. If (and only if) the mapping function represents the actual situation accurately, the gain of accuracy of position solutions due to low-elevation observations is significant.

The fluctuations of water vapour constitute a highly nonstationary process. Temporal characteristics must be studied carefully in order to derive realistic Kalman filter parameters and to trim the solution parameters in order to obtain minimum bias results for geodetic positions (Elgered et al., 1991). Additional complication arises when spatial water vapour gradients occur. These originate primarily in weather fronts, but can also persist, e.g. across coastlines, during stable weather conditions. Implementation of gradient parameters in the geodetic solutions is currently considered (Davis et al., 1993; Jarlemark, 1994). Alternatively, separate solutions for observations in the respective local quadrants are conceived, however suitable only for GPS as simultaneous observations at widely separate azimuths are required.

The development of mapping functions and the tailoring of the Kalman

filter parameters has been dependent on progress in microwave radiometry.

Microwave radiometry

Indirect estimates of the integrated water vapour content of the atmosphere can be obtained by observation of the microwave radiation that the vapour emanates. Water vapour has a week molecular resonance at 22 GHz that is thermally activated. Located at ground level, measuring the intensity of the radiation at the resonance frequency and comparing it with an unperturbed frequency gives an account of the total radiation emission due to water vapour and hence an indirect measure for the altitude-integrated density. Models or other evidence for thermodynamical conditions that describe gross variations of water vapour with height are required to compute wet delay estimates from the two- or more-frequency sky brightness observations. The broadening of the resonance line, which increases with atmospheric pressure, and sensing it off-centre is exploited to enhance the sensitivity of the method in the lower troposphere.

Instrumental development of microwave radiometers for water vapour measurement (often called a Water Vapour Radiometer, WVR) and research on the algorithms needed to convert brightness temperature into wave propagation delay, has been a major area of activities and competence at Onsala Space Observatory (Elgered, 1993; Jarlemark, 1994); c.f. Chap. 3.1.3.

Wet delay algorithms have been derived to cover a wide range of meteorological conditions, including the presence of liquid water in clouds. Problems persist, however, during rain; the radiometer data will typically overestimate the delay, however with a very high variance.

Typically a radiometer receives radiation from within a narrow cone of the field of view, defined by the design of the microwave feed horns. Narrow beam width is desirable since admittance of ground radiation must be eliminated. The sky is scanned by means of pointing maneuvers. Thus, the sky can be mapped by laying out a regular angular pattern. Alternatively, the instrument can be pointed in parallel with a VLBI radio telescope, or successively pointed at GPS satellites. A critical part of the instrument is the reference source which must provide high long-term stability.

There are several applications. Delay estimates from WVR observations can be used directly as corrections in the geodetic parameter solutions. The demand on accuracy is very high in this case. Deriving parameters for water vapour variability is somewhat less crucial; they can be applied to down-weight observations taken in unfavourable conditions, leading to

reduced random and systematic error in a least-suqares fit.

Operating a WVR, however, implies also a substantial amount of data processing and experience with the technique. To consider WVR as a regular ancillary device at geodetic observation sites at present appears not really feasible. Size and delicacy of the instrument also argue against that prospect. Instead, a few of these instruments at fundamental stations, where they can run in parallel with several geodetic techniques has been and will probably also in the future be a more successful route.

Experience from comparison of wet delays from WVR with estimates from GPS and VLBI data has resulted in a number of data analysis strategies, concerning

- the length of single observations and the distribution of sources in VLBI schedules,
- lower elevation cut-off limits,
- the discrimination of systematic errors as being instrumental, geometric or atmospheric,
- to determine realistic confidence limits for estimated geodetic parameters
- to improve data weighting in the observation equations

In short, findings based on VLBI and GPS suggest that despite tropospheric parameters being estimated water vapour variations affect baseline determinations at the millimetre to 1 cm level; horizontal components are more accurate than vertical in a 1:3 proportion and show a clear proportionality with length; in long-term observations a noise background can be found on all baselines, and provided they are short (below 2000 km) the VLBI and GPS determinations give similar repeatability. We find no baselines that show outstandingly better repeatablities (which would be expected if ground motion, be it tectonic or monument deformation were the limiting factor). If we find baselines with significantly worse repeatability, however, error sources can almost always be pointed out.

1.4.3 Local site displacements

The three-dimensional position and motion of a geodetic point in the global cartesian coordinate frame is conceived according to the following terms:

$$\mathbf{X} = \mathbf{X}_0 + \dot{\mathbf{X}} \cdot t + \Delta\mathbf{U}_T(t) + \Delta\mathbf{U}_A(t) \qquad 1\text{-}11$$

where $\mathbf{X}_0$ is the reference position at a specific epoch. $\mathbf{X}_0$ a plate tectonic velocity or any other small position migration rate. $\Delta\mathbf{U}_T(t)$ is a local displacement due to earth tides. and $\Delta\mathbf{U}_A(t)$ is the effect of loading of the crust due to barometric pressure. These displacement terms correspond to modelling procedures in the data analysis tools. Of course, mean position and site velocity are parameters of primary interest, and they will in the first case be solved for. But also amplitude and admittance parameters for the tides and loading effects are available to be solved for. The regular case is, however, that accurate parameters are supplied from external models and/or the literature.

The tidal displacement is composed of a solid earth part, directly induced by the gravity and orbital accelerations of the celestial bodies involved (earth, moon, sun), and a loading part induced by the changes of ocean bottom pressure associated with the tides in the oceans.

The tidal displacements are largely sinusoidal and confined to primarily three frequency bands (semi-diurnal, diurnal, and long-period, the latter containing semi-monthly, monthly, semi-annual, annual and slower terms). Accounting for the response of the solid earth, the displacment field distinguishes between radial (vertical) and transverse (horizontal or tangential) components (u, v, w). At mid and northern latitudes, the solid earth tide has typical amplitudes of 10 – 20 cm in the vertical and 3 – 6 cm in the horizontal. The geographical variation of the solid earth tides is regular, whence these motions can be computed with relative ease.

Ocean loading tides

The loading tides depend largely on the oceanic tides in the neighbourhood. However, an accurate account in the modelling of the effect requires that the global ocean tides are encompassed, and that computational accuracy requires algrithmic refinement in the case of tidal loads at short distance (Scherneck, 1983, 1991, 1993). Due to uncertainties in available ocean tide maps, the case of adopting an optimum loading tide model is still not closed, although the results recently concluded from TOPEX/POSEIDON missions have largely improved oceanic tide solutions particularly in the open oceans.

Figures 1-2 through 1-y show typical examples of tidal displacements and their amplitudes for a number of sites. The swedish GPS sites are seen to have fortitiously low loading tide effects. Largest effects at European geodetic sites appear at Tromsø and Madrid.

Modelled predictions of ocean tide loading is feasible in a once-for-all scheme, accepting the notion of stationarity of at least the largest oceanic oscillations. Among computational methods one can principally distin-

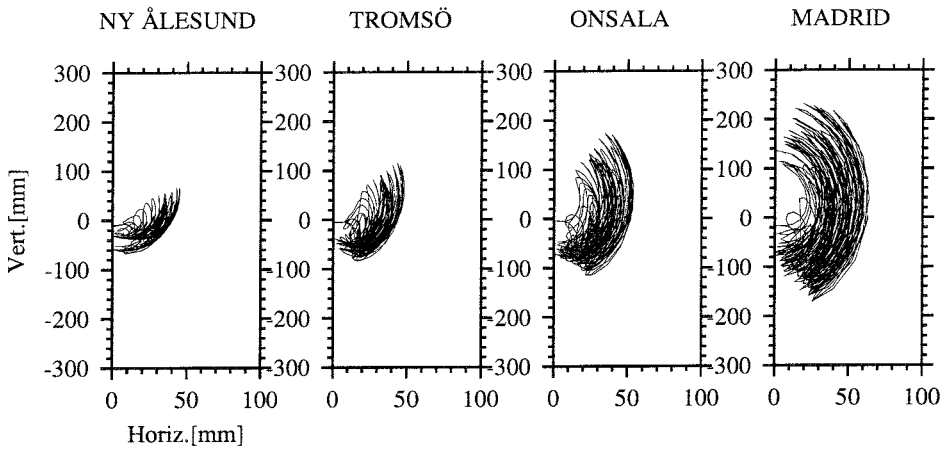

Figure 1-2. *Solid earth tides at four IGS sites. Shown is vertical displacement versus horizontal displacement (i.e. the absolute value of the east and north components) during 1000 hours, sampled every hour. Notice how solid earth tides decrease with latitude.*

guish between spherical harmonics methods and point load integration with a kernel function representing the loading solution to a point load that is applied sinusoidally in time (Scherneck, 1990). The latter method is due to Farrell (1972) and has been applied in Scherneck (1991) as a contribution the IERS Standards (McCarthy, 1993).

Air pressure loading

In analogy to the loading of the oceanic tide also air pressure variations induce deformation of the earth. The transient, aperiodic nature of the time evolution of the barometric field implies that predictions of the loading effects must be explicitly time-dependent and to be based on global pressure data.

The loading response is most efficient on continental areas. Where air pressure variations occur over water-covered areas, the water body will adjust in order to attain hydrodynamic equilibrium, meaning that the pressure along the bottom will become constant in the long-time limit. This adjustment is efficient in the deep oceans, typical relaxation times being on the order of tens of hours. It is termed the **inverse barometer effect**, henceforth termed IB,

$$p_w = -\beta_{ib} p_a \qquad 1\text{-}12$$

where p_w is the water bottom pressure increase due to the water surface displacement, p_a the surface pressure of the atmosphere, and β_{ib} is the

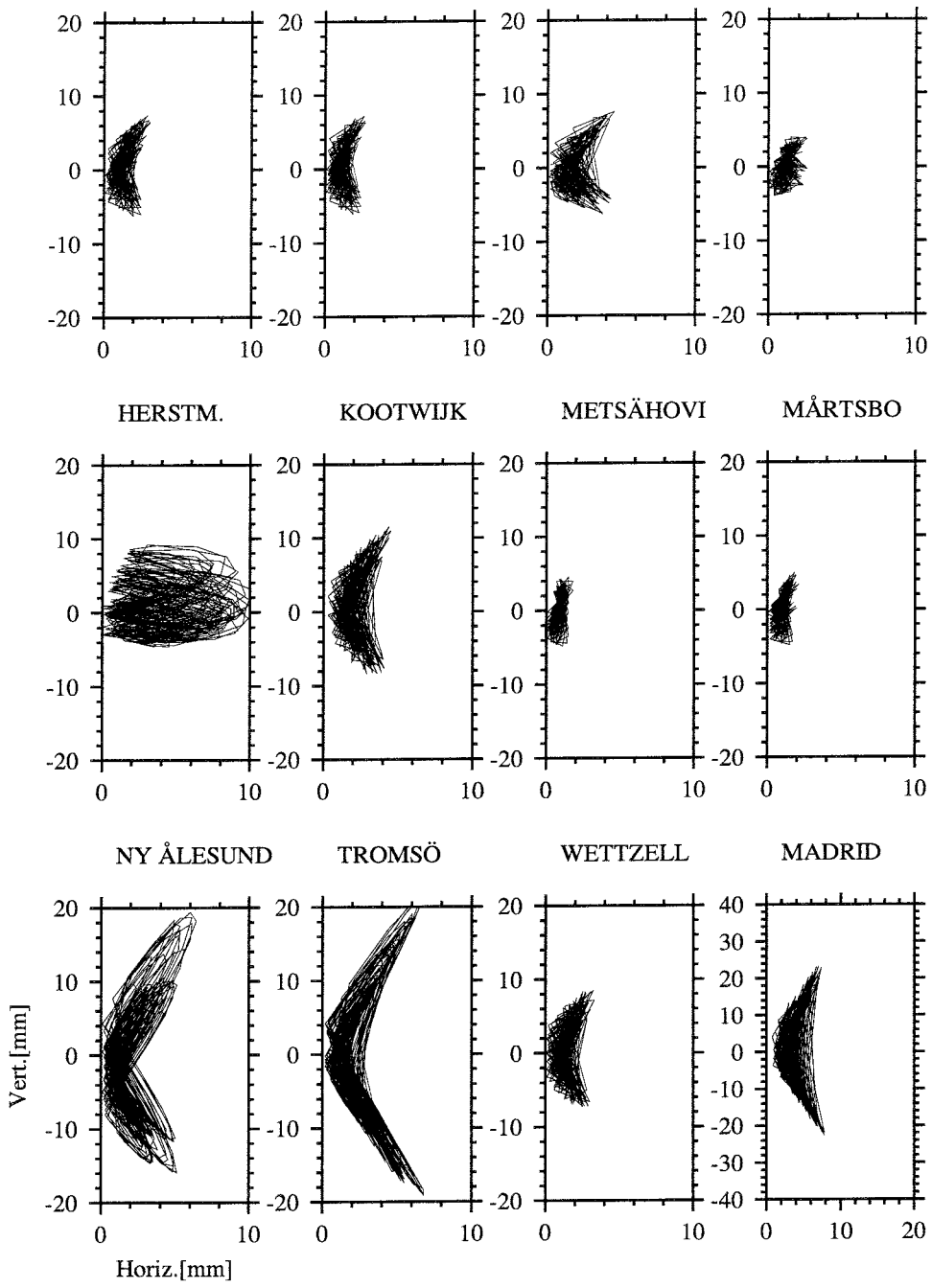

Figure 1-3. *Ocean loading tides at selected IGS and SWEPOS sites. Shown is a tangle plot of vertical versus horizontal instantaneous displacement. Ocean loading tide amplitudes depend on the regional ocean tide range; they decrease with the distance from the coast.*

inverse-barometer coefficient. In the ideal case of perfect compensation, β_{ib} is unity.

In shallower basins the relaxation time is first reduced roughly with the square root of water depth. Enclosure effects are also at work, like in the Baltic Sea, where air pressure perturbations of typical 1000 km wavelengths must displace the water through the Danish-Swedish sounds. This process has typical relaxation times of weeks, longer than the persistence of most barometric perturbations.

The inverse barometer condition is not exactly fulfilled, not only because of the limited extent and depth of the oceans, but also because wind fields accompany high- and low-pressure areas in a systematic way; earth rotation causes geostrophic conditions, approximately right-angle relations between pressure gradients and wind vectors. This causes the inverse barometer coefficient to be less than unity by at most 10 percent. The deviations are greatest at high latitudes due to geostrophy.

Vertical displacements of the crust amount typically to 1 cm, but in extreme situations, particularly in the centre of large continents where loading is not compensated by oceans, up to 3 cm. Horizontal displacement of the crust occurs at roughly a 1:3 ratio with respect to the vertical ones. The precision ratios of space geodetic methos are typically similar, so both displacement directions are equally important.

Thus, in order to predict displacements of air pressure basically the same loading integral applies, to carried out over the total surface of the earth. The deep oceans can be excluded assuming that the IB is perfect there. This method can predict all three spatial components of the loading field. A much more simple account, restricted to the vertical component, assumes that air pressure perturbations occur in a limited range of wavelengths. The vertical displacement of the crust in the centre of the pressure perturbation can be computed. The ratio between the centre pressure and the loading effect can then be used as an admittance coefficient α, giving

$$\Delta w \cong \alpha \Delta p_a \qquad 1\text{-}13$$

where -0.3$\times$ 10^{-3} < α < -0.42$\times$ 10^{-3} m/hPa. Figure 1-4 shows a time series of predicted vertical displacement at Onsala based on Equ. 1-13 and regular pressure observations at the same site. The predictions can be compared to estimated vertical positions obtained from SWEPOS GPS solutions, for the single site position and a vertical baseline variation, Onsala-Visby in the example. The figure shows that air pressure loading implies peturbations at the order of magnitude of the repeatability of GPS determinations. Dissimilarities between the signals exist for a number of reasons (simple formulation by Equ. 1-13; inhomogeneity in the GPS network, particularly different antennas and receiving conditions at the IGS sites; the baseline case cannot be compared to pressure effects

known at one end only). But there is also the possibility that this local site effect is admitted in the modelling of the wet troposphere, and that the GPS solutions only show residual effects, which would be strongly dependent on satellite geometry as the vertical crustal displacement maps into the satellite range as the cosine of the zenith angle, $\cos \psi$, and the tropospheric delay largely as $1/\cos \psi$.

We plan to implement air pressure loading predictions by obtaining global pressure fields from ECMWF on a regular basis. The data management in conjunction with this work, however, is not negligible.

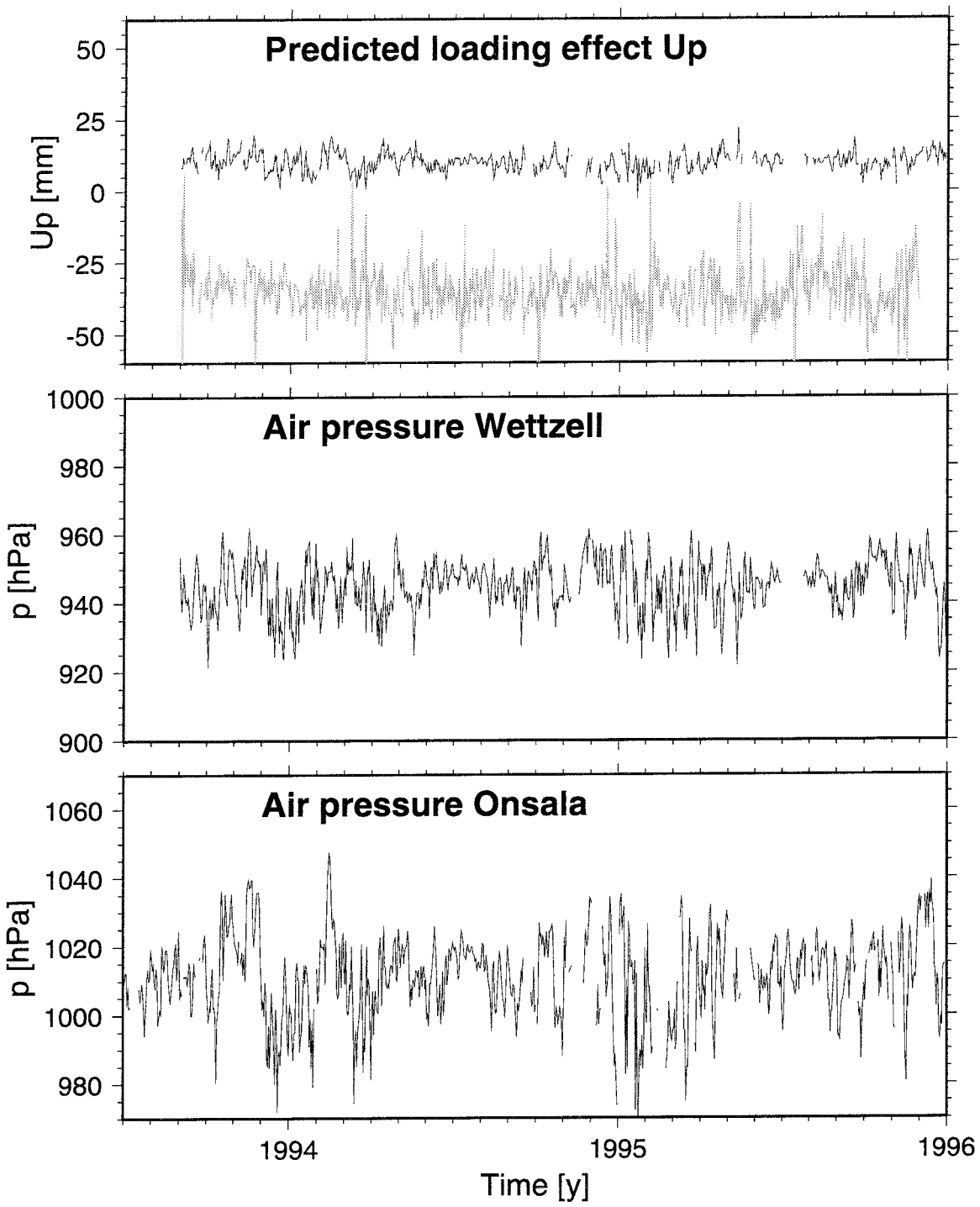

Figure 1-4. *Air pressure loading on the Onsala–Wettzell baseline predicted from local barometric recordings. Uppermost frame shows predicted loading effect in the Up component. The faint curve shows the observed motion inferred from GPS, evidently suffering from a noise level in excess of the pressure loading signal power.*

2 GEOPHYSICAL APPLICATIONS

The development and the use of space techniques for studies of tectonic plate motion on a global scale was the key element of the Crustal Dynamics Project (CDP), a coordinating and research supporting effort of NASA during 1980 to 1990 (Bosworth et al., 1993). The results of the CDP have been able to confirm the plate tectonic model in its essential parts—tectonic plates act to a large extent as if rigid, and deformation, accretion, and consumption is predominantly confined to plate boundaries. Signatures for lower scale deformation in certain regions started to become evident. Focussing on intercontinental geodetic baselines and hence transsecting many important tectonic plate boundaries, roughly 200 sites were participating in the measurement campaigns. The techniques initially used were VLBI and SLR (Robbins et al., 1993; Ryan et al., 1993; Smith et al., 1994; Gordon and Stein, 1992), gradually introducing the other satellite ranging techniques starting after around 1986, particularly GPS (Blewitt, 1993).

A summary of techniques, results and achievements has been compiled in a three volume set of publications (Smith and Turcotte, 1993a-c).

A second group of applications, which will be of lesser interest in the context of this report, concern earth orientation and rotation studies. As already mentioned these projects are necesary to provide scale and orientation for the deformation networks (Himwich et al., 1993).

2.1 TECTONIC DEFORMATION

Most importantly, the achievements of CDP in terms of relative plate velocities and positions of plate motion poles have provided important benchmarks for the drawing of the changing face of the earth. At the project's origin, the Anderson-Minster model was the major source of reference concerning the geological evidence. Concurrent geological and geophysical research during the 1980's, especially where the marine areas were probed, has been providing more and more accurate dating and mapping of geological formations and magnetic anomalies. At the end of the CDP epoch, NUVEL-1 (DeMets et al., 1990) presented the best and most consistent picture of contemporary plate motion.

In successive studies a slight disagreement in the global comparison of geodetically determined plate motion with the NUVEL-1 model (correlation coefficient 0.94) was found (Robbins et al., 1993). Revision of the paleomagnetic time scale led to a succeeding NUVEL-1A model being identical with the predessesor except for a global scaling constant, 0.9562

(DeMets et al., 1994). The evidence was judged as convincing despite of the vast difference between the geological time scale, being on the order of tens of million years, and space geodesy which is based on observations over tens of years. The discrepancy could have been accepted as being indicative of episodic evolution of plate tectonic also in a global mean. It should be noted that relative velocities of plates lacking an accretional boundary (like the Caribbean plate) are difficult to determine from geological data, and earthquake source mechanisms along subduction zones can only give evidence for the direction of the motion. Here, geodesy has filled in unique information.

As another important outcome of the CDP it was realized that plates do deform on a regional scale, though at one to two order of magnitude lower rates than what is engendered at plate boundaries. Most of this deformation appears to occur in continental crust in 100 to 200 km wide zones, but not necessarily next to an active plate margin. In many areas (like southern California) deformation was found at levels sufficient to be measured with the evolving techniques. From about 1987 on VLBI and SLR repeatabilities and campaign lengths became good enough to allow deformation rate determinations at or below the 1 mm/yr level. Even the displacement associated with single large earthquakes could be determined (Ma et al, 1990; Clark et al., 1990). The most frequently remeasured transatlantic VLBI baselines were shown to have length rates like 17.2 $\pm$ 0.2 mm/yr (Westford–Wettzell, 6000 km length) or 17.2 $\pm$ 0.5 mm/yr (Westford–Onsala, 5600 km length; Ryan et al., 1993).

In Europe, the Mediterranean area, especially the eastern part, obtained much attention. As an area with a complex tectonic setting, earthquakes occur frequently with considerable devastation, loss of life and health. The Nort and East Anatolian Fault systems could be seen as an Asia Minor equivalent of the San Andreas Fault, i.e. as a major fault system which is sufficiently concentrated and active to try to develop seismic prediction methods. In Greece, compressional regions of the Hellenic Island Arc and pull-apart basin tectonics e.g. in the Gulf of Korinth also show considerable seismic activity causing dangerous hazard. The space geodetic determinations of plate motion mostly using SLR within the WEGENER-MEDLAS program (Wilson, 1987) and several GPS campaigns by a consortium of MIT, UNAVCO, IfAG, and ETH-Zürich helped to clarify the tectonic deformation patterns (e.g. Oral et al., 1993; Smith et al., 1994a; Straub and Kahle, 1995), adding unique information as to the regionally integrated total slip, seismic plus aseismic.

European VLBI network started with the array of observatories all located in the northern and western parts (Germany, Spain, Sweden, Northern Italy). The baseline between the sites north and south of the Alps and Pyrenees were found to contract at a rates of 2.1 $\pm$1.3 mm/yr (Onsala–Medicina), 2.2 $\pm$0.5 mm/yr (Wettzell–Medicina), and insignificant length changes to Madrid. With the new sites in southern Italy

(Noto on Sicily; Matera in Apulia), movements in the border zone between the African and the European plate can be studied (Rius et al., 1992; Zarraoa et al., 1994). First findings produced by these authors show the Sicily site moving mostly with the velocity of the African plate and the Apulian site to at least possessing a significant component of this movement.

As GPS became available, an economical opportunity was created to monitor a large number of geodetic monuments in regional networks. Towards the end of the CDP period, from approximately 1989 on, GPS started to contribute seriously. There were notably two projects, the first Iceland campaign in 1986 (Rothacher and Beutler, 1988) during which important experience was collected, and the CASA UNO (Central America – South America) project (Kellogg and Dixon, 1990) which concluded tectonic motion between the Nazca, Cocos and North American plates determined with satisfactory precision.

First evidence of plate boundary zone deformation, the importance to determine the associated patterns of motion and to assess its consequences has been identified in the objectives of the DOSE program (Dixon and Bills, 1992). At this time the techniques were capable to be aimed at deformation rates one order of magnitude lower, which widened the view to include phenomena like vertical movement of the crust induced by varying ice and ocean loads. The quick progress that GPS was showing prompted development of particularly this technique in order to find out its full use and capabilities.

Recently Argus and Heflin (1995) demonstrated that the dense GPS networks start to provide comparable solutions for plate tectonic rates and positions of the plate rotation poles. Especially in the case of the Australian plate, earlier determinations hinged on VLBI at one eastern location. Three GPS sites at large separation appear to provide the crucial geometric stength to pin the plate rotation pole equally well in all components.

Large-scale GPS networks for tectonic motion are now operating in Central and Southern California (Bock et al., 1995) and in Japan (Sagiya et al, 1995; Shimada and Bock, 1992). Decimetre scale ground displacements at the network sites have been concluded in conjunction with major seismic events, notably 1992 at Landers and 1994 at Northridge, both on side faults of the San Andreas fault system (Bock et al., 1993; Hudnut et al., 1995), 1994 at Hokkaido (Tsuji et el., 1995), and 1995 at Kobe, Japan, (EOS, 1995; Geographical Survey Institute, 1995). In California the scale of motion across plates is on the order of 40 mm/yr, and important deviations from rigid plate require precisions of better than 10^{-7} and rate determinations of 1–5 mm/yr. The start of the projects dates at 1982 (VLBI) and 1986 (GPS). The three Californian studies presented similar confidence limits, around 5 mm, in the horizontal compo-

nents, and in the latter two cases could the displacement field be sampled satisfactorily by the networks. The geodetically determined strain field could provide essential information as to delineate the seismic source regions and mechanisms of these events. The shear movement across the San Andreas Fault (SAF) system was already well observed in terrestrial trilateration networks. However, detection of dilatation, specifically a shortening across the southern Coastal Ranges and across the Santa Barbara Channel, required the long-range precision of VLBI and GPS (Feigl et al., 1993).

Typically, the maximum relative displacements in the areas that are studied for their tectonics using GPS are on the orders of centimetres. Yearly campaigns in projects that encompass a three to five year period obtain thus the necessary statistical strength to conclude tectonic motion and discrepancies from initial models at the level above at least 5 mm/yr. At current this is satisffactory, giving ample opportunity for field studies in the active regions. The earthquake applications mentioned above show that with this resolution coseismic and postseismic deformation associated with large events can be studied at great detail. For example in the Hokkaido event, 20 GPS sites in a 10^5 km^2 area showed motions between 20 and 450 mm, determined at 5 mm precision.

However, it is not clear how active the so-called inactive regions in reality are. A one millimetre per year resolution in the monitoring of motion is not fully sufficient. We should be reminded that on geological time scales like 10^7 years and typical lithospheric length scales of 200 km (crustal length scales of 20 km), the total deformation that is equivalent to this uncertainty may accumulate to 5 (50) percent.

2.2 EARTH ROTATION

The success of CDP drew also from efforts to monitor the orientation of the earth with an accuracy compatible with the baselines. Today the position of the sites and the movement of the earth-fixed coordinate system with respect to "inertial space" is repeatable at or below the centimetre level. This implies standard deviations for the determination of earth orientation parameters of 0.2 marcsec in the case of pole position and 0.05 ms in the case of UT1, respectively.

Utilizing this precision, a large number of studies have produced a wealth of scientific results which reflect the global character of changes and dynamics in all parts of the earth, solid and liquid core, mantle, oceans and atmosphere. For a summary we refer to Eubanks (1993) and mention just a few examples. Changes in the length of the day occur in response to the El-Niño Southern Oscillation; seasonal changes of global wind patterns appear to be the most effective source of power for the

free Chandlerian wobble: length of day and polar motion also appear to shows signs of influence from seismically induced mass movements in the solid earth (Chao and Gross, 1995). The orbits of LAGEOS and similar laser reflector satellites are sensibly influenced by atmospheric mass redistribution (Chao and Eanes, 1995). Specifically the secular change of the rate of rotation of the orbital node is closely related to the oblateness of the earth and thus to mass flux in the course of postglacial isostatic adjustment (Rubincam, 1984): the decreasing oblateness is in turn causing an acceleration of the earth rotation, placing contraints on the tidal despinning parameters.

Neither the satellite laser ranging method nor GPS can provide a strictly nonrotating reference since satellite orbits undergo slight, slow evolution with time, the terms of which are not completely understood. However, as VLBI is tied to an ensemble of radiosources — quasars which belong to the most distant astronomical objects — this technique can realize such a quasi-inertial system. The major product of this kind of survey is a group of time series of Earth Orientation Parameters (EOP), specifying deviatoric angles with respect to the adopted precession-nutation model, the position of the pole of rotation and the earth rotation angle (which translates to mean Universal Time, UT1).

Although the satellite techniques can provide short-range variations of EOP's (sub-daily to weekly/monthly), the long-term changes as well as those motions which are most prominently influenced by planetary gravity fields, namely precession and nutation, which also perturb the satellite orbits. Observations of these motions will therefore be the domain of VLBI in all forseeable future.

2.3 GLOBAL CHANGE

Regional tectonic deformation may imply risk to population, industry, and infrastructure in the course of seismic or volcanic hazard. Problems pertaining to this field have been formulated and studied already for a long time, and it appears consequent to utilize the technical and scientific accomplishments towards more refined measurement, promising not only accuracy at greater detail but also greater consistency in the total picture. On the other hand, evidence converged from several geoscience disciplines that our environment is subject to change also on a global scale, where the earth's atmosphere rather than its mantle plays the key role. A number of geodetic methods are already available which are capable to monitor key parameters of global change, namely global sea level (tide gauges in combination with GPS determined positions; satellite altimetry), the ice caps (GPS; satellite altimetry), global water budget (gravity field modelling in conjunction with low-flying satellite orbits). The DOSE program promotes studies to focus on these global change issues, among

others motions in relation with the rebound of glaciated areas, and in particular changes of mean sea level.

The International Association for the Physical Science of the Ocean (IAPSO) promotes a global project to determine the positions of tide gauges with GPS (Carter, 1994). As long-term changes of the gravity field will affect the sea surface absolute gravity measurements are also carried out at existing tide gauge sites. Given the current accuracy, 3 μGal (1 μGal = 10^{-8} ms^{-2}), this is useful in areas which undergo movements at 3 mm/yr or more. Considering the global coverage of mean sea level observation that satellite altimetry can provide (Nerem, 1995), considering further the long-term record of tide gauges that exists and will (must) continue, and realizing that it is a change in relative sea level that implies the environmental threat, GPS is seen as a necessary component to obtaining the evidence.

In the context of global change, basic research in the field of geophysics and geodesy may have an important bearing on the development of civilisation and culture in the broadest sense, in particular through contributions to resolve questions of regional stability and safety, and the formulation of methods for sustainable development.

2.4 POSTGLACIAL ISOSTATIC ADJUSTMENT

One important phenomenon that is prominently seen in vertical motion is the isostatic rebound of the earth to a history of loading events, primarily glacial loading in the course of climatic change during the recent 100,000 yr. Together with response to the corresponding loading history of oceanic counterpart of the total water mass involved in the glacial cycle, the rebound effects entail practically the entire surface of the earth in movement. The motion is supposed predemonantly vertical, but also horizontal components exist. The motion is upward at the order of one centimetre per year in the central uplift areas, those that were glaciated during the holocene. It is downward at rates of some millimetre per year in the so-called forebulge zone, which is peripheral to the glaciated areas, and upward again in the far field beyond 2000 km distance.

As a consequence, relative sea level is falling not only in the centre of Fennoscandia, but also at equatorial latitudes. The question as to whether increasing greenhouse warming prevails and will cause the volume of water in the oceans to grow via a net mass influx from e.g. melting ice caps and thermal expansion cannot be resolved without monitoring the vertical movement of each of the tide gauges.

Earlier evidence for vertical movement is based on primarily tide gauge (mareograph) records and strand line dating. The precision of the for-

mer is roughly one millimetre per year using records of more than 50 (in the case of Stockholm 220) years length (Ekman, 1995; Balling and Banda, 1992; Kakkuri 1986), despite individual readings are affected by air pressure, wind, temperature and salinity. The influence of these perturbations is efficiently supressed when monthly and annual averages are computed. However, the number of tide gauges with histories exceeding 50 or even 100 years is limited and their geographic distribution is not homogeneous. Regionally, differential effects of the uplift pattern, more specifically the decrease of the tilt of the land surface, can be seen in the shoreline history of lakes.

The uplift can also be determined with precise levelling. Here one compares successive epochs of relevelling of the country, which is now being carried out in Sweden, Norway and Finland for the third time since the availability of the technique at the turn of the century (Ekman, 1995; Bakkelid, 1986; Kakkuri and Vermeer, 1985).

In Figure 2-1 we show an isoline map of the uplift field using kriging of only the available numerical data (precise levelling, mareographs, lake shorelines) yielding rugged isolines in areas of data scarcety. (The map renderings in Ekman, 1995, have been admitting older drawings by Ussisso and in other ways been drawing from human expertise; Ekman, 1995, pers.comm.)

Vertical motion components

All terrestrial techniques observe with respect to a reference surface, the sea level, w or its geodetic abstraction, the geoid N. A mareograph senses relative sea level u at the same location r, levelling senses relative uplift differences Δu between pairs of locations,

$$\begin{aligned} u &= r(t_0+t) - r(t_0) \\ &- [w(t_0+t) - w(t_0)] \qquad (Mareograph) \\ \\ \Delta u &= r(x, t_0+t) - r(x, t_0) \\ &- [N(x, t_0+t) - N(x, t_0)] \\ &- \{r(x_0, t_0+t) - r(x_0, t_0) \\ &- [N(x_0, t_0+t) - N(x_0, t_0)]\} \qquad (Levelling) \end{aligned} \tag{2-1}$$

Here, $N(t)$ emphasizes a time dependent geoid, expected to have rates on the order of 1:20 with respect to the vertical movement in the centre of the region[1]. In levelling we notice the need of a reference station or—at least—a regional verification of a unique relative vertical position, i.e. a unified geodetic height system. With the mean sea surface as a reference, these measurements determine **apparent land uplift**, sometimes also called **land emergence**.

[1] off-centre the ratio tends to increase

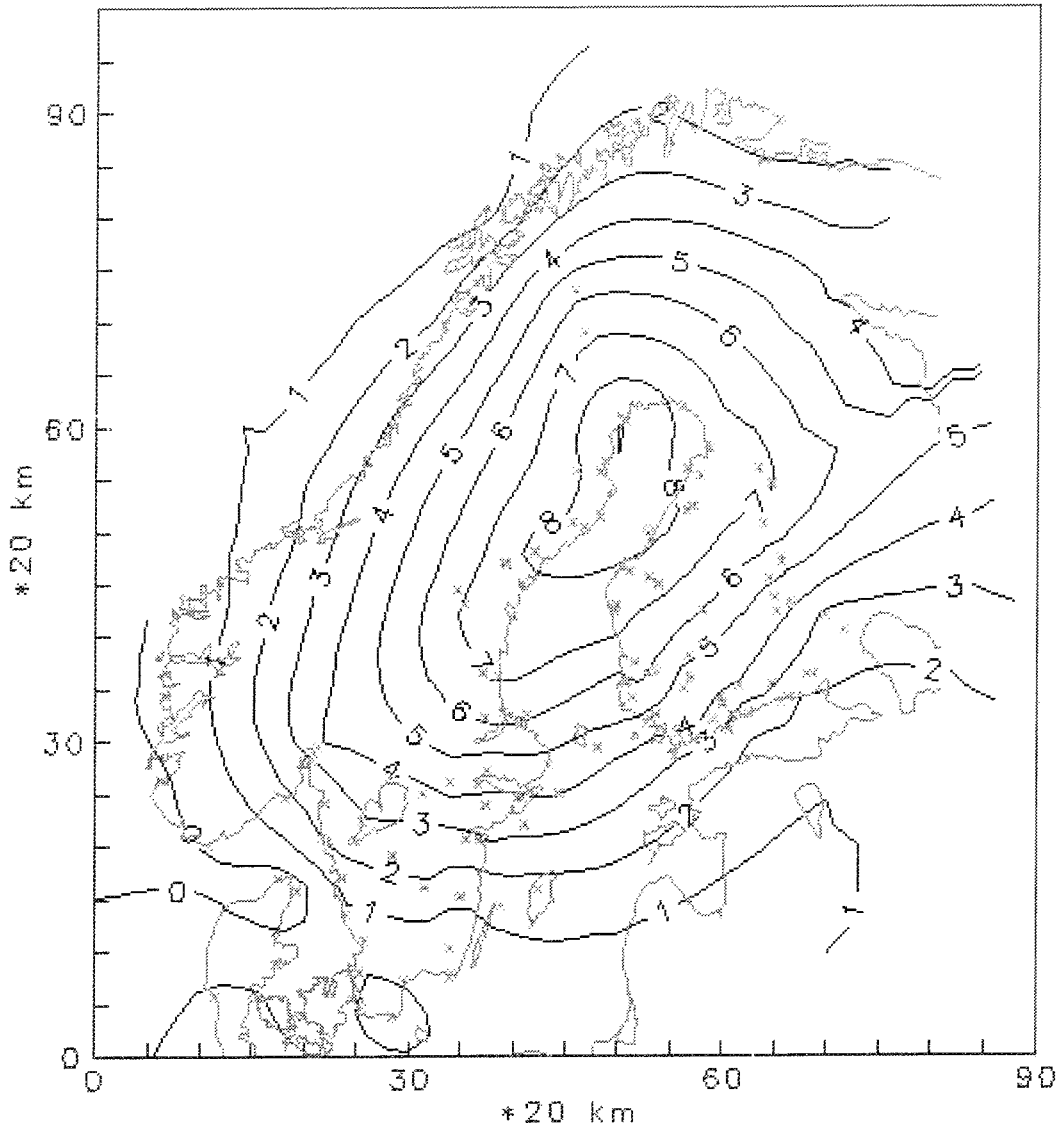

Figure 2-1. *Uplift map based on the available tide gauge and precise levelling data (sites marked by crosses). Observe the large areas where inference of vertical motion is only weakly supported by measurement.*

In contrast, satellite orbit modelling techniques are capable to determine the geopotential separately from height changes at the earth surface. GPS, VLBI and the other space based positioning techniques are independent from the sea surface. One obtains vectorial baseline changes $\Delta\mathbf{u}$

$$\begin{aligned} \Delta\mathbf{u} &= \mathbf{r}(x, t_0 + t) - \mathbf{r}(x, t_0) \\ &- [\mathbf{r}(x_0, t_0 + t) - \mathbf{r}(x_0, t_0)] \quad (GPS) \end{aligned} \tag{2-2}$$

(Some techniques may directly provide single point positions with respect to the geocentre, however usually with much less precision.) To obtain single point position solutions the baseline results are translated and rotated into the global reference system.

The dependence on a geoid or any other vertical reference is only one

disparity between terrestrial and space geodetic data, the latter appearing to have one less problem. However, the situation is more complicated. Even a limited size space geodetic network must be monitored in a global reference system, and the reference positions are allowed to have rates to account for e.g. tectonic plate motion. The translations and net rotations of the coordinate system are relatively weakly determined parameters. Considering translation, one centimetre of geocenter offset may induce a tilt of a 2000 km diameter network of up to 4 mm, but the curvature effects will be less than 0.15 mm. Due to the sphericity of the earth, horizontal plate motion implies a change of baseline orientation in both up and transverse directions; thus, inaccurately known plate motion will affect GPS and VLBI determinations of vertical rates. Along a baseline of length l, mismodelled plate motion δv affects the vertical rate as lv/R where R is the radius of the earth; i.e. 10 mm/yr due to **net plate rotation** with respect to the reference frame can offset true vertical motion by 1.3 mm/yr along a baseline from Hässleholm to Skellefteå. We will return to this problem in Chapter 5.1.1.

Still the situation is considerably improved compared to having the nearest tide gauge as the only reference, and having to rely on hydrodynamic models to account for changes of sea surface topography in the uplift region.

But if one is to combining all efforts, the objective must be to adopt a feasible definition of the geoid, including its time dependence, and to monitor changes of the water level with respect to the geoid (Nerem, 1995, BIFROST project members, 1996).

Observables in spherical harmonics

Most approaches of modelling postglacial rebound treat the problem for a spherically symmetric earth model (Peltier, 1974). Spheroidal surface displacement developed in spherical harmonic base functions (Y_n^m, degree n order m) is then

$$u(\theta,\lambda) = \sum_{nm} U_{nm} Y_n^m(\theta,\lambda)$$

$$v(\theta,\lambda) = \sum_{nm} V_{nm} \nabla Y_n^m(\theta,\lambda)$$

The relation of the motion components u to the load history $\Psi_{nm}(t)$ is formulated with the so-called Love-number functions

$$U_{nm} = h'_n(t) * \Psi_{nm}(t)/g$$

$$V_{nm} = l'_n(t) * \Psi_{nm}(t)/g$$

The *-symbol signifies the convolution of the response functions $h'_n, k'n$ with the load history.

The perturbation of the gravity potential that accompanies the deformation and causes the geoid change is similarly given by

$$\Psi'_{nm} = k'_n(t) * \Psi_{nm}(t)$$

and is a consequence of redistribution of mass in the earth's interior.

Rebound gravity

A consequence of rebound motions are changes in gravity at the surface. Due to the vertical motion u gravity changes by $\delta g = -2g/Ru$. Redistribution of mass in the earth's interior adds a secondary term.

$$\delta g_{nm} = [n\delta(t) + 2h'_n(t) - (n+1)k'_n(t)] * \Psi_{nm}(t) \qquad 2\text{-}3$$

Two subsequent epochs of free air gravity campaigns will relate their results to the two corresponding epochs of the geoid, therefore

$$\Delta g^{(FA)}_{nm} = [(n-2)\delta(t) + 2h'_n(t) - (n-1))k'_n(t)] * \Psi_{nm}(t) \qquad 2\text{-}4$$

According to equation 2-3 δg is gravity measured at the same surface point at two separate times without corrections for height changes necessary. Determination of the interior mass redistribution parameter, however, requires that the vertical motion is known. The free air problem, equation 2-4 has no advantage in that respect, but requires an accurate determination of the geoid.

The project of the land uplift gravity profiles, which has been started around 1966 (Mäkinen et al., 1986), takes advantage of surface gravity measurements and observed vertical movement to determine changes of the geoid and infer mass flow in the asthenosphere (Ekman and Mäkinen, 1995). The amplitude of the geoid anomaly associated with the uplift together with uplift rate estimates can serve as a rough estimate of the total uplift that is remaining.

Within the WEGENER project, absolute gravimeters are used to determine δg at a number of locations in Fennoscandia (Onsala, Mårtsbo (Gävle), Skellefteå, Helsinki, Vaasa, Trysil, Tromsø).

Modelling approches

Equations of motions that compute the response functions from radially structured earth models have been solved by a number of authors The literature resulting from the roughly fifteen groups that have produced detailed models with realistic results during the recent fifty years in geophysical journals is extensive. We refer only to some of the latest publications—interested readers may use the mention as an entry (Lambeck, 1993, 1993a; Mitrovica et al., 1994; Peltier, 1995; Spada et al., 1992; more references follow below).

Elastic structure and density profiles are usually adopted from a seismological model (e.g. PREM. Dziewonski and Anderson, 1981). and these parameters are relatively well constrained. The long time-scales which are encompassed in the glacial loading problem. however, admit motion due to the rheological properties of primarily the earth's mantle. The generally adopted view considers a set of exponentially decaying modes with time scales between 10^3 and 10^5 years, the dominating modes near 8000 yr. The exponential decay is intimately related with linear viscoelasticity (Mitrovica and Peltier, 1993; Mitrovica and Davis, 1995).

Thus, the major issue is the determination of mantle viscosity from model computations and parameter inversion from comparison of predictions and observations (mostly historical heights of mean sea level and present-day rates of change; in some cases gravity anomalies; rarely rates of gravity change).

Many of the theoretical models have been adjusted with respect to the relative uplift history in Ångermanland where a long geological record is available. Present day rates of relative uplift (Ekman, 1995) are largely compatible with the total relative uplift, given the uncertainty of sea level changes in the early stages of the rebound, 8000 to 10,000 yr BP. A slight northward migration of the uplift center can be discerned (Ekman, 1995). A general trait in model inversion results is that additional observations from the periphery of the glaciated regions would help constrain viscosity profiles and other rheological parameters, lithospheric thickness etc.

The role of the lithosphere in these models is generally a modification of the forces which drive the system back to isostatic equilibrium. The flexural rigidity of the lithosphere prevents predominantly short wavelength loads to excite large motion. Systematic searches for parameter sensitivity in inverse solutions show that there is a trade-off between upper mantle viscosity, lithospheric thickness and lithospheric flexural rigidity (Mitrovica et al., 1994). In other words the impact of the lithosphere can be attributed to a few key parameters, detailed structure cannot be resolved.

Additional issues that have been discussed by modellers are

- Spherical models contra half-space models (Wolf, 1985);
- Effect of compressibility (Wolf, 1991);
- Radial symmetry contra lateral heterogeneity (mainly concerning viscosity) (Gasperini et al., 1990; Breuer and Wolf, 1995);
- Rheology - transient (Burgers body, generalized Maxwell) contra steady-state (Mueller, 1986; Yuen et al, 1986; Rümpker and Wolf, 1996);

- The effect of oceanic mass redistribution as a secondary isostatic rebound process (Mitrovica and Peltier, 1991)
- Adiabaticity in the mantle (Fjeldskaar and Cathles, 1984).

Inferred mantle parameters are discussed in the light of models for the generation of gravity anomalies due to mantle convection and plate tectonics, seismic tomography and implications of mantle viscosity and lithosphere elasticity on the geological timescale.

Rarely found are computations of stress at depth levels where—at least indirect—evidence exists, namely near the surface or in the brittle part of crust. The problem is whether analysis of stress measurement could discriminate the pattern in a background of tectonic origin, of ambient sources and localisation effects.

Much of the discussion reflects the uncertainty of individual tide gauges, markers of sea level history, age dating methods, assumed glacial mass loading histories. Construction of the ice load history (the spatial distribution during the succession of stages) fits practically the same data set, sea level curves, as the rebound process.

This beds for an inherent problem in self-consistency, circular argument. The history and spatial features of recent ice load models (ICE-4G, Peltier, 1995; ICE-3G, Tushingham and Peltier, 1991) have been reconstructed at high detail. They have been inferred using the same, comparitively simple earth models that are also used in the inversion for viscosity structure. By simplicity we mean specifically that the earth models assume laterally homogeneous steady-state rheology. Contemplating that laterally heterogenous viscosity and/or transient viscosity may play a significant role, the spatial and temporal evolution of the load will tend to absorb those transients and irregularities. A virtual self-consistency which operates on a grantedly large but limited data set can only be falsified by presenting new, reliable observations, preferably of a new kind.

We hope that determinations of horizontal movement from GPS will play this role. First attempts to monitor the movement using VLBI have already been started (James and Lambert, 1993; Mitrovica et al., 1994; Peltier, 1995) but the network is somewhat sparse and misses details. Especially in the uplift centres stations do not exist.

A case study for lateral heterogeneity has recently been published by Breuer and Wolf (1995). At least in the case of the large ice-covered regions, attempts to resolve laterally heterogeneities in mantle and lithosphere parameters or nonlinear viscosity appear still to be premature. Breuer and Wolf (1995) have considered the regionally more confined ice loading problem in Spetsbergen. It appears to provide clearer clues as to

the importance of lateral variations at the continental shelf edge. Horizontal motion is seen to be sensitive to the viscosity of the upper mantle and thus discriminate the trade-off of lithosphere thickness against viscosity.

2.4.1 Inferring strain

A conceptually clear separation of deformation and rigid-plate orientation effects can only be obtained if the field of displacement rates is analyzed in terms of strain and rotation. The basis of this is the fundamental separation of velocity fields into strain-rates and infinitesimal rotation parts

$$\Delta u_i = \sum_j \left[\frac{1}{2} \left(\frac{\partial u_i}{\partial x_j} + \frac{\partial u_j}{\partial x_i} \right) + \frac{1}{2} \left(\frac{\partial u_i}{\partial x_j} - \frac{\partial u_j}{\partial x_i} \right) \right] \Delta x_j \qquad 2\text{-}5$$

or in vector-tensor notation

$$\Delta \mathbf{u} = \left(\dot{\mathbf{E}} + \Omega \right) \Delta \mathbf{x} \qquad 2\text{-}6$$

where the target quantities are the elements of the strain rate tensor $\dot{\mathbf{E}}$ and the rotation matrix Ω. The former requires regional parametrization since measurements will generally be sparse and since the derivatives can be approximated by finite differences only in a very crude sense.

A parametrization $\mathbf{U}_n$, $n \leq N$ of $\mathbf{u}$ together with a minimum strain energy condition can be formulated in general as

$$\mathbf{u} = \sum_n \sum_i \hat{\mathbf{i}} D_{ni} U_{ni}(\mathbf{x}) + \begin{pmatrix} 0 & \omega_z & \omega_y \\ -\omega_z & 0 & \omega_x \\ -\omega_y & -\omega_x & 0 \end{pmatrix} \mathbf{x}$$

$$E_\epsilon = \sum_{(ij)} C_{ij} \int_{\mathcal{R}} \left(\sum_n \partial_{ij} \mathbf{U}_n \right)^2 d\sigma$$

where ∂_{ij} denotes the differential operator that yields the strain component ij from displacements as in Equation 2-5, C_{ij} are apparent viscosity parameters, $\lambda \delta_{ij} + 2\mu$ for bulk and shear deformation, and the integral is to be performed over the region $\mathcal{R}$.

The $3 \times (N+1)$ parameters D_{ni} and ω_x, ω_y, ω_z are to be solved e.g. by least-squares

$$w \sum_{pq} \left\{ \dot{\mathbf{b}}^{(pq)} - \left[\mathbf{u}(\mathbf{x}^{(q)}) - \mathbf{u}(\mathbf{x}^{(p)}) \right] \right\}^2 + E_\epsilon = \min$$

from the baseline rate observations $\dot{\mathbf{b}}^{(pq)}$, the fit of which is weighted in as a Lagrange multiplier w.

There is a certain degree of subjectivity in such an analysis, especially concerning the type of base functions $\mathbf{U}_n$ and the outline of the region. We expect that strain rate analysis becomes meaningful only after several years of network operation, leading to improved separability of seasonal cycles from steady deformation rates, more homogeneous data coverage with respect to time, and damping the effect of perturbations at the sites and receiving conditions during the first phases of the experiment until the system is totally settled.

2.4.2 Postglacial contra tectonic movement

Debates exist as to the importance of postglacial rebound for stress and stability in the Fennoscandian shield. Generally the rate of seismic energy release in Fennoscandia is low compared with e.g. the centre of Europe (Ahos and Uski, 1992). Several authors note that stress measured in boreholes (e.g. Stephansson et al, 1991) or seismically inferred stress (e.g. Gregersen, 1992) in Scandinavia shows little resemblance with stress patterns expected from postglacial rebound (Müller et al., 1992). Instead, the stress field in Fennoscandia like the one on the opposite side of the North Atlantic spreading zone appear largely to be aligned with respect to the plate tectonic setting (Adams, 1989).

Turning to seismological evidence the presence of earthquakes in the interior of a craton undergoing isostatic rebound requires a plausible mechanism for the generation of sufficient deviatoric stress. This is difficult in either case since tectonic stresses are imposed at distant boundaries, and postglacial rebound in simple crustal structure generates a specific stress pattern which is difficult to reconcile with actually observed events and inferred source mechanisms, notably reverse faulting events (Wahlström, 1989). Modifying effects like topography or weak zones must be invoked (e.g. Hasegawa, 1991; Hasegawa and Basham, 1989; Talwani, 1989).

Away from the continental margin, stress levels due to ridge push or postglacial flexure appear comparable at a level of 10 MPa (Stein et al., 1989), but advocates for the prevalence of either source of stress generation exist, proposing additional sources stress in either one of the settings. Notably Muir Wood (1993) argues in favour of predominantly post-glacially induced seismicity in Fennoscandia. Stein et al. (1989) are doubtful as according to their models sediment loading would generate stresses along the continental margins at a 100 MPa level, yet little correlation is found between seismicity and locations of heavy sedimentation.

If the Mid Atlantic Ridge and the collision zones between the European, African and Arabian plates are considered to be the nearest regions with

prevailing tectonic activity, then experience from CDP and similar space geodesy projects suggest that a shield area like Fennoscandia being near a passive continental margin will only show low levels of tectonic deformation. On the other hand, detailed models have been presented (Talbot and Slunga, 1989) that picture the shield as being squeezed in a vice. The jaws of this vice have complicated shapes, for instance along the Mediterranean boundaries, but also in the complicated system of ridge segments and transform faults to the north of Iceland. Iceland itself is situated on the top of a crustal productivity anomaly. As an effect major shear zones are predicted to develop in the continent. However, quantitative upper limits for the movements are not stated while the maximum age of the features hints at rates of 0.1 mm/yr or less.

An interesting prediction of horizontal shear rates has been made by Slunga (1991) based on moments, mechanisms and recurrence of earthquakes in southern Sweden. It appears that during one year more than 500 km of fault length may move by one 1 mm. Along the fault, on the average 25 km long segments would be associated with one larger earthquake. On the average twenty such events occur per year, however entangling only minor namely the locked sections of the fault. The coseismic slip during one event is on the order of 1 mm. The argument for having the total fault length move is closed by asserting a rate of aseismic to seismic slip of 20,000:1. An indication that a value this high is yet not unreasonable refers to the seismicity of Finland and to the deformation of terrestrial networks in Finland (e.g. Kakkuri, 1988). This work has more recently been reevaluated (Kakkuri and Chen, 1992).

In this latter work millimetre to centimetre per year relative movement between tectonic subunits is inferred. However, the Finnish data consists of heterogeneous observations, triangulation in the first-order skeleton network proceeding during 40 years, and three to four remeasurements by trilateration using different instrument types with different accuracies inside the triangulation loops. The analysis of the combined data was difficult; it had to be separated into individual adjustments from which rates were concluded, rather than determining positions and rates together for a unique epoch in a single stage of network adjustment. Even the largest baseline rates given in Kakkuri and Chen (1991) are significant only at the one sigma level. If one of the concluded strain rates, 0.15 ± 0.07 ppm/yr, had been persistent over the last 2 Myr, a time period during which alpine collision and North Atlantic spreading occurred at roughly uniform conditions, distortion at the 40 percent level would result. The rates of movement between the blocks which Kakkuri and Chen (1991) discern reach 20 mm/yr, a level usually found only across mayor tectonic boundaries.

Active processes at the boundary of the shield have been suggested, like onset of subduction along the Norwegian continental margin, but also less dramatic ones like sediment loading on the shelf which activates weakness

zones and fault complexes (Bungum, 1989). This work also reports of seismicity in conjunction with the Senja and Jan Mayen fracture zones, zones which may be seen as continuing into the shield where they widen to form shear lenses and duplex structures (Talbot and Slunga, 1989).

Tertiary uplift along the Norwegian coast, extending into the Caledonian Mountain belt has been concluded from studies of sediments and topography using a model that incorporates crust and mantle rheology and deep crustal rock phase change (Riis and Fjeldskaar, 1992).

On-going motion has been claimed as evident in regionally limited areas like in the Lappijärvi area of mid western Finland. Referring to the theory of elasticity, specifically the principle of Saint Venant, one might expect that structures having a typical horizontal extent of x km would require a source region at a depth $\leq x$.

Considering the effective thickness of the lithosphere for processes on the time scale of 10^4 yr at low strain rates ($< 10^{-16}$ s^{-1}) to be at least 200 km (cf. Cloetingh and Banda, 1992), a network with 200 km mesh width is adequate to sample the gross lithospheric deformation. This is certainly applicable to the vertical motion field associated with postglacial rebound, with a reservation concerning the 0.1 to 0.5 mm/yr deviatoric features on scales less than 100 km which can be seen in Ekman (1995). Assuming these to be real or at least representative, it appears reasonable to consider separate geodetic networks depending on the scale size, 200 km being a starting point relevant for the lithosphere.

Spatially more concentrated features like weakness zones, subsidence lenses, visible faults that extend to the surface require concentrated efforts in dedicated local studies. Several of such projects are under way at KTH Stockholm and at Uppala University.

2.4.3 Potential contribution of GPS

To consider the use of GPS for the vertical and horizontal motion, prospectively connecting the international tide gauge network, appears in its prospect fully in line with the aims of DOSE. It combines tectonics, postglacial dynamics and applications to mean sea level. Starting with baselines of at least 200 km, a network diameter extending to some thousand kilometres would require less than 50 stations. Considering a timeframe of say ten years, however, one finds that this demands extremely high precision, in fact at levels which currently cannot be garanteed in regular field campaign experiments, referring to the repeatabilities of similar studies for tectonics. Using the estimate of Coates et al. (1985) of

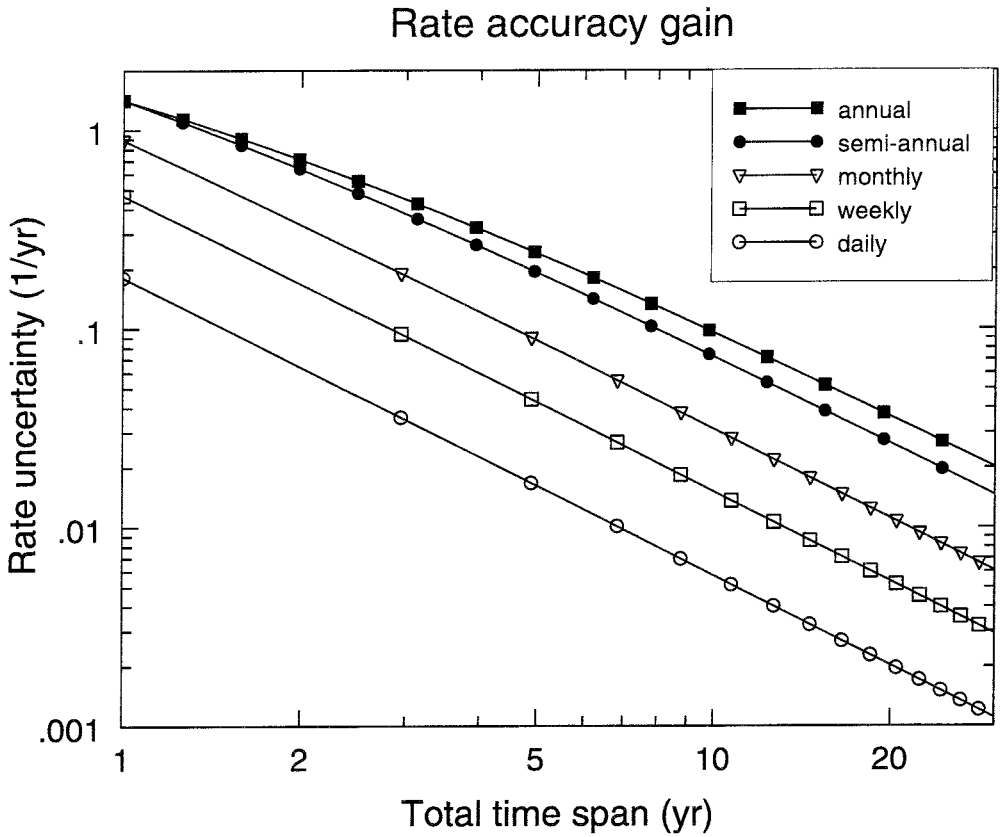

Figure 2-2. *Gain in accuracy versus total time of a network experiment, repeated at various rates. Shown is the rate uncertainty assuming unity uncertainty in each single experiment. If experiments are correlated over time, a greater effective repetition interval must be assumed. In daily repeated sessions correlation typically persists for two to three days.*

the rate uncertainty σ_r

$$\sigma_r = \frac{\sigma_m}{T}\sqrt{\frac{12T/\Delta t}{(1+T/\Delta t)(2+T/\Delta t)}} \qquad 2\text{-}7$$

where T is the total time span and Δt the repetition interval of observations, and σ_m the single position uncertainty. Whence, 4 (8, 20) years of daily (weekly, semiannual) analysis results are needed to obtain 0.1 mm/yr precision for vertical movement (cf. Fig. 2-2) if σ_m is 5 mm.

Operating a network continuously offers major benefits. Primarily there is the opportunity to concentrate on environmental and instrumental error sources and to explore the technical limits, work which draws from a large amount of data collected at short, regular intervals. At the same time the risk can be kept low to introduce heterogeneity or failure in the instrument setup since transport, re-installation, and conditions prone to human error can largely be avoided.

Prerequists are good in Scandinavia as e.g. access to bedrock is almost always given. Also, site stability is then hardly incurred by seasonal

ground water fluctuations or other problems typical for thick, diagenetically unsolidified sediment layers.

2.4.4 VLBI AND GPS TOGETHER

GPS observation points have been established in close colocation with all geodetic VLBI observatories. The European VLBI baselines now include Ny Ålesund, Spetsbergen. Spetsbergen contains another postglacial rebound centre within the European plate. Horizontal motion within the subnet of colocated VLBI and GPS sites is prospectively sensitive to Fennoscandian rebound owing greatly to the existence of the sites at Onsala and Ny Ålesund. However, long records entirely in the same plate with no major tectonic zone intervening exist only for the baseline Onsala to Wettzell.

The colocated sites define an outer network and provides constraints on the large spatial scale, actually in two ways: (1) colocated techniques at a number of sites will mutually strengthen parameter solutions; (2) inference of motion in post-analysis interpretation will also obtain contraints from the large-scale network.

3 HISTORICAL REVIEW: ONSALA

Geodetic research at the Onsala Space Observatory was introduced by Very-Long-Baseline Interferometry (VLBI). It has been the main component of the space geodesy research program for more than two decades. The first geodetic VLBI experiment to Onsala, using the Mark–I data acquisition system at the 25.6 m antenna, was carried out in April 1968 (Whitney, 1974). This was actually the first experiment using the bandwidth synthesis technique (Rogers, 1970). The results from the Mark–I experiments have been summarized by Ryan et al. (1986).

The first experiment using the Mark–III system at Onsala was carried out in November 1979. This experiment had only two channels recorded at S-band (and five at X-band) and it turned out that it was impossible to obtain accurate ionospheric delay corrections. In July 1980 this mistake was corrected (three channels were used at S-band and four at X-band) and the precision of the estimated intercontinental baseline lengths reached the cm-level. In this first experiment and in many to follow during the next seven years the X-band was received at the new radome-enclosed 20 m antenna, whereas S-band reception stayed at the larger, old telescope 600 m west of the new one.

Thereafter, many improvements have been added to the geodesy VLBI technique. Below we will discuss the most important ones, and when they were implemented at Onsala. We will also summarize the VLBI observations so far carried out at Onsala during the Mark–III era and give a couple of examples of the geodetic results from the these experiments.

In this chapter we will also review in short the GPS activities until the building-up of SWEPOS. This latter phase will instead be covered in chapters 4 and 5 of this report.

Towards the end of this chapter we report on recent occupations by absolute and relative gravimeters at the Onsala site. These independent measurements are important for the interpretation of the variations of the local vertical position inferred from the space geodesy techniques of VLBI and GPS.

3.1 VLBI—Technical developments at Onsala 1980–date

3.1.1 The telescopes and the feeds

The original Mark–III setup was to use the 25.6 m antenna for reception of the S-band signals and the 20 m, radome enclosed, antenna for the X-

band signals (Lundqvist, 1984). Because the 25.6 m antenna could not operate during wind speeds >13 m/s a significant part of many experiments was lost at Onsala. Therefore, the S-band operation was moved to the radome enclosed 20 meter telescope in March 1987 using a dichroic surface design to allow for the two (S- and X-band) beams to be pointed in the same direction. A couple of years later, the feed system was improved using a new design of the dichroic surface (Jaldehag, 1992).

A large upgrade of the 20 m antenna performance started in 1991 which included a new drive system allowing for faster slewing rates and new panels of higher surface accuracy. The new steering system, including numerically controlled motors, resulted in slewing speeds of 2.4 °/s in the azimuth coordinate and 1.0 °/s in the elevation coordinate compared to the previous 0.83 °/s in both coordinates. The actual maximum speeds are significantly higher but the new values take into account part of the acceleration and retardation cycle. The rest of this effect is taken care of by the "setup" times in the scheduling program. The improvement of the rms surface accuracy from approximately 0.23 mm to 0.13 mm has little impact on the S/X-band aperture efficiency ($\approx$ 0.5% improvement at 9 GHz). The first experiment using the new drive system was carried out in January 1992.

A second part of the antenna upgrade is still in the design phase. This may result in two new subreflectors—one smaller for high frequency radio astronomical observations and one larger for S/X-band observations—and the goal is to significantly improve the aperture efficiency of the antenna at both S- and X-band. The present design has been evaluated in detail by Jaldehag (1992) and Jaldehag et al. (1993).

In 1980 parametric amplifiers were used at both X- and S-band, with total system temperatures, including a typical atmospheric contribution, of 180–200 K and 80–90 K, respectively. Cooled FET amplifiers were installed in the 20 m telescope in September 1986 reducing the total system temperatures to 80–100 K and 50–65 K, respectively. At first, only the X-band part was used but after the move of the S-band to this telescope in March 1987 (mentioned above) also the S-band part of the receiver could be used.

Cooled HEMT (High electron mobility transistor) amplifiers were installed in the fall of 1991. The total system temperatures in the zenith direction and for fair weather are now approximately 70–90 K at X-band and 45–60 K at S-band. The major contributions to these temperatures are from losses and ground noise pick-up caused by the feed system and the radome. The HEMT receiver was first used in January 1992.

Concern about the deformation of the concrete foundation of the antenna was raised recently. This pillar is 12 m tall and supports the 20 m telescope. Inside the radome it is exposed to the daily and seasonal tem-

perature cycles, which might introduce height variations and tilts on the order of millimeters and thus introduce bias in diurnal and annual parameters. In December 1994 temperature sensors were placed at strategic points in the pillar. The observations are recorded in a small computer. The analysis of one year of data shows yearly variations of 4 mm peak-to-peak. Tilts and daily variations are on the sub-mm level (Carlsson, 1996).

3.1.2 The Mark–III data acquisition system

Compared to the first Mark–III setup at Onsala in November 1979, another 7 channels (video converters) were added to the previously incomplete system before a VLBI campaign in June 1982. Since then the standard setup has been to record 8 channels at X-band and 6 channels at S-band.

A high density tape drive was installed in September 1990. The result of this improvement was that the number of tapes needed for an experiment was reduced with a factor of twelve.

The maximum possible spanned bandwidth was increased when the HEMT amplifiers started to be used in January 1992. This upgrade also required an additional IF distribution unit (often referred to as IF3). The wide band recording mode at X-band presently spans 720 MHz whereas the standard setup is 360 MHz wide.

3.1.3 The water vapour radiometer (WVR)

Microwave radiometry has been used continuously during VLBI experiments since the first successful Mark-III campaign in July 1980 in order to provide independent estimates of the excess propagation path caused by atmospheric water vapour (Elgered, 1993). Instrumental comparisons have been carried out at the Onsala site with the NASA owned J03 WVR in the summer of 1988 (Kuehn et al., 1993) and with two WVRs from ETH, Zürich, during October 1992 (Bürki and Elgered, 1993).

The impact of using WVR data for correction of the wet propagation delay has been studied for the experiments carried out during the period 1980–1990 (Elgered and Davis, 1993). A couple of examples from this study will be presented below in the section on VLBI observations (Figures 3-1 and 3-2).

The WVR was upgraded during the time from October 1990 to February 1992. Instead of controlling the data acquisition from the Mark–III "Field System" computer a more flexible, PC based, system was built

which allow faster slewing and more frequent data sampling. This is an advantage in general but especially it will imply improved estimates of spatial gradients in the wet delay (see. e.g., Davis et al., 1993).

3.1.4 Observations

We will give a brief summary of the geodetic Mark–III VLBI experiments carried out at the Onsala Space Observatory from 1980 through November 1995. Table 3-1 lists the baselines observed to the Onsala site and, thereafter, we comment on the different networks with Onsala participation. We have included experiments with data of acceptable quality from more than half of a 24-hour session. Another twenty or so experiments were planned, or only partly carried out, during this period. Most of these were lost due to strong winds before March 1987 when the S-band operation was moved to the radome enclosed 20 m telescope. After that date it has mainly been problems with the antenna drive system or the hydrogen maser that have forced us to cancel observations.

Individual campaigns

We detail a subset of campaigns with a primary focus on geodesy. The first group is devoted primarily to plate tectonics and the second group (MERIT *ff*) to earth orientation.

US–Onsala, 15 experiments, 1980–1983, was the first network observed using the Mark–III system including Haystack, Fort Davis, Owens Valley, and NRAO in the US and Onsala in Sweden. These were the first measurements of contemporary motion between the North-American and the Eurasian plates (see, e.g., the early paper by Herring et al. (1986a). From 1983 to 1987, 27 experiments continued on this baseline under the **TRANS-ATLANTIC** title with emphasis on monthly experiments in difference to the earlier long-duration campaigns once to twice per year. Wettzell was added in January 1985 and Westford replaced Haystack in May 1985. The 11 **NORTH-ATLANTIC** 1984–1987 sessions extended TRANS-ATLANTIC with the addition of Fort Davis, Owens Valley, and later on Mojave. Here, a deformation transect of the North American continent was obtained. Successor projects along this line were **EAST-ATLANTIC**, 7 experiments 1988–1989 (Westford, Onsala, Wettzell, Richmond (Fl.), Medicina (Italy)), and **WEST-ATLANTIC**, 3 experiments 1988, (Wettzell, Onsala, Westford, Mojave, and Fort Davis).

Between 1985–1995, 14 **POLAR-N** have been carried out approximately twice per year, involving Fairbanks, Westford, Kashima, Mojave, Wettzell, and Onsala. The network configuration has slowly changed over the years and in 1993 the sites were: Fairbanks, Westford, Kashima,

Table 3-1. *VLBI baselines including Onsala measured at least three times during 1980–1995 using the Mark-III system.*

Onsala to	Number of baseline measurements per year																Total
	80	81	82	83	84	85	86	87	88	89	90	91	92	93	94	95	
Haystack, MA, USA	19	8	8	7	7	3	1	-	-	-	1	2	2	1	-	-	59
NRAO, WV, USA	-	4	4	-	-	-	-	-	-	-	-	-	-	-	-	-	8
Owens Valley, CA, USA	17	4	10	-	2	3	3	3	-	-	-	-	-	-	-	-	42
Fort Davis, TX, USA	16	9	11	11	10	11	13	14	15	13	12	-	-	-	-	-	135
Effelsberg, Germany	7	-	-	1	-	-	-	-	-	-	-	-	1	1	2	1	13
Chilbolton, England	7	-	-	-	-	-	-	-	-	-	-	-	-	-	-	-	7
Westford, MA, USA	-	5	12	11	10	19	23	23	21	16	14	8	10	15	12	11	210
Mojave/DSS15, CA, USA	-	-	-	-	1	5	5	5	5	-	1	8	10	1	2	1	44
Wettzell, Germany	-	-	-	4	9	21	23	21	20	23	15	11	25	24	15	13	224
Richmond, FL, USA	-	-	-	1	5	8	10	11	16	13	12	8	1	-	-	-	85
Fairbanks, AL, USA	-	-	-	-	-	2	2	2	2	1	2	2	2	21	12	12	60
Kashima, Japan	-	-	-	-	-	2	2	2	2	1	2	1	2	1	2	1	18
Medicina, Italy	-	-	-	-	-	-	-	-	5	1	3	4	7	4	8	6	38
Madrid, Spain	-	-	-	-	-	-	-	-	-	2	3	3	5	3	4	9	29
Noto, Italy	-	-	-	-	-	-	-	-	-	1	3	1	2	1	2	4	14
Tromsø, Norway	-	-	-	-	-	-	-	-	-	3	-	-	4	-	-	-	7
Metsähovi, Finland	-	-	-	-	-	-	-	-	-	4	-	-	-	-	-	-	4
La Silla, Chile	-	-	-	-	-	-	-	-	-	-	3	-	-	-	-	-	3
Matera, Italy	-	-	-	-	-	-	-	-	-	-	2	2	5	9	5	4	27
Kokee Park, HI, USA	-	-	-	-	-	-	-	-	-	-	-	-	-	11	10	10	31
Fort Davis (VLBA), TX	-	-	-	-	-	-	-	-	-	-	-	-	-	11	10	6	27
Los Alamos (VLBA), CA	-	-	-	-	-	-	-	-	-	-	-	-	-	11	10	6	27
Mauna Kea (VLBA), HI	-	-	-	-	-	-	-	-	-	-	-	-	-	-	2	1	3
Algonquin Park, Canada	-	-	-	-	-	-	-	-	-	-	-	-	-	6	-	-	6
Ny Ålesund, Spetsb	-	-	-	-	-	-	-	-	-	-	-	-	-	-	4	7	11
Hartebeesthoek	-	-	-	-	-	-	2	2	1	-	1	-	-	-	-	2	8
Crimea, Ukraine	-	-	-	-	-	-	-	-	-	-	-	-	-	-	6	4	10
Total[a]	66	30	45	35	44	74	84	83	87	78	74	50	76	120	106	98	1150

[a] The low number of baselines measured during 1991 was caused by extensive upgrade work on the 20 m telescope (making it impossible to operate the antenna for long periods during September, 1991 – March, 1992). Because of the European mobile VLBI campaign during the summer of 1992 there was still a relatively large number of baselines observed this year.

Medicina, and Onsala. The purpose of these experiments is to tie sites together around the pole and thereby also different VLBI networks which together include sites that have poor common visibility of the extragalactic sources.

The dedicated **EUROPE** network—including Noto, Matera, Medicina, Madrid, Wettzell, and Onsala—started to observe in 1990 and has been scheduled 3–6 times per year, currently with a record of 23 experiments. Additionally, the Effelsberg antenna has been used occasionally during the last couple of years. The geodetic results from these experiments have been proven to be of high quality (see, e.g., Rius et al., 1992).

An effort of **EUROPE MOBILE** experiments proceeded 1989, 1992, and 1993 with 22 sessions. During the summers of 1989 and 1992 Onsala participated as a base station to support the MV–3 and MV–2 occupations at different European sites. Metsähovi and Tromsø was observed by MV–3 in 1989 and Kirchberg, Karlsburg, Høfn, and Tromsø by MV–2 in 1992. Furthermore, in May 1992, one 24-hour experiment was made when MV–2 was located at the Onsala site, approximately 20 m from the permanent GPS tracking station. The vector estimated from the VLBI data has formal one-sigma errors of 2 mm in the horizontal components and 4 mm in the vertical component (Potash, 1992). The disagreements with conventional surveys and GPS measurements are 2–3 times as large. In January 1992 and in March 1993 Onsala also participated in IRIS-A experiments which included the mobile station MV–2 at Trysil, Norway.

A geodetic baseline between Onsala and the SEST antenna on La Silla in Chile was measured a few times during April and May 1990 (Jaldehag, 1992).

MERIT, 14 experiments, 1980 (Monitor Earth-Rotation and Intercompare the Techniques) "short campaign", during two weeks in September and October 1980, used the US–Onsala network and alternatingly Effelsberg in Germany and Chilbolton, England, as additional stations in Europe.

The 29 **POLARIS** (POLar-motion Analysis by Radio Interferometric Surveying) experiments 1980–1984 had the major goal of study earth orientation monitoring. In the beginning an experiment was carried out every second week. Originally only the Haystack and the Fort Davis sites were regularly available and it was only when a third station joined the network that it was possible to estimate all three earth rotation parameters (the x- and y-components of the pole and the rotation rate). Onsala participated approximately once per month. Westford replaced Haystack in 1981 and then the experiments were scheduled once a week. The Richmond site in Florida was added to the network and participated on a regular basis starting in 1984.

The **IRIS-A** experiments. 90 in number during 1984–1993 continued POLARIS. scheduled at every fifth or seventh day. As in the POLARIS network Onsala has participated in these experiments regularly (approximately once per month). The stations in the network have varied but most often they were: Westford. Richmond. and Fort Davis/Mojave/Fairbanks. in the US. and Wettzell in Germany. The Fort Davis antenna in Texas was closed in 1989 and replaced by Mojave in California. Mojave in turn was closed in 1992 and replaced by Fairbanks, Alaska.

Starting in May 1993 the IRIS-A experiments were replaced by **NEOS-A** and **NEOS-B** experiments, 15 sessions 1993–1994 (NEOS = National Earth Orientation Service). The NEOS-A observes once per week using an identical network each time which makes it impossible for stations such as Matera and Onsala to participate on a monthly basis. Instead a separate network, NEOS-B, has been defined which observes at approximately one month intervals. The stations used have been: Algonquin Park, Fairbanks, Green Bank, Matera, Onsala, and Wettzell. As a side-effect of NOAA passing responsibility for NEOS to USNO, NEOS-B has been discontinued at the beginning of 1995.

As plate tectonics studies shifted towards regionally more refined projects VLBI obtained the role of a large-scale network stability custodian. This the border between earth orientation and plate tectonics appliciations started to disappear. In this context NASA's **R&D Network** has been operating, comprising 27 monthly experiments since 1993. The 1995 R&D network consisted of Fairbanks, Fort Davis (VLBA), Kokee Park, Los Alamos (VLBA), Onsala, Westford, and Wettzell, i.e. an exceedingly global network, striving for pushing the limits of parameter estimation of both baseline vectors and reference system orientation. By coordination with NEOS, NAVEX and VLBA, two week-long **CONT** sessions have been performed in 1994 and 1995, in which Onsala was observing during the whole time span. The purpose of the CONT sessions is to assess the consistency individual VLBI-networks as regards short-term variations primarily in earth rotation. Discussions on the demonstrated repeatabilities using different networks have been presented by, e.g., Rogers et al. (1993) and MacMillan and Ma (1994).

Onsala participation currently

By the beginning of 1996 Onsala participates in the CONT, EUROPE, and GTRF networks. The typical precision of estimated baseline lengths is now well below 1 cm and the typical repeatability of estimated trans-atlantic baselines is at the 1 cm level over time periods of many months.

3.1.5 VLBI results

Results from the two most frequently observed baselines to Onsala are shown in Figure 3-1 (Onsala–Wettzell) and Figure 3-2 (Onsala–Westford) together with NUVEL-1 predicted rates for the time period 1982–1995.

Results are presented for the baseline to Westford in Figure 3-3, demonstrating the difference in the analysis between the use of WVR data and estimating a Markov process for the wet propagation delay at the Onsala site (Elgered and Davis, 1993). Here we have used only that subset of the solutions which were analyzed with roughly the same methods (until the hardware change in WVR October 1990).

In each method an optimum elevation cut-off angle is determined by the criterion to minimize the weighted RMS of the fit. These cut-off angles are wastly different. Using WVR data, the inferred wet delay is accurate primarily at high elevations, giving an optimum cut-off between 17 and 20°. Estimation of the tropospheric delay from the observations themselves, on the other hand, requires low elevations down to 5° as these carry the effect most strongly.

In general we conclude that the formal one-sigma uncertainty of the estimated baseline lengths as well as the repeatability improve with time regardless of which method is used for the atmospheric corrections at Onsala. It is seen that the short time repeatability is much better than that over longer time scales. The impact of using WVR data is a lowering of the error level mostly during the later periods, presumably in the course of other critical error sources having been brought under control.

In the case of the baseline to Wettzell we note that the estimated rates are -0.2 ± 0.2 (1σ) mm/yr for the WVR solution and -0.7 ± 0.2 (1σ) mm/yr for the Markov solution. The expected change in the baseline length due to the postglacial rebound is of the order of -1 mm/yr (Onsala towards Wettzell) (Mitrovica et al., 1994). Clearly systematic errors prevent us from claiming to have detected such a motion today.

The Onsala–Westford baseline is more than six times longer than that to Wettzell and is, therefore, more affected by atmospheric errors as the local verticals at the endpoints project more into the baseline's length component (Herring, 1986)). Systematic effects in the estimated baseline lengths are clearly seen in the WVR solution, c.f. Figure 3-3. The estimated rates are 17.6 ± 0.3 (1σ) mm/yr for the WVR solution and 14.8 ± 0.3 (1σ) mm/yr for the Markov solution. If we, however, only use the 1988–1990 data both rate estimates are consistent ($\approx20\pm2$ (1σ) mm/yr) and in reasonable agreement with the geological estimate from the NUVEL–1 model (≈18 mm/yr) (DeMets et al., 1990). The solution using the Markov process and elevations larger than 5° gives a weighted rms of the residuals of 13.7 mm for the whole data set (133 exp.) and 11.8 mm for

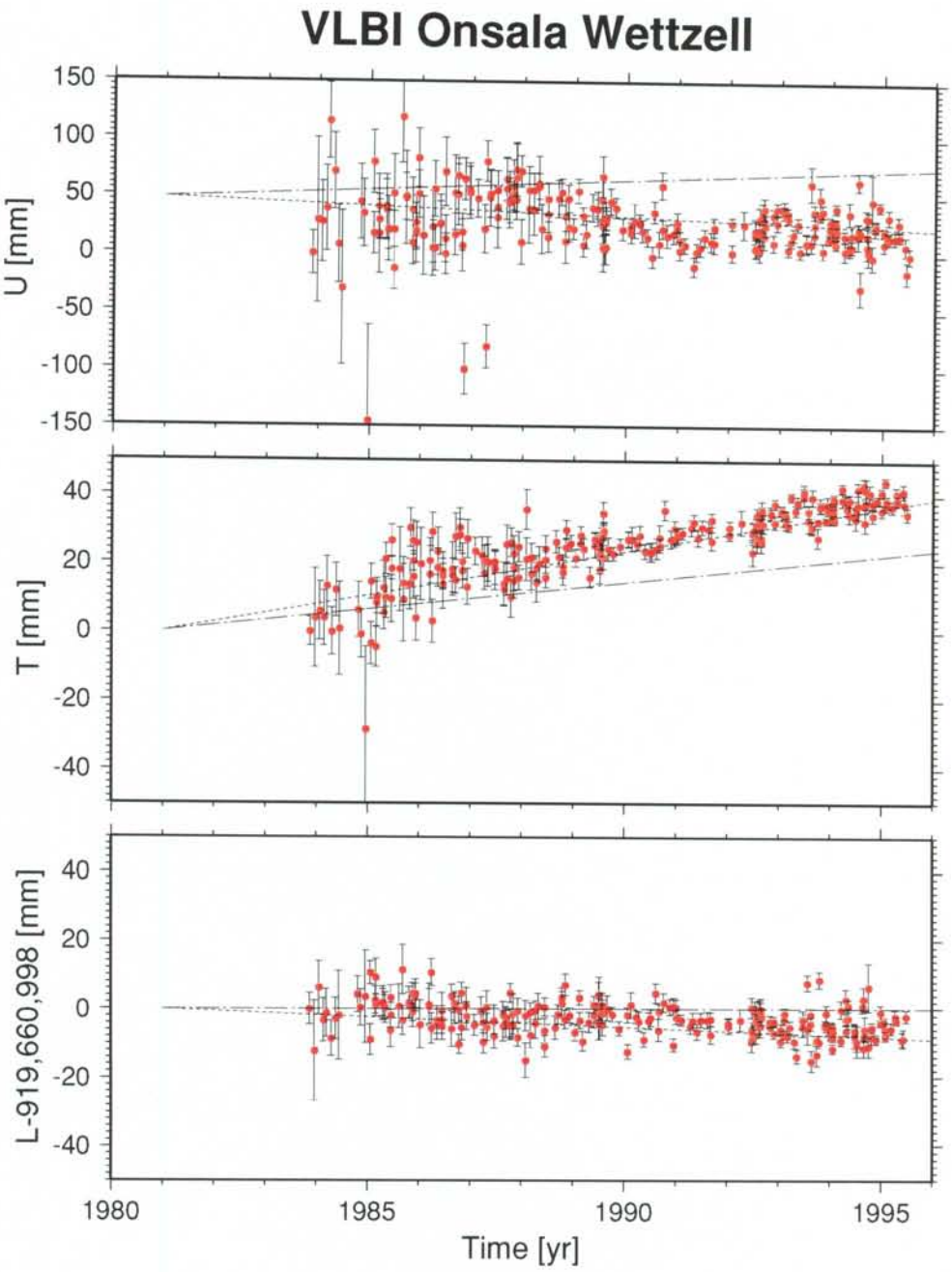

Figure 3-1. *Estimated baseline lengths Onsala–Wettzell in the three orthogonal baseline components, Length, Transverse, and Up. (The plane spanned by Length and Up contains the geocentre.) This is the GSFC standard solution, not using Water Vapour Radiometer (WVR) data nor using a Markov process to estimate wet tropospheric delays from the data. The weighted rms of fit for each component is 3.6, 3.3, and 13.7 mm, respectively. Using WVR data, the estimated Length rate changes from 0.6 ±0.1 mm/yr (dotted line) to 0.25 ±0.1 mm/yr. Shown are also the rates predicted from NUVEL-1a plate motion (dash-dotted lines)*

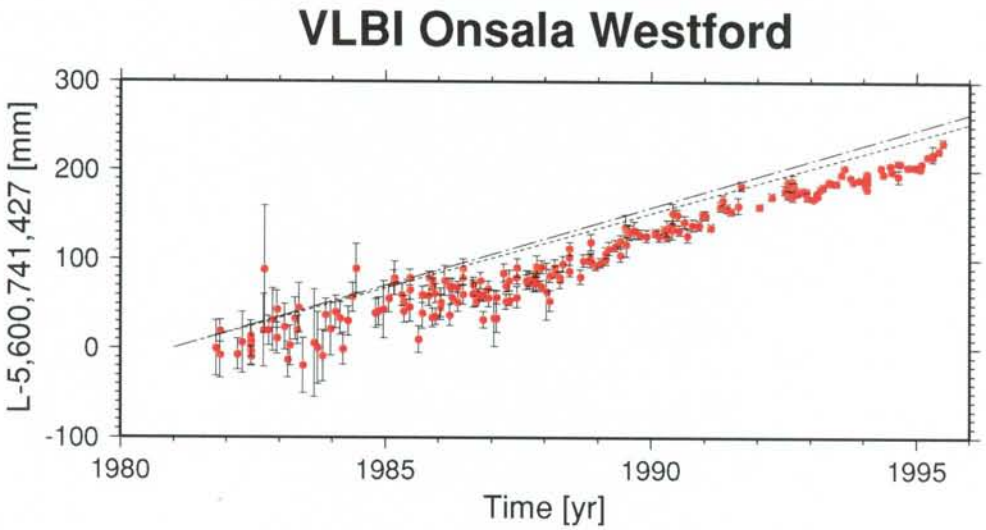

Figure 3-2. *Estimated baseline lengths Onsala–Westford. This is the GSFC standard solution. Shown is also the rate predicted from NUVEL-1a plate motion (dash-dotted line) and the mean observed rate (dotted line), 16.9 ±0.2 mm/yr.*

the last three years (42 exp.). When the WVR data are used a larger elevation cutoff is adopted (20°). In this case we obtain a weighted rms of the residuals of 13.8 mm for the whole data set and 10.4 mm for the last three years.

3.2 GPS—1986 to 1993

Operations with receiver equipment for the Global Positioning System started at Onsala in conjunction with the Iceland campaign summer 1986 (Rothacher and Beutler, 1988). At this occasion Onsala was selected as a fiducial site. Since colocation with a well-established VLBI point was feasible, the observations with a TI4100 receiver at Onsala would tie the Iceland network into the International Terrestrial Reference Frame (ITRF). Similar high-latitude fiducial sites were maintained at Algonquin Park and at Westford. The deployment of satellites was by far incomplete, and the network suffered from a low number of simultaneously visible space-craft.

The fiducial site concept was developed further, converging into the establishment of a world-wide infrastructure of today, the Internations GPS Service (IGS). A major stage leading there was CIGNET (Cooperative International GPS Network), a network of permanently observing GPS receivers colocated at VLBI or SLR sites and thus tied into the ITRF. The CIGNET station at Onsala was put into service in December 1987. After a couple of monument changes and relocations of the antenna, a concrete 1 m high pillar has been the permanent place for the CIGNET

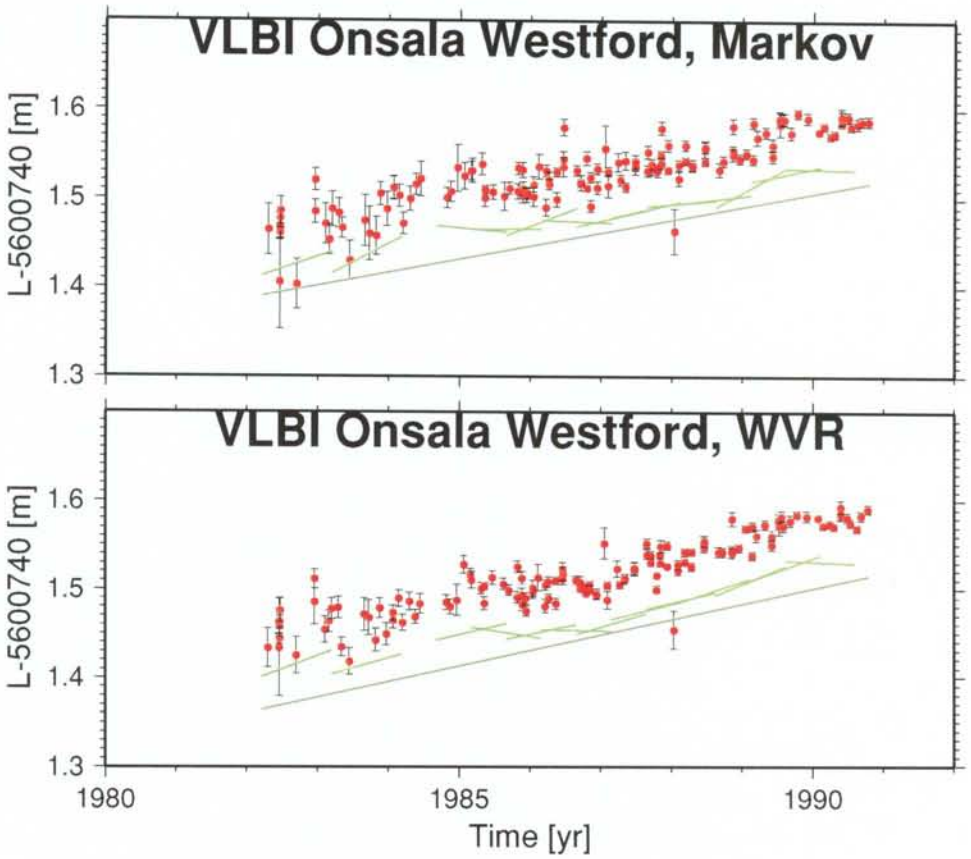

Figure 3-3. *Estimated baseline lengths Onsala–Westford, using a stochastic filter (Markov method) or Water Vapour Radiometer observations (WVR) to reduce the propagation delay due to variations in atmospheric water vapour. Wastly different elevation cut-off limits are required in each case to obtain minimum rms of the residuals (WVR 20°, Markov 5°). The observed baseline rate turns out to be sensitive to the method, 15.0 mm/yr resp. 17.6 mm/yr, more details see text. Using the WVR the residual shows less rms* **and** *systematic signatures, which may ar may not be of atmospheric origin. The Markov-modelled troposphere is suspected to falsely pick up such systematics.*

point. Today it is used as the primary antenna point for the permanent operations in both SWEPOS and IGS.

A number of support points have been founded, and local ties have been measured to establish and maintain the coordinate ties to the different reference systems (Swedish national RT, Nordic NORDREF, European EUREF, World WGS) and between the VLBI and GPS ground reference points (Johansson et al., 1992).

Today, Onsala is a core station of the IGS network. The satellite observations have also been used in research and development projects carried out by various companies for the purpose of navigation and rapid differential positioning.

Recent developments concern providing estimates for the wet propagation delays from GPS measurements, comparing these results with those similarly derived from VLBI, and with independent WVR observations of the thermal emission from atmospheric water vapour. Research on GPS antenna design, radiation fields and scattering effects will be mentioned below in the SWEPOS context.

The photograph in Figure 3-4 shows the VLBI-facility, the GPS monument, and the water vapour radiometer.

3.2.1 Gravity measurements

The GPS observation cabin at Onsala is built around a concrete ground plate furnished for gravimeter observations. Several occupations by absolute gravimeters have occurred during 1992–1994. The first visit was by the Swedish National Land Survey in November, 1992. The next observation period used the absolute gravimeter of the Finnish Geodetic Institute in March 21–23, 1993. Two absolute gravimeters from NOAA (FG5 102) and IfAG (FG5 101) [*Klopping et al.*, 1991] occupied the site during August 7–10, 1993. A remeasurement with the NOAA instrument was carried out September 28–29, 1995. Gravity gradients along the gravimeter bed have been surveyed by Jakko Mäkinen of FGI Helsinki in April 1995. Another visit occurred on May 16, 1994, from "Kort og Matrikelstyrelsen", Denmark.

3.3 FUNDING

Geoscience and related research at Onsala Space Observatory is to the largest extent basic research. Support for the establishment of the technical facilities and the localities has been granted by Knut and Alice Wallenberg's Foundation and the Swedish Council for Planning and Co-

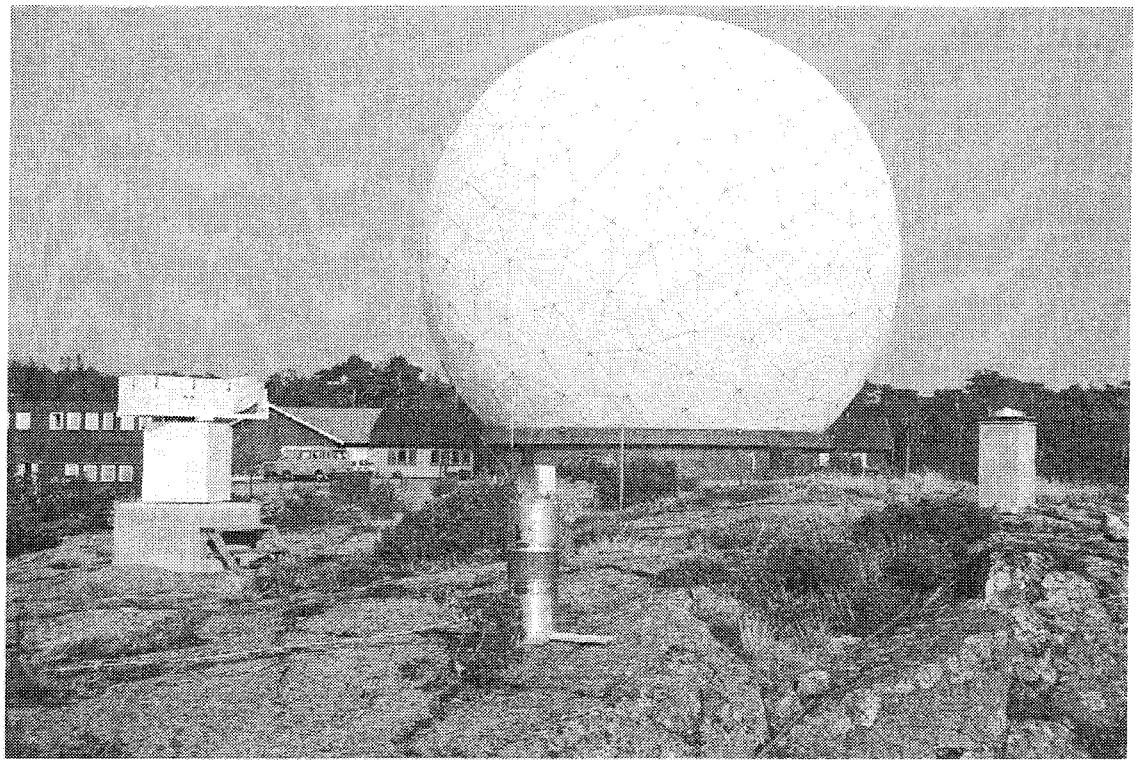

Figure 3-4. *Facilities at Onsala Space Observatories include the 20 m radio telescope for VLBI (covered with the large radome), the water vapour radiometer (left hand side, foreground), and the GPS antenna monument on the square pillar to the right. Another 20 m to left outside the picture is the hut housing the GPS receiver equipment and the measurement platform and reference points for gravity. Located at half this distance is a reference point for large mobile geodetic instruments like VLBI or satellite laser ranging equipment. (The device in the foreground is a test assembly of an ESRANGE rocket element on which a GPS antenna has been mounted.)*

ordination of Research (FRN). Projects have been funded by the Swedish Natural Science Research Council (NFR) and the Swedish Research Council for Engineering Sciences (TFR). Together two European Community and European Union (EU-SCIENCE) projects have been supporting specific projects in conjunction with VLBI, GPS, and WVR.

Thanks to long-term loans by and unbureaucratic exchange with NASA, VLBI equipment has been kept operating in healthy conditions during more than fifteen years.

The radio telescope itself is supported by the government as the Swedish National Facility for Radio Astronomy.

4 GPS NETWORKS

In the following discussion of GPS networks we will consider only those the aim of which is to monitor movement at the centimetre to millimetre level. This has become feasibe technically. In comparison to VLBI as the still most precise technique, the precision gap to GPS is less than an order of magnitude, but the costs involved in creating and operating an equivalent VLBI network would be more than two orders of magnitude greater.

Among different concepts to operate GPS networks we may distinguish according to the degree of activity

- **field campaigns,** re-occupation at monuments, mobile instrumentation incl. antenna support (e.g. tripods);
- **permanent installations,** but data retrieval and analysis sparse in time;
- **continuously operating,** retrieving and analyzing as much data as can possibly be observed.

The first type requires a high level of manpower and runs risks of technical problems in the course of the field work, which will put limits on the number of network nodes. The second set can avoid these problems; a large number of sites may be included in simultaneous network solutions since long periods of time can be expended in the data processing phase. In the third type the number of network sites is traded off against the gain in precision offered by producing dense time series of solutions. Also the cost per data point is minimized.

Analyzing daily sections of GPS data each 30 h long, we find that individual position determinations decorrelate statistically already after two to three days. Thus, 24 h to 48 h solution intervals already contribute to improving the stability of estimated mean positions and rates of change. The search for transient perturbations can be extended to these short time scales.

Once the decision converges towards establishment of a permanent network, a large number of organisational details need to be resolved. The number of sites to be included will have a lower limit imposed by the application. The required data throughput will determine the data facilities for acquisition, processing and archiving, and some trade-off can be achieved by simplifying or sacrificing certain phases of the computing process (like obtaining satellite orbits from a central service) while the amount of data would facilitate the attenuation of errors.

Ultimately the success of the system as a whole will depend upon an assemblage of individual features and technical/logistical/infrastructural details. A large number of decisions is needed to optimally tailor and fine-tune the system, cf. Chapter 6.

The detailed technical specifications for SWEPOS sites are given in the following sections. We estimate the additional cost for adding one station to be 0.5 MSEK (that station would include one receiver and no RTCM service, but else have the same quality as a standard SWEPOS station).

4.1 TECHNICAL REQUIREMENTS FOR PERMANENT OBSERVING SITES

Permanent operation of observing sites causes a number of consequences concerning the installation of the basic equipment, supporting equipment, and infrastructure.

The minimum equipment required to carry out observations within a limited period of time, say from some hours to a couple of days, would consist of an antenna, a receiver, data recording media, and battery power. At a minimum the site would be established by installing a permanent geodetic marker (brass bolt) in a large outcropping boulder or an accessible bedrock surface. The antenna could be placed on a tripode and the eccentricity between the antenna's reference point and the geodetic marker be measured to within one millimetre.

Many surveys have been carried out using this minimum setup. Additionally, observations of air temperature, pressure and humidity have oftentimes been made as processing software containing options to model the signal delay in the troposphere may accept such data. The usefulness and representing power of near-surface meteorological data, however, is highly debatable.

Permanent installations raise concern about the inherent stability of the system. The reference point of an antenna, the point to which the geodetic determinations are effectively been made, will in general differ from the reference marker by the site tie. The site tie (and the monument itself) will not be ultimately stable and thus will affect the position of the antenna reference point. But seen from the electrical point of view the antenna reference point is an abstraction; it is an effective position given the actual distribution of angles of the incident waves and the actual effect of wave scattering and other signal perturbations in the antenna assembly and its environment. Thus, in both the aspects of mechanical and electrical reference point stability, possible routes of attack may consider to (i) avoid or at least suppress, (ii) to compensate and (iii) to survey and model the pertubations.

Permanent sites necessitate stable structures to support the antenna, a cabin to house the receiving equipment and peripherals, and infrastructure to provide electrical power and to off-load the recorded data. This section will present general points of view considering critical properties and trade-offs to be resolved in the planning of observing stations. Further down we will present the SWEPOS solution, its benefits and its limitations.

4.1.1 Antenna support structures

Satellite observing sites are preferably located in areas remote from cities, industry, mines, electrical power lines, roads, and railways for a number of reasons. Tall standing structures may not obscure the antenna horizon. Metal surfaces in the antenna environment may not reflect the incoming waves causing nonstationary multipath or scattering conditions. Inflictions on ground stability must be avoided. The permanence of the site may not be limited for a forseeable future due to infrastructural development, land-fills or exploitation for e.g. ground water.

For the purpose of

- staying clear from a ground snow cover,
- standing out of reach of animals and humans
- extending the horizon mask

the antenna is preferably mounted on a standing structure, e.g. a concrete (rock, ceramic ...) pillar or a metal framework tower. Typically such a structure will have to be between one and several metre tall. Exposed to the seasonal thermal cycle and exposed to the daily insolation and thermal cycles, the structure will undergo deformations which — in the present context — may be considerable. Also, concrete will expand in reponse to increasing humidity, but tailered composition and surface treatment can limit these effects.

- **A minimum of perturbing objects in the field of view of the antenna.**

Preventive measures are required to keep the antenna itself clean from snow and other objects that may settle on its top or accumulate at places where they perturb the antenna radiation field. The required protection is usually accomplished with a plastic or glassfiber radome. The radome should shield off the antenna to all sides. Its material must be chosen

with care, i.e. the refractive index in the 1.2 to 1.6 GHz frequency interval should be low. The shape and a low surface roughness of the radome is to be designed to counteract raindrop and snow adhesion and snow and ice pile-up. Birds should be discouraged from perching, which can be accomplished attaching a sharp spike on top.

- **The structure must be stable.**

The antenna support must be resistive to wind loads, preventing deformation beyond the one millimetre level. It must withstand frost. Additional stabilization (temperature control, thermal compensation) must be considered in order to maintain a sub-millimetre limit on temperature induced movements within the mount assembly. Firm mechanical coupling of the monument within the bedrock environment is required. Means and measures for monitoring eventual movement of the antenna with respect to the ground are required in order to assess the long-term stability.

- **A standard structure should be adopted.**

Analysis has shown that monuments at a height of at least two metres imply an effective averaging of multipath perturbations due to the reflections from the ground as the satellites move over the daily range of elevations (Elósegui et al., 1995; Jaldehag et al., 1995; Jaldehag and Ying, 1995). The phase variations induced in the received signals is an oscillating function of satellite elevation, the number of zero-crossings in an elevation interval being largely proportional to the monument height (for details cf. Chapter 4.1.2).

However, the antenna mount, the design of the top of the pillar, and the structures at decimetre distances from the antenna may cause large multipath perturbations with much fewer zero-crossings over the satellite elevation interval, causing considerable systematic error in the data analysis. The studies suggest that identical structures (monuments and mounts) inflict the smallest systematic errors, and thus that the monuments can favourably be produced in a series. This goes hand-in-hand with the economy of the project.

A wide range of solutions exist in the precision networks, from tripode-like leg supports (the UCLA Pinñon Flat model) via metal framework (FGI, Finland) to concrete and stainless steel pillars (GSI Japan). As all of these projects are new, evaluation of monument and mount stability and determination of the optimum design at this point of time would be premature.

The Working Group on Permanent Networks of the Nordic Geodetic Commission is on the way to define such a standard in order to facilitate homogeneous network solutions when sites within the different subnets are combined.

- **Horizon mask must permit visibility above 10° elevation.**

Satellites need to be tracked to elevation angles typically down to 15° above the horizon. In network analysis, common visibility from all stations will strengthen the results, but at least one pair is required. Observations at low elevation angles are required to increase the resolution power of site height and the troposphere parameters. Considering the carrier frequencies of the GPS signal, practically all kind of buildings (wooden, stone, ...) and all kinds of conducting material will block or severly attenuate the signal. Even thin layers of metal will block the signal, and thin sheets of plastics or other dielectric material (plant's leaves) will perturb the signal or at least introduce undesired delays and scattering patterns.

Thus, material from which antenna covers can be made must be chosen with care.

Considering the preference for a remote location of sites, this implies that sufficiently open areas must be found or trees and other vegetation around the antenna monument must be clipped. Raising tens of metres tall structures, however, is less feasible as these would be even more susceptable to thermal variation and wind loads.

The cabin will generally not inflict on the horizon mask if the monument has a height of three metres or more. However, near-by location of the cabin may imply reflection of the GPS signals from the roof and introduce a multipath problem. For countermeasures the gable of the cabin should face the monument, and the distance to the monument should be sufficient, e.g. 10 m (most sites) appears better than 1 m (at Furuögrund).

The solution preferred in Finland (Vermeer, 1994) devises a steel framework tower 3.0 m tall. At Metsähovi the tower is 8 m tall and is compensated for thermal expansion by an Invar-steel rod. This rod effectively clamps the antenna mount to the monument base very near the geodetic ground reference marker, while the steel tower provides the horizontal support.

4.1.2 Antennas

Using antennas of different designs within the same network can introduce serious site-to-site heterogeneities in receiving conditions. Schupler and Clark (1991) and Schupler et al. (1994) specify correction methods for experiments which mix different antenna types. The major conclusion of the recent work of Jaldehag (1995) is to use antennas of identical type throughout the network. Reducing the errors due to different antennas by using a model to describe the sensitivity patterns is considered as a too uncertain method. Still, the particular antenna type which introduces an acceptably low level of perturbations needs careful consideration.

The sensitive antenna element consists usually of two dipoles, arranged crosswise in the horizontal plane. The dipoles are electrically coupled for circular polarization. This arrangement obtains omnidirectional sensitivity in azimuth and approximately cosine sensitivity with respect to the zenith angle. The main lobe of a simple dipole at finite distance above a finite ground plate extends to angles below the horizon. At still larger angles perturbations are admitted through the sidelobes of the radiation pattern.

Owing to the design of the antenna assembly, particularly enhanced ground plane models, scattered or reflected waves impinging on the antenna dipoles at sub-horizon angles can be attenuated with high ratios.

One of these antenna types, the choke ring design, obtains an enhanced ground plane by virtue of deep, concentric metallic corrugations. Their attenuating effect must be tailored to fit the particular frequencies. The method works strictly only at one frequency. Already with two frequencies modelling criteria and trade-offs become considerably complex, yielding many different design options (number of choke rings, vertical profile, horizontal spacing). A number of technical solutions have been realized and are available from antenna manufacturers.

A widely used GPS antenna is based on the cross-dipole assembly originally designed by JPL and manufactured by Dorne & Margolin, N.Y. Suppliers of GPS equipment add a choke ring and preamplifier assembly. Chocke ring antennas have become the standard choice for Allen Osborne's TurboRogue and recently also Ashtech receivers. The following variants exist: Original DM-T, a DM-TA type, and an older DM-B model. They are practically identical. The DM-TB has a different bottom plane housing the pre-amplifier assembly, which has no demonstratable effects on the radiation pattern.

The original Ashtech antenna that came with the Ashtech Z-12 or P-12 receiver and is similar to the Trimble antenna has been used in SWEPOS only temporarily.

4.1.3 Receivers

For high-precision purposes, receivers must be capable to acquire and process both phase and P-code measurements simultaneously for the two frequencies and for as many satellites as can be visible, which is more than eight but less than twelve. This restricts the candidate receiver models to the product palette of about five manufacturers

During Anti-Spoofing, P-code measurements require a sophisticated procedure to derive an equivalent P-code variable from the Y-encrypted signal, which is accomplished by real-time cross-correlation in TurboRogue and Ashtech receivers. Satellite clock dithering under Selective Availability favours the use of receivers with stabilized oscillators, or the use of external Rubidium or Caesium oscillators as an alternative.

An extensive list of receivers and their specifications for a wide range of applications is found in GPS World (1996).

4.1.4 Other station equipment

At remotely located sites the following equipment may be considered: Backed-up uninterrupted power supplies; data communication modems or other connectors to data networks; air heating and/or cooling devices. The use of frequency standards (Rb or Cs time standards) may in the first case be indicated in connection with the Ashtech Z12 receiver and its drifting oscillator. Evaluation is under progress.

4.2 THE SWEPOS SITES

Here we describe the actual realisation in SWEPOS of the antenna, its monumentation and other site facilities in conjunction with the instrument cabin, supposedly meeting the demands above. We will discuss the cases where problems have been detected, the solutions we devised and problems that might still persist.

A map of the network is shown in Figure 4-3. Figure 4-1 shows SWEPOS along with similar networks in Finland (FinnNet) and Norway (SATREF).

Geodetic positioning solutions in the SWEPOS network with the non-fiducial strategy (c.f. `\ref{sec:NONFID}`) utilize IGS data observed at several sites within Europe, all being located on the same tectonic plate and well separated from active margins. Thus, the regional solutions can be postfit to the GPS subset of the ITRF which is maintained by these IGS sites. The small deformations known to exist across the Alps and

Pyrenees do not inflict on this strategy. The IGS sites used in the Onsala solutions together with the SWEPOS sites are shown in Figure 4-3.

4.2.1 SWEPOS sites design and equipment

The SWEPOS pillar

The SWEPOS network is furnished with a standard 3 m tall concrete steel-inforced pillar of circular cross-section. The standard pillar design is due to the National Land Survey (cf. Figure 4-4). The Division of Structural Mechanics (Doc Ola Dahlblom) at Lund Technical University has assisted in its development with studies on the thermally induced deformations. The foot of the pillar consists of a 0.75 x 0.75 m concrete plate. The pillar's steel inforcement continues through the bottom plate into holes drilled into the bedrock. The concrete of the foot plate is cast into a shallow bowl-shaped mould hammered out of the bedrock.

Under an insulating outer cover that extends over the height of the pillar and consists of a helically wound corrugated plastic sheet, rockwool insulating material aids in attaining a homogenous temperature field throughout the pillar. The temperature level is controlled attaching a heating wire to the pillar, helically wound. A temperature sensor is fit into a small cavity inside the pillar and connects to a thermostat unit in the instrument cabin (on-off regulator, powered with AC from the mains).

The pillar set temperature is 15 °C. Present temperatures exceeding this limit may deform the pillar. At 40 °C the length change is still below one millimetre. Figure 4-5 shows a photograph of the Vänersborg site, which is furnished in the standard design.

Exceptions are as follows: The Jönköping pillar is a 1 m lowered version of the standard pillar (for air traffic safety); actual coupling to bedrock is unclear and confirmation would be desirable. Lovö and Mårtsbo monuments rest on pre-existing pillars with a rectangular cross-section. Onsala continues to use the CIGNET monument on a 1 m tall pillar with a square cross-section (cf. Fig. 4-2).

Local control network

At ten to twenty metres distance from the monument, geodetic markers (stainless steel studs) are driven into the surface of the bedrock. Usually six such markers, as regularly distributed as possible with regard to healthy bedrock accessibility, form a local network within which eventual deformations of the top of the antenna monument can be detected.

Figure 4-1. *SWEPOS, the Permanent Swedish GPS Network and its Norwegian (SATREF) and Finnish (FinnNet) neighbours.*

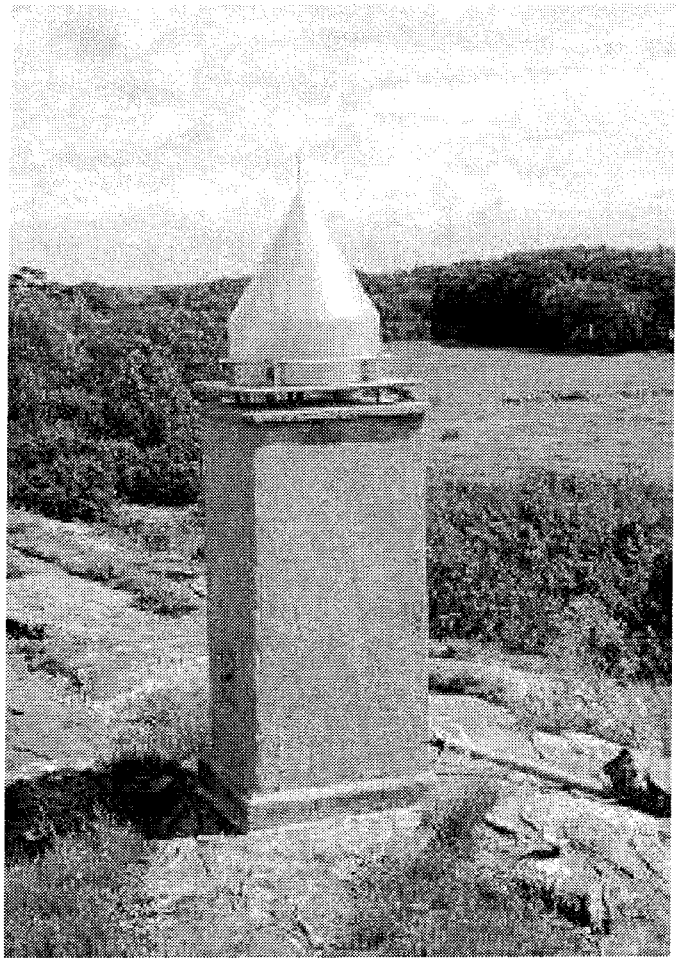

Figure 4-2. *SWEPOS monument at Onsala, old radome. Eccosorb material in-line with the antenna bottom plate has been removed for the photo.*

Figure 4-3. The SWEPOS Permanent Swedish GPS Network and the European IGS sites regularly included ("n.u."—not included) in the solutions derived for the BIFROST project.

Figure 4-4. *The SWEPOS standard pillar (left). Layout of the Kiruna site near Esrange with two monuments (A, B) and local reference marks. The latter serve as control points for surveying monument movements.*

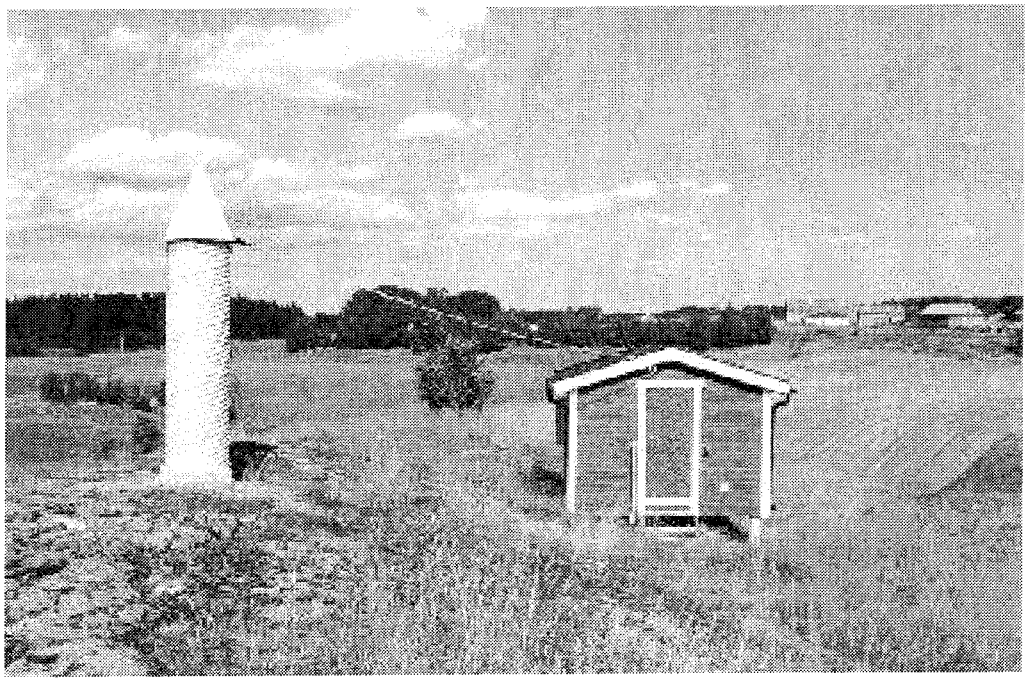

Figure 4-5. *The SWEPOS station at Vänersborg. SWEPOS standard pillar and new radome*

In a control survey, the antenna is removed and replaced with a theodolite. The horizontal and vertical angles to the steel studs are observed. The detection level for horizontal and vertical movement of the pillar within the control network is 0.1 mm.

The National Land Survey carries out the control measurements. Leksand has been used as a control site where the local network has been observed twelve times with at minimum one-month intervals during 1993–1995. In general the monuments have been measured and remeasured once in two years. Preliminarily, in some cases the surveys seem to indicate movements of one to two millimetres.

Independent evidence that helps discriminate interannual and seasonal signatures from secular trends is considered extremely important. The strategies for the local control measurements must suit these needs in terms of how regular and how frequent they are carried out. Recovery of an annual cycle requires that measurements repeat from year to year on a calender basis. On the other hand, the circumstance that the antenna must be removed and an optical observing device be installed in its place introduces a source for systematic errors (the remounted antenna must return to the previous position and the parts and pieces must not change electrical environment of the antenna). At present we need to develop the strategies for the control surveys further to obtain greater significance while simultaenously reducing systematic perturbations.

The SWEPOS antennas

All sites are now equipped with Dorne-Margolin choke ring antennas. Where stations are furnished with the standard pillar a profoundly homogeneous geometry in the aspect of EM propagation, diffraction and scattering has been achieved.

The shorter pillar and the special antenna mount at Onsala has caused some concern as to the wave scattering conditions in its near field. Also, the site is just outside our laboratories so that testing alternate arrangements is less time consuming. Our experiments have converged to the following solution: Scattering perturbations originating from the mount and backplate structure has been attenuated with the help of EM wave absorbing material (Eccosorb AN-W). A $61 \times 61 \times 5.7$ cm square piece has been put directly above the metallic back plate, yielding satisfactory preformance (Jaldehag et. al. 1995b).

Extended antenna choke ring designs have been considered using computer modelling, and some have actually been manufactured (Jaldehag and Ying, 1995). The extension concerns the number of choke rings as well as their thickness profile and spacing.

The SWEPOS radome

After a first winter of experience with a fiberglass radome manufactured by Delft University, a new design was developped by our group in order to avoid snow/ice accumulation. Large (40 mm) vertical variations in the vertical component determinations were observed primarily at the inland sites of northern Sweden. Jaldehag et al. (1995) found correlation with precipitation and the local temperature at ground-level. The study suggested that snow was accumulating around the top of the pillar and the mounting elements of the Delft radome which together present many surfaces for snow and ice to attach and settle on. The OSO model was developed from this experience and eliminates edges due to its straight inverted icecream cone design with an aperture wide enough to extend over the top surface of the pillar with an overhang (cf. Fig. 4-5).

Owing to the electrical properties of the radomes, the transition from the Delft to the OSO model induces a detectable, virtual change in the site position, generally less than 20 mm in the vertical and smaller than that in the horizontal. It was found that this change in position is different at each site and therefore must be determined individually. The variability is probably related to surface inhomogeneities in the plastic molding process.

The SWEPOS receivers

At present all SWEPOS sites house two receivers. Employed models are eight channel TurboRogue and/or twelve channel Ashtech Z-12. Table 4-1 shows the currently deployed receiver/antenna combinations at all sites. At stations that house two receivers a power splitter connects both receivers to the same antenna. The remainder of this chapter gives a short historic review.

In the first phase (1993–94) 15 sites were equipped with TurboRogue receivers, all of which connected to DM antennas. At the time AS was switched on by the US DoD, the TurboRogue was the only receiver model capabable of full wavelength L2-measurements. Some stations were equipped with Ashtech P-12 receivers of which the larger part was connected to Ashtech antennas. In order to achieve homogeneity in receiving conditions, which was a primary concern, DM antennas replaced the Ashtech ones in 1995. From July 1, 1995, all 20 (21) stations could be included in the BIFROST data analysis.

Sites that are used for Differential GPS require the full RTCM capability and Doppler measurements (for terms cf. Chapter 4.3.4 below). Also, the sampling rates preferred in this application are high. The receiver matching this purpose is the Ashtech Z-12. Presently, 13 of the DGPS reference sites house an additional TurboRogue receiver. A 15 s sampling rate is the standard for the data used in the BIFROST analysis. The preference for this receiver, however, has been due largely to its oscillator being more stable and being controlled in a more suitable way, but recently the increased number of simultaneously visible satellites has motivated to favour the Ashtech model.

In order to control the Ashtech oscillator, an external frequency reference is supplied by precision quartz oscillators or Rb clocks installed at Lovö and Mårtsbo. Onsala uses the observatory's hydrogen frequency standard. On the other hand, the uncontrolled oscillator has not caused noticeable problems.

Instrument cabin

The standard SWEPOS instrument cabin has a size of 3×2 m and houses

- one or two satellite receivers,
- optionally one precision quartz frequency standard,
- one data collecting computer for each receiver (486 PC, typically a Laptop model),

- one telecommunication modem for each receiver.
- one modem for remote control of electrical power supply to all instruments.
- Uninterrupted Power Supply (UPS) including batteries.
- heater control of the antenna pillar

(cf. Fig. 4-6) Thermal insulation helps to maintain the ambient temperature range of the equipment, and ventilation safeguards for lead-acid rechargable batteries. Considering an outdoor temperature range between -40 °C and +35 °C, the additional heating effect due to insolation on the cabin's surfaces, and the power dissipation of the apparatus (15 W/receiver; 40 W/PC; 40 W/LapTop; 50 W/modem) necessary heating and cooling devices have been installed.

Power mains and telephone installation must be properly protected against transients, primarily those induced by lightning strikes.

Attendance or visual inspection is done on the average four times per year.

Table 4-1 *Summary of site equipment*

site[a]	Latitude[b] [°]	Longitude[b] [°]	Height[b] [m]	receiver(s)[c]	pillar[c]	cable[e] [m]	antenna[f]	remark
Arjeplog (ARJE)	66.31	18.12	489	2 A	3-m CC	15	DM-T	
Borås (BORA)	57.71	12.89	219	A + TR	3-m CC	60	DM-TA	
Hässleholm (HASS)	56.09	13.72	114	A + TR	3-m CC	12	DM-T	DGPS
Jönköping (JONK)	57.75	14.06	260	A + TR	1-m CC	22	DM-T	
Karlstad (KARL)	59.44	13.51	114	A + TR	3-m CC	17	DM-T	DGPS
Kiruna (KIRU)	67.88	21.06	498	A + TR	3-m CC	15	DM-T	DGPS
Leksand (LEKS)	60.72	14.88	478	2 A	3-m CC	20	DM-T	
Lovö (LOVO)	59.34	17.83	80	2 A	3-m RA	10	DM-TA	DGPS
Mårtsbo (MART)	60.60	17.26	75	A + TR	3-m RA	25	DM-T	DGPS
Norrköping (NORR)	58.59	16.25	41	2 A	3-m CC	26	DM-TA	DGPS
Onsala (ONSA)	57.40	11.93	46	A + TR	1-m SQ	20	DM-B	DGPS
Oskarshamn (OSKA)	57.07	16.00	150	2 A	3-m CC	42	DM-TA	
Östersund (OSTE)	63.44	14.86	490	2 A	3-m CC	10	DM-T	
Överkalix (OVER)	66.32	22.77	223	2 A	3-m CC	18	DM-TA	
Skellefteå (SKEL)	64.88	21.04	81	A + TR	3-m CC	7	DM-T	DGPS
Sundsvall (SUND)	62.23	17.66	31	A + TR	3-m CC	18	DM-T	DGPS
Sveg (SVEG)	62.02	14.70	491	A + TR	3-m CC	10	DM-T	DGPS
Umeå (UMEA)	63.58	19.51	54	A + TR	3-m CC	20	DM-T	
Vänersborg (VANE)	58.69	12.03	170	A + TR	3-m CC	15	DM-T	
Vilhelmina (VILH)	64.70	16.56	450	A + TR	3-m CC	19	DM-T	DGPS
Visby (VISB)	57.65	18.37	80	A + TR	3-m CC	12	DM-T	DGPS

[a] Four-letter abbreviations.
[b] Approximate WGS-84 coordinates.
[c] A - Ashtech-Z12 and TR - SNR-8000 TurboRogue.
[d] Height and cross-section of pillar; CC - circular; RA - rectangular; SQ - square
[e] Antenna cable length.
[f] Type of antenna mount is shown in annotated figure.

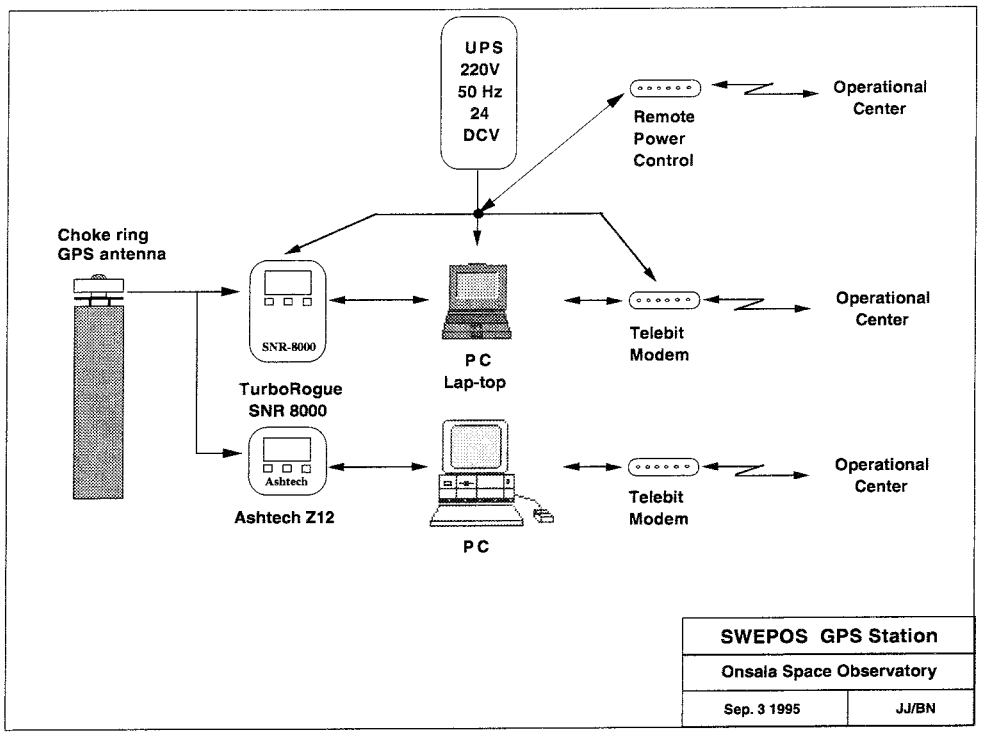

Figure 4-6. *SWEPOS site equipment in the instrument cabin*

4.3 DATA FLOW, PROCESSING, ARCHIVING

The data flow in conjunction with daily solutions is described. In addition to the data produced by each receiver, ancillary data is acquired from services in order to concentrate efforts, utilizing the available service products as far as these are compatible with our demands on quality.

4.3.1 Data from the satellite receivers

The data that are produced by a GPS receiver may consist of individual measurements of phase, of pseudorange derived from codes, and possibly measurements of Doppler frequency shift. Each of the receiver channels locks to one satellite during its time of visibility. For each acquired satellite, space-craft identification, time, and status indicators are recorded. The receiver adds manufacturer-supplied respectively user-supplied information as to its identification, location, operator etc. Additional data sections record the broadcast navigation messages (satellite orbit ephemerides, UTC parameters, ionosphere parameters, satellite clock parameters). The observation data is read out and moved into a local memory at specific sampling instances while the receiver keeps (tries to keep) continuous track of the signal phase.

In order to facilitate data exchange, a specific Receiver Independent Exchange Format (RINEX) data format has been agreed upon. Its second

version accomodates data taken under anti-spoofing (Gurtner and Mader, 1990). Interfacing software accomplishes the RINEX conversion of data from a specific receiver. These programs are usually available from the manufacturers. Compliance with the RINEX standards definition cannot always taken as granted. Our experience suggests that thorough testing by users is indicated in the succession of new hard-, firm- or software releases. We don't mention any name.

The RINEX format definitions concern observation data, navigation message, and site meteorological data.

There are a number of ways with which the quality of the observed and archived data can be characterized. A quality indicator is valuable for prospective users of the data e.g. in connection with regional GPS networks and campaigns. Quality indicators are obtained from the number of samples available, signal to noise ratio, the RMS of the code measurements, satellite health, the L1/L2 cross-correlation parameter. A medium-level quality factor is derived from the number of samples passing the automated editing process prior to subjecting the data to parameter inference. At this stage cycle slips are detected; low numbers are indicative of good data. A high-level quality indicator is derived from the daily analysis, reflecting the consistency of parameter estimates. Low values for the variance of the position parameters, of the atmospheric parameter (zenith wet delay) or local clock terms, are indicative of good data. So are low post-fit variance/covariance matrix elements of the site position parameters.

The particular sampling rate at which the phase and code measurements are taken, can be set within wide limits. It is determined from the main purpose of the data. The storing of high-rate data storage may be preferred as decimation to lower sampling rates is always possible, but size constraints on data to be archived might be critical.

In application to daily solutions from 30 hour observation windows with emphasis on site positions regarded fixed during each session, the variability of critical parameters is a determinant for the sampling rate. Clock dither during SA calls for synchronous sampling. Clock parameters especially under SA conditions are the fastest varying quantities. Based on our experience data decimation to a sampling rate of 240 to 300 s is still uncritical for the network solutions.

4.3.2 Data flow in SWEPOS

Since November 1, 1994 the National Land Survey (NLS) hosts the operational centre of SWEPOS, responsible for the downloading, RINEX-conversion, and archiving of data from the SWEPOS sites. Data sampling rate is 15 s and the elevation cutoff level is 4 ° or 10 ° in the Tur-

boRogue or Ashtech case, respectively. The PC which connects to the TurboRogue (Ashtech) receivers' RS232 port serves as a backup storage with a capacity of 180 (500) Mbyte of disk memory. Storage operations to the PC's are performed several times per day. A total of four weeks worth of data will fit on the disk. In the case of the TurboRogue, four days worth of data is kept in the internal memory.

To offload the data the site is dialed up from the control centre in an automated process. One day's load of data is transferred at a time (2.5 Mbyte in compressed form) through a 19,200 baud high-speed modem, consisting of the following data types: Pseudorange measurements from C/A-code and from the P-code on both L1 and L2 frequencies; carrier phase observations on L1 and L2; Doppler frequency observations; and satellite broadcast ephemeris.

The Onsala Space Observatory keeps an independent archive, obtaining the data mostly from the NLS operational center via the INTERNET. Prior to this date, and eventually in the case of problems, data have been downloaded to OSO from the SWEPOS stations directly.

Data from the IGS of satellite observations incorporated into the standard solution concerns the following sites: Tromsö and Ny Ålesund (Norway), Metsähovi (Finland), Herstmonceux (UK), Kootwijk (Holland), Madrid (Spain), Matera (Italy), Wettzell (Germany). This data is acquired regularly via Internet.

Ancillary data bases specifying the reference sites setup, local ties bewteen monuments etc. are also provided in the IGS archives.

4.3.3 Solving geodetic parameters

Standard data analysis uses in the first case the GIPSY/OASIS-II software from JPL. Occasionally the Bernese Software is used mainly to assess various analysis problems along independent routes.

The parameters estimated in the standard analysis are:

- stations clocks (white noise parameter)
- satellite clocks (white noise parameter)
- phase ambiguities (white noise parameter)
- stations coordinates (constant bias)
- tropospheric delay (random walk parameter)
- ionospheric delay (calculated from dual frequency observations)

Tides, earth orientation parameters and satellite positions are acquired from the IGS network and not further estimated. However, at the post-processing stage also these parameters are investigated.

4.3.4 Differential GPS

In passing we shortly mention the Differential GPS service based on the SWEPOS network, which is a joint venture of NLS, OSO and Teracom Swedish Radio Broadcasting. The latter organisation is the commercial provider of the service, which is termed Epos. Those SWEPOS stations that serve as DGPS reference points transfer their data derived from C/A-code measurements continuously over dedicated telephone lines to the central TV tower in Stockholm for further distribution by Teracom as part of the RDS signal of the P3 program on the public FM band. This data consists of pseudorange corrections according to the RTCM-104 industry standard (Radio Technical Commission for Maritime Services) at a rate of about 0.5 Hz for all satellites with elevations above 5 °. Special FM receivers and subscription to the service are required to perform the RDS decoding. Relative positions of roving surveyors can be obtained in real-time regularly at 2 m accruacy level.

More advanced developments make use of the carrier frequency, which can provide accuracies below 1 m, optimistically as good as 0.1 m. For the part of Sweden, a service in this context is currently under development.

5 RESULTS FROM TWO YEARS OF OPERATION

As of current, more than two years of SWEPOS operation and daily analyses within the BIFROST project have resulted in a large number of repeated independent determinations of positions and baseline variations. BIFROST stands for Baseline Inferences for Fennoscandian Rebound Observations, Sea-level and Tectonics. The main final products from the analyses are

- estimates of site positions and variance/covariance between the estimates in the ITRF geocentric reference frame;
- estimates of baseline components between the sites and variance/covariance between the estimates.
- estimates of the tropospheric delay parameters for each site.

For item 2 a reference solution is selected. The differences of successive baseline determinations are then displayed in e.g. local coordinates North, East, Vertical (NEV) or baseline natural coordinates (Length, Transverse, and Up (LTU). Refer to Figure 5-1 for these systems.

5.1 Baselines from SWEPOS/BIFROST

The LTU representation has the advantage that one obtains a set of three components with each a characteristic error level, generally being lowest in L, intermediate in T and greatest in U. On the other hand, NEV components are more practical since the results can directly be drawn on maps.

In both cases, however, one has to keep in mind that baseline vector increments contain an orientation part. In the LTU representation the length (L) component is invariable under rotation.

5.1.1 Adjustment of reference frame motion

For the sake of the argument let us assume a perfectly rigid tectonic plate. Global plate motion affects the orientation of an intraplate baseline. If the plate motion has a nonvanishing component **along** the baseline, the **Up** component is affected, and the motion **across** the baseline direction affects the **Transverse** component.

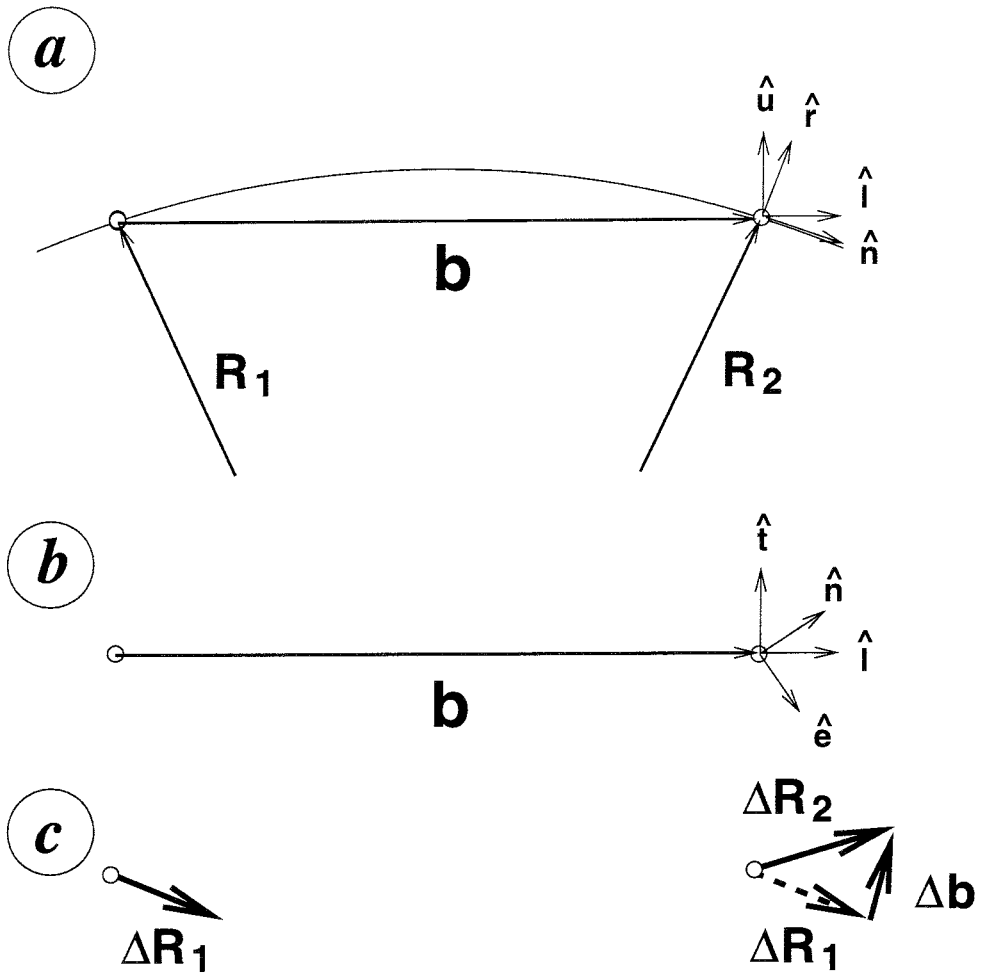

Figure 5-1. *Local coordinate systems for the display of variations of baseline components. LTU = Length, Transverse, Up, oriented at the baseline itself. NEV = North, East, Vertical conventional geodetic coordinates. Top view (a) cuts earth through baseline and geocentre. Mid view (b) shows the same situation from "above". Bottom (c) shows that the result of movement at each end point gives the baseline variation vector* $\Delta\mathbf{b}$. *Forthcoming figures show GPS estimated baseline variation vectors as a function of time.*

As GPS baseline determinations are given in the global ITRF system, plate motion is manifest in the station coordinates (cf. Equation 2-2). Thus, global (intercontinental) displacement rates in LTU are obtained from repeated baseline determinations in the global ITRF. Rates relative to known plate motion is obtained after subtracting a suitable plate motion model. One possible choice is the GPS-independent NUVEL 1a (Pacific plate fixed) or NUVEL 1a-NNR (no-net-rotation), see DeMets et al. (1990, 1994). Alternatively one might consider to monitor the changes with respect to a regional subnet of ITRF sites.

In general, regional deformation implies an orientation component. The deformation component can only be resolved if the motion of an equivalent **rigid** plate is subtracted. This is principally possible with a tectonic

model like NUVEL 1a-NNR. However, at the required level of sensitivity the different net motions between the ITRF-NAR (the no-average-rotation variant of ITRF) and NUVEL 1a-NNR are a problem.

One reason is that the ITRF site motion consists of a seven-parameter affine transformation, including translation and scale in addition to rotation. The tectonic motion in NUVEL, however, is described in terms of rotations only. Inspecting the site catalogues (ITRF93 and ITRF94, for the former cf. Boucher et al., 1994) we find in the case of the European IGS stations (GPS monuments included in the ITRF, and particularly those that are included in our SWEPOS analysis) that the motions in the Up component appear closely tied to Wettzell while Wettzell appears to have a vertical rate between -3 to -4 mm/yr (common to all monuments there, including VLBI, GPS, and SLR). The Italian stations which contribute to the IGS frame also have predominently downward movement; we don't consider these to be related to Fennoscandian vertical movement. We find more convincing Up-rates for Onsala-Wettzell if the regional motion model is reduced to **pure rotation** but otherwise follows the SWEPOS analysis subset of ITRF93 in a least-squares sense. The results of the analysis shown below are derived after removing these three parameter rotations (which is the designation of the subtitle "IGS/SWEPOS 3 p R" in Figures 5-3 to 5-12).

5.1.2 Individual baseline results Sep. 1993–Nov. 1995

In the following we show baseline rate results in Figures 5-3 to 5-12 and more completely in Table 5-2. The ingredients in the signal reduction model are indicated in this table. Choosing the most plausible of parallel solutions, Figure 5-2 compares our GPS results for the baseline up components with the vertical motion obtained from interpolating the tide gauge and levelling data (c.f. Fig. 2-1). Hässleholm has been used as the pivot for this analysis for the practical reason of this site having the smallest expected uplift rate.

Baseline rates are estimated relative to site anomaly models. These are least-squares fits using a tidal analysis procedure. The signals which are fitted to reduce the long-term site position offsets are

- **time-limited biases;** anomalous jumps are allowed to occur for known reasons, e.g. at times where antennas were refitted or their radomes were replaced. These time intervals are taken from the site service books.
- **time-limited anomalous rates** in a few special cases.
- **seasonal cycles;** for the least-squares fit the solar radiation tide (Cartwright and Tayler, 1971) was demodulated at the 24 h daily

solution interval and the resulting annual, semi-, ter- and quarter-annual cycles are admitted into the baseline variations with a separate admittance coefficient each.

- **local barometer observations** where available at both end points of a baseline; at the present—in lieu of meteorological recorders at the SWEPOS sites—this reduction can anly be made with Onsala-Wettzell. The effect is supposed to account for crustal loading deformations induced by the time-varying atmospheric load, at least as a first-order approximation.

Removal of processes that correlate with the solar radiation tide is useful during the first 2.5 years of operation since the seasonal cycles are not fully completed. Candidates are ambient temperature of the antenna, snow and frost deposition. The estimated rate can be significantly offset if an annual signature is present. When longer data series are available, discrimination of rates in a background of noise and annual cycles will probably operate better. Where data records were shorter, like in the case of Skellefteå, alternate solutions with and without the seasonal cycle fit have been prepared.

5.2 Discussion

Results for air pressure loading effects (Onsala Wettzell) are discouragingly weak. Only the Up component was modelled as the horizontal effects are expected much smaller still, and also they are at first order proportional to the horizontal gradient of the local pressure, which is not recorded at the sites. The admittance coefficient is barely significant and one order of magnitude smaller than expected. Obviously other parameters that are estimated, presumably the tropospheric delay, have the capability to mimic air pressure induced vertical motion quite well.

The seasonal signatures which we try to resolve are supposed to remove possible climatic or insolation effects. In those cases where we obtain strong effects in the Up components we attribute these primarily to snow and ice covering the antenna radomes. After the radome changes we are to expect different (hopefully more modest) behaviour. Reliable results can only be expected after several repetitions of the annual cycles since we need to discriminate periodic from nonperiodic behaviour.

Long time series straddling the $\simeq$ 800 days of SWEPOS analysis presently available obtain relatively stable determinations of the baseline rate parameters. However, the rate of the Onsala-Wettzell baseline, which can be compared to independent VLBI results, is correlated with both the estimation of a horizontal offset after refitting the Onsala antenna in September 1994 and to the seasonal parameters. In addition, also the

annual cycle is highly correlated with this antenna offset as it unfortuitously took place in autumn. Depending on the modelling setup, length rates can be obtained which are different on a two-sigma level (-0.16 ±0.4; +0.97 ±0.4 mm/yr). The VLBI determinations were nonunique depending on whether the data were processed with observed or stochastically modelled wet troposphere. We recall the results from Chapter 3.1.5, -0.2 (-0.7; -0.4) ±0.2 mm/yr for the WVR (Markov wet delay; GSFC standard) solutions. We note that the GPS rate uncertainty is at the level of the VLBI-inferred rates, suggesting that more data needs to be collected.

The sites showing anomalous horizontal rates are Vänersborg, Leksand, and Skellefteå (at Norrköping, Oskarshamn, Lovö and Överkalix conclusions have to await processed results of Ashtech data). At Leksand the local monument surveys introduced perturbations; at the other sites the lengths of the data series are somewhat shorter. Thus, we hesitate to correlate the anomalous rates with ground instability indicators, increased local seismicity (Ahjos and Uski, 1992), presence of long, connected fault zones and fault duplex structures (Henkel, pers. comm.). Later this year we will have sufficient time coverage to decide on whether additional sites in these areas are needed. The level of seismicity in the area will be a key factor; thus we will concentrate on densification of the network in a circular area of 250 km radius around lake Vänern and in a strip in the Norrland area between Umeå and Kiruna.

The prospect of analyzing strain from BIFROST displacements argues for a widening of the network. At present we resolve the shield only be two rows of sites in the north, implying a weakness on derivatives taken along NW-SE directions, and the influence of the IGS stations at Tromsö and Metsähovi becomes undesirably large (unless—or better: until their observing conditions resemble those in SWEPOS). Addition of sites in Norway and Finland, four or five stations each, and one in each of the Baltic states as a segment in the cooperation under NKG for the purpose of maintaining EUREF geodetic system is already on the way. It will provide valuable data for the strain determination problem.

Table 5-1. *SWEPOS sites, codes and approximate locations*

Site code	National RT90 coord.[a] x [m]	y [m]	h [m][b]	Expl. location
ARJE	7359601	1604007	466	25 km northeast **Arjeplog**
HASS	6220164	1370095	84	Göinge Åsen 7 km south **Hässleholm**
JONK	6403644	1396053	229	**Jönköping** airport
KARL	6593758	1369556	83	7 km north **Karlstad**
KIRU	7540983	1720732	479	2 km southwest ESRANGE, **Kiruna**
LEKS	6734262	1449346	447	Top of Granberget 20 km northwest **Leksand**
LOVO	6581414	1615165	49	RIT[c] geodetic observatory **Lovö**, Stockholm
MART	6720630	1579635	45	NLS geodetic observatory **Mårtsbo**, 10 km south Gävle
NORR	6496477	1525659	10	**Norrköping** airport
ONSA	6369962	1266801	14	**Onsala** space observatory 30 km south Göteborg
OSKA	6326607	1511622	119	35 km southwest **Oskarshamn**
OSTE	7037462	1452746	462	32 km nne **Östersund**
OVER	7375050	1811940	201	3 km west **Överkalix**
SAAR	7538409	1717072	371	**Saarijärvi** ESA Kiruna
SKEL	7207532	1748254	56	13 km north **Skellefteå**
SUND	6903590	1596440	3	Lörudden, 25 km southeast **Sundsvall**
SVEG	6878736	1442132	461	17 km east **Sveg**
UMEA	7057523	1683924	27	Nordmaling, **Umeå**
VANE	6514005	1281454	138	40 km west Mellerud, **Vänersborg**
VILH	7177238	1536018	423	10 km northwest **Vilhelmina**
VISB	6394988	1652943	49	**Visby** airport

[a] B G Reit, NLS, pers.comm.
[b] Antenna height above Bessel's ellipsoid.
[c] Royal Institute of Technology, Stockholm.

Table 5-2 *Baseline rate results, values in mm/yr. Rates are relative to a three parameter plate motion model following with the European IGS sites. Least-squares reduction model is indicated in rightmost column, designating: s–southern, n–northern sites radome change: o–Onsala antenna re-orient in Length and Transv.; c–seasonal cycles: r–anomalous rate (Up only); t–truncated (Up only); pU–pressure loading, Up only.*

Baseline	Length	σ_L	Transv.	σ_T	Up	σ_U	model
ARJE HASS	1.48	0.69	3.34	0.64	-10.60	1.78	s n c
HASS JONK	0.08	0.28	2.55	0.43	3.50	0.86	s c
HASS KARL	0.81	0.48	0.41	0.56	7.01	1.38	s n c
HASS KIRU	1.72	0.57	-0.50	0.48	4.87	1.44	s n c
HASS LEKS	-1.86	0.50	6.52	0.86	6.35	1.66	s n c
HASS MART	-0.78	0.33	0.78	0.37	8.03	0.91	s c
HASS ONSA	0.24	0.28	1.32	0.31	6.05	0.68	s o c
HASS ONSA	-0.77	0.31	-0.10	0.35	6.57	0.80	s o
HASS OSTE	0.89	0.64	2.15	0.58	-0.26	1.85	s n c
HASS OSTE	1.01	0.67	1.80	0.62	1.40	2.20	s n
HASS OSTE	-	-	-	-	1.24	3.07	s n t
HASS SKEL	6.14	0.77	1.41	0.63	-6.03	1.45	s n c
HASS SKEL	2.86	0.78	0.48	0.67	15.35	1.57	s n
HASS SKEL	-	-	-	-	-10.53	1.45	s n r
HASS SUND	0.65	0.40	1.60	0.38	8.51	0.91	s n c
HASS SVEG	0.65	0.35	2.41	0.33	5.84	0.89	s c
HASS UMEA	0.95	0.50	0.45	0.42	10.30	1.00	s n c
HASS VANE	6.12	0.62	9.41	0.63	-15.63	1.29	s c
HASS VANE	3.07	0.63	4.16	0.70	0.94	1.35	s
HASS VILH	1.64	0.49	1.78	0.43	6.84	1.01	s n c
HASS VISB	-1.41	0.31	0.03	0.28	0.30	0.70	s c
HASS WETB	-0.56	0.37	-2.99	0.44	2.54	0.92	s c
JONK ONSA	1.38	0.51	-0.03	0.20	2.45	0.76	s o c
KARL ONSA	0.58	0.40	1.08	0.44	-0.15	1.23	n o c
KARL VANE	6.62	1.11	-1.34	1.08	-5.28	3.09	s n
ONSA VANE	-2.69	0.47	2.64	0.62	-13.08	1.49	s o c
ONSA VANE	-2.71	0.49	2.60	0.64	-11.36	1.68	s o
ONSA TROM	2.17	0.57	-0.50	0.57	0.35	1.12	o c
ONSA WETB	0.97	0.40	3.82	0.44	-2.34	0.88	o c pU
ONSA WETB	-0.16	0.41	1.34	0.49	-2.29	0.91	o
TROM WETB	2.44	0.57	0.82	0.61	-2.46	1.24	c

Table 5-3 *Length of the baselines of Table 5-2 and repeatabilities around the modelled biases and seasonal signatures.*

Baseline	Length [m]	Repeatability [mm]		
		Length	Transv.	Up
ARJE HASS	1 161 572.521	3.6	3.3	9.2
HASS JONK	185 273.635	1.9	3.0	6.0
HASS KARL	373 468.736	2.3	2.7	6.7
HASS KIRU	1 363 816.076	4.7	3.9	11.8
HASS LEKS	519 992.488	2.5	4.4	8.4
HASS LOVO	436 424.542			
HASS MART	542 375.545	2.6	2.9	7.1
HASS NORR	317 045.385			
HASS ONSA	181 879.343	2.5	2.9	6.1
HASS OSKA	17 7073.496			
HASS OSTE	820 849.977	3.4	3.1	9.8
HASS OVER	1 234 248.155			
HASS SAAR	1 360 406.944			
HASS SKEL	1 055 912.292	4.1	3.6	8.3
HASS SUND	719 515.506	3.1	3.1	7.2
HASS UMEA	893 415.010	3.7	3.2	7.5
HASS VANE	306 778.785	2.8	3.1	5.9
HASS VILH	970 397.822	3.9	3.4	8.0
HASS VISB	332 452.747	2.7	2.4	6.1
JONK ONSA	133 519.317	4.4	1.6	6.4
KARL ONSA	246 142.448	2.2	2.4	6.8
KARL VANE	118 792.921	2.2	2.2	6.2
ONSA TROM	1 406 186.550	4.7	4.8	9.3
ONSA VANE	144 693.992	2.0	2.7	6.5
ONSA WETB	919 697.274	3.6	4.0	8.0
TROM WETB	2 296 365.672	5.0	5.3	10.3

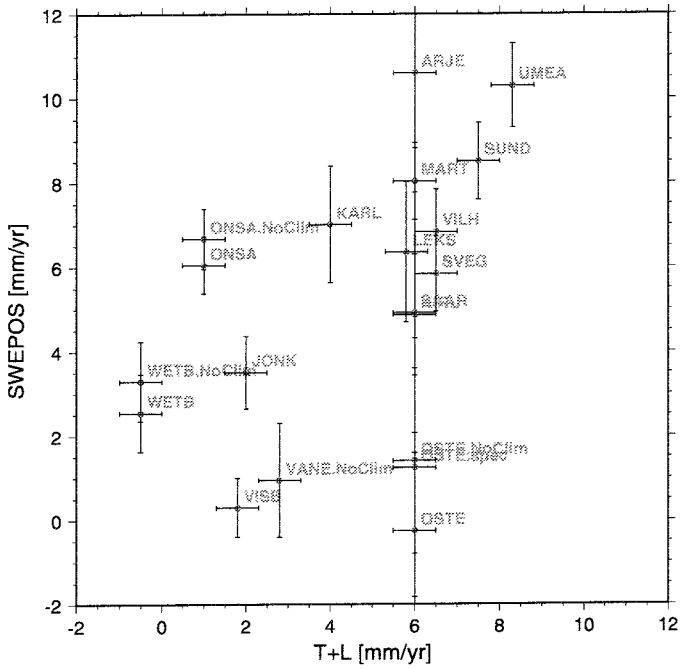

Figure 5-2. *Rates of the GPS baseline up component versus levelling and tide gauge results interpolated using the field shown in Fig. 2-1.*

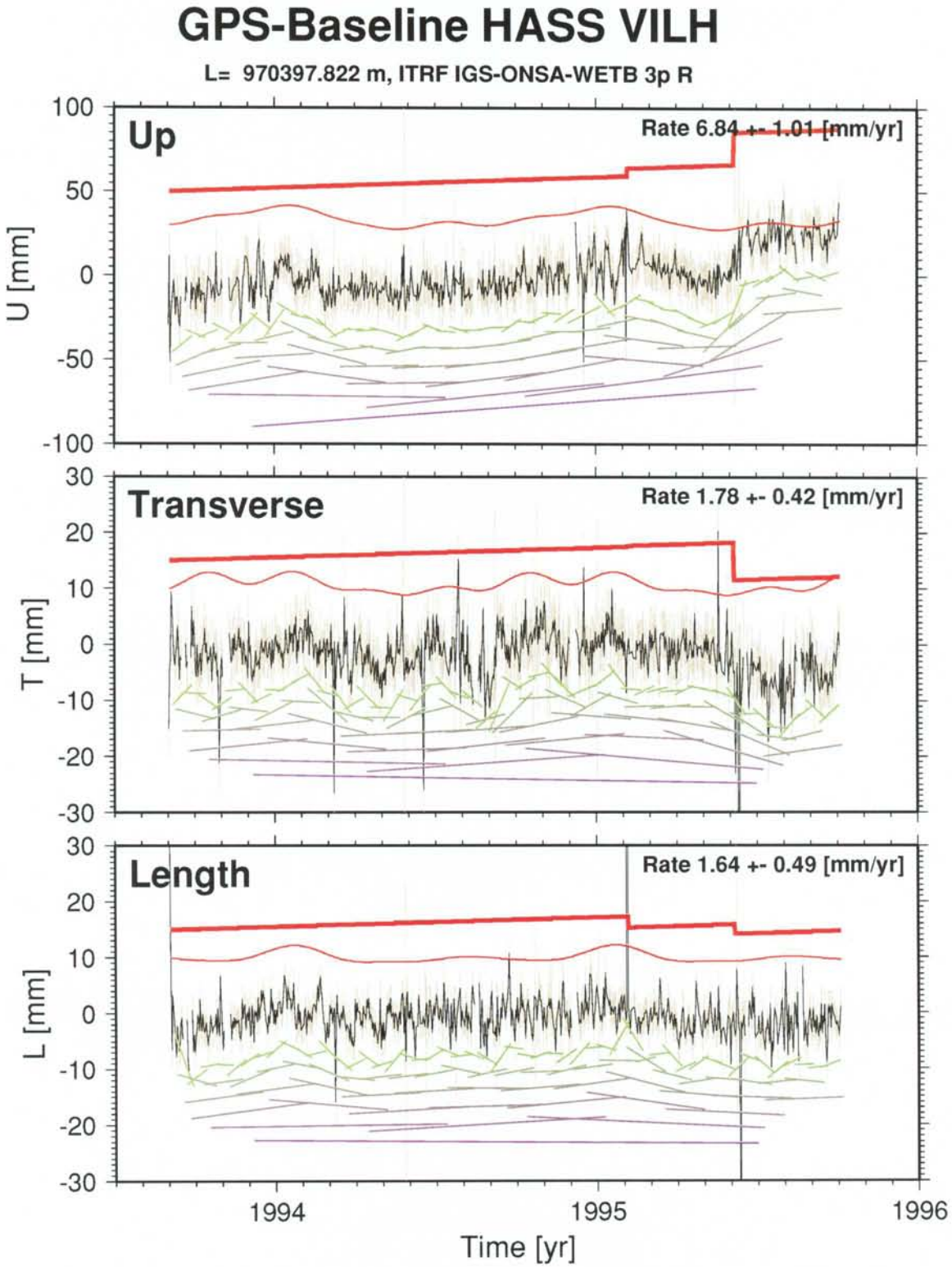

Figure 5-3. *Baseline Hässleholm–Vilhelmina, 970 km, variations around a 1994 mean solution, projected into LTU components and reduced for the global plate motion model NUVEL-1a-NNR (black curve, centre). Model fit: One rate but different biasses at antenna radome changes (Hässleholm: May 1995, Vilhelmina: Feb.1995), seasonal solar radiation (thin smooth line). Sliding-interval slopes of doubling lengths below the observations intend to highlight breaks in levels and rates.*

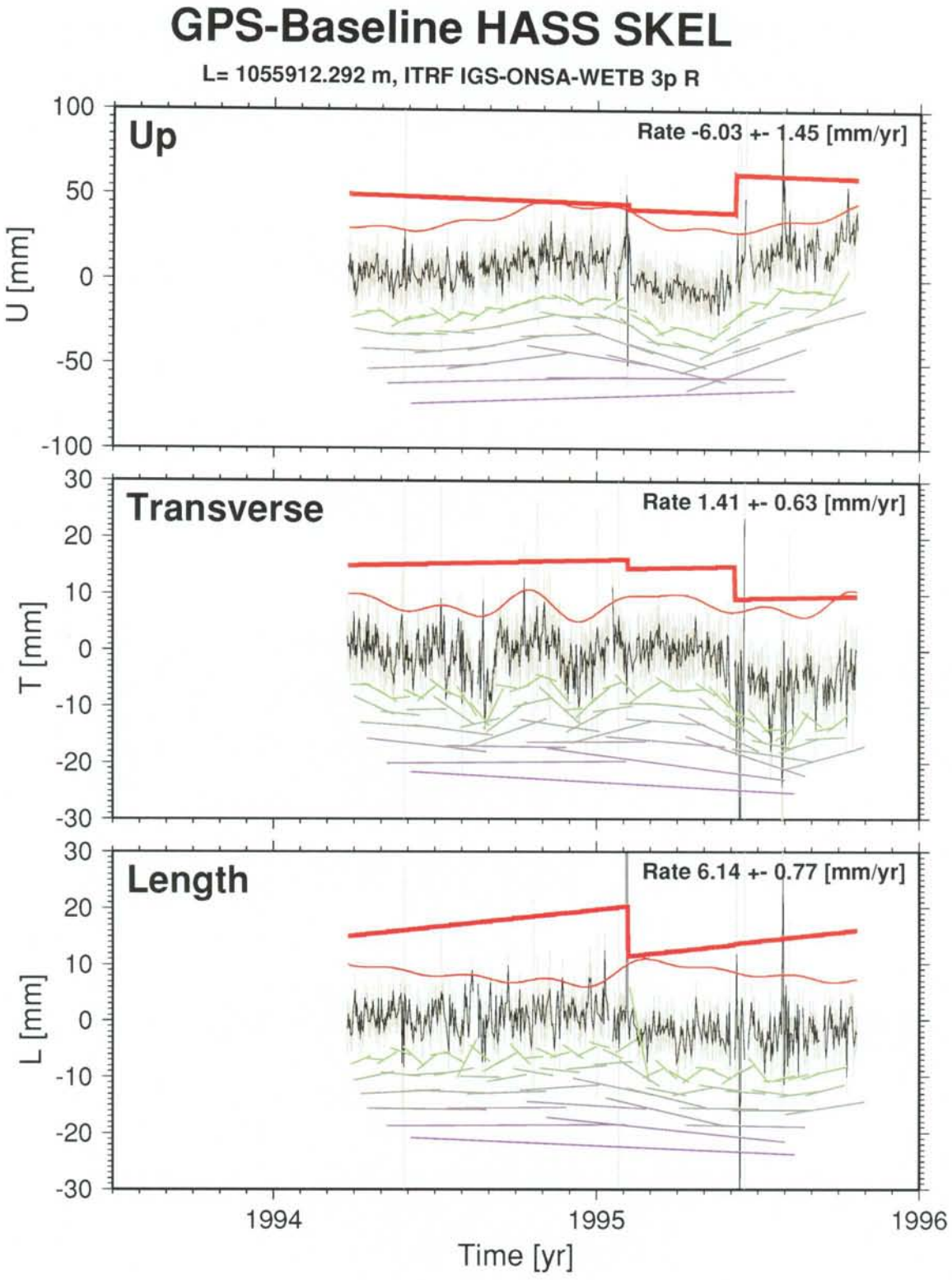

Figure 5-4. *Baseline Hässleholm–Skellefteå, 1056 km, like Fig. 5-3.*

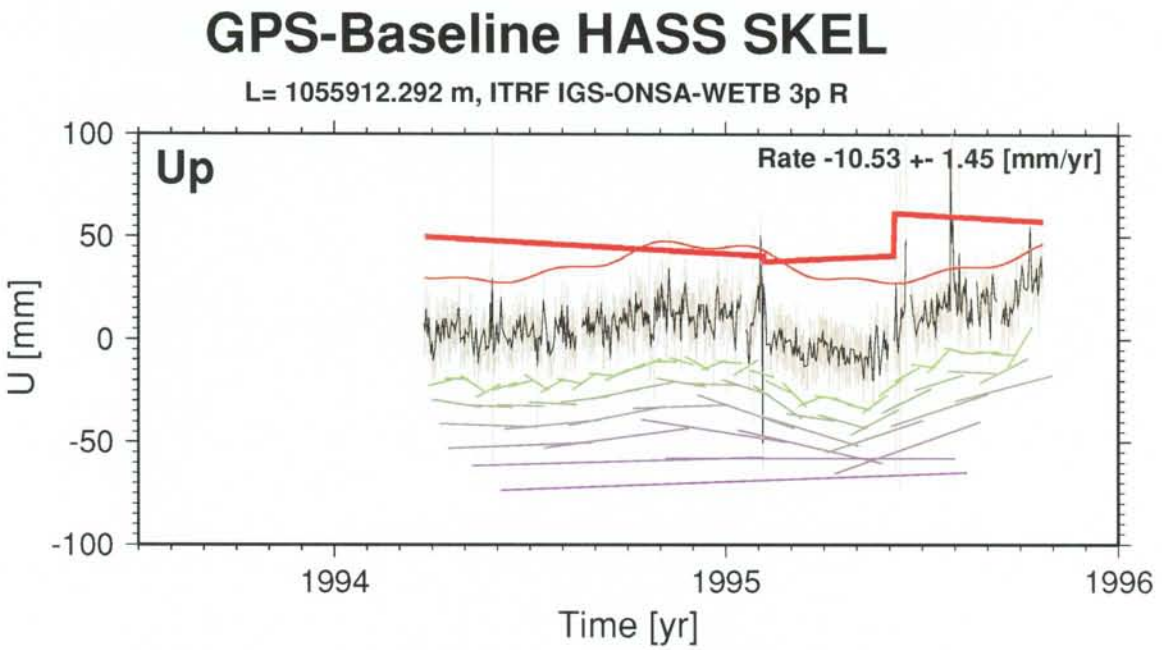

Figure 5-5. *Baseline Hässleholm–Skellefteå, 1056 km, like Fig. 5-4. In the Up component an anomalous rate is allowed between radome changes (determined: 6.5 ± 5.5 mm/yr). The rate for the entire period assuming no breaks is 7.5 ± 1.1 mm/yr.*

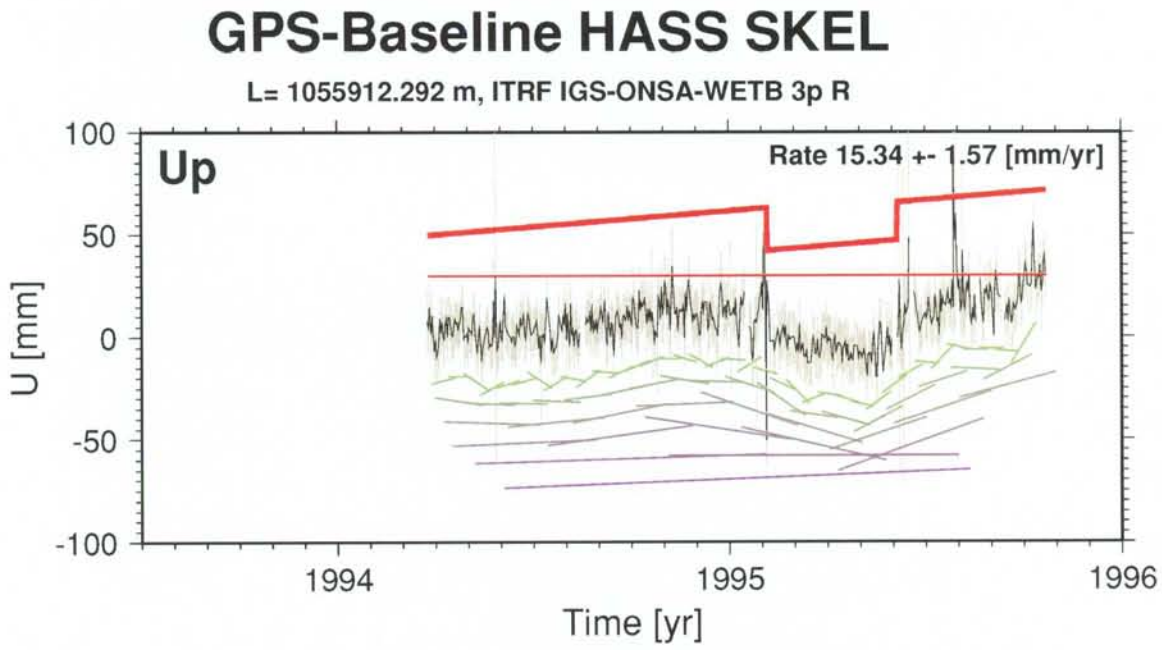

Figure 5-6. *Baseline Hässleholm–Skellefteå, 1056 km, like Fig. 5-4, in the Up component no climatic cycles have been fitted though.*

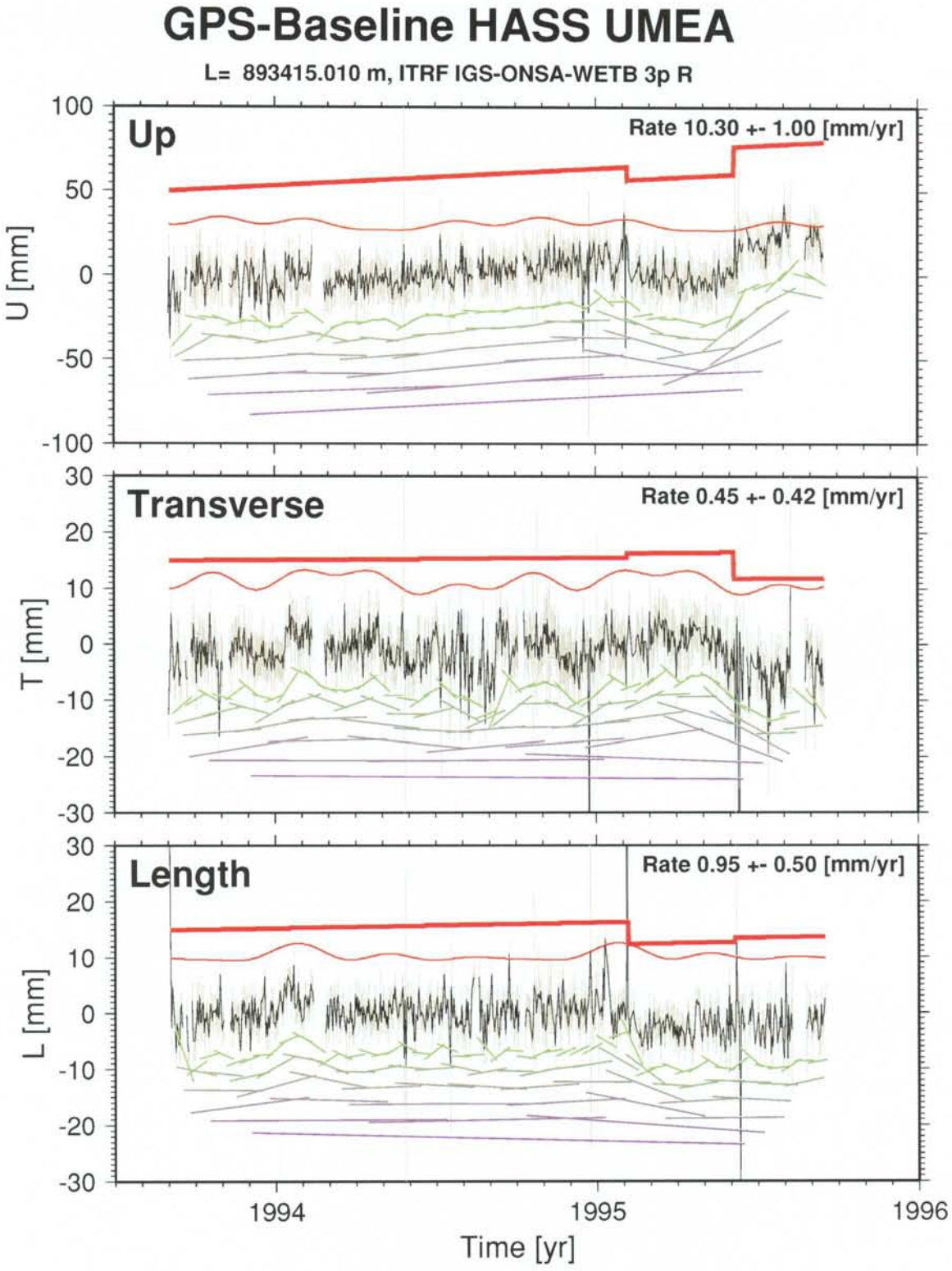

Figure 5-7. *Baseline Hässleholm–Umeå, 893 km, like Fig. 5-3.*

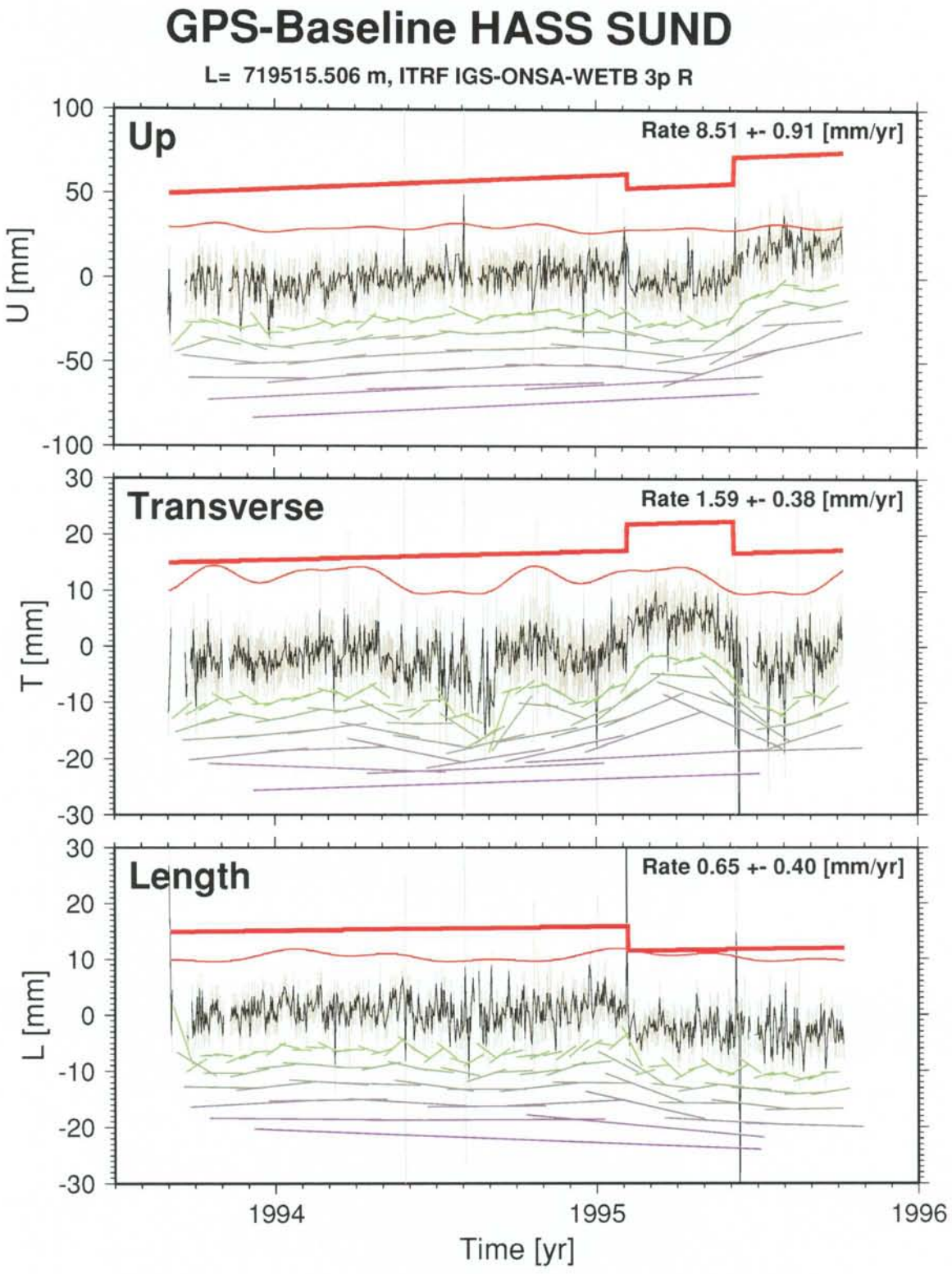

Figure 5-8. *Baseline Hässleholm–Sundsvall, 720 km, like Fig. 5-3.*

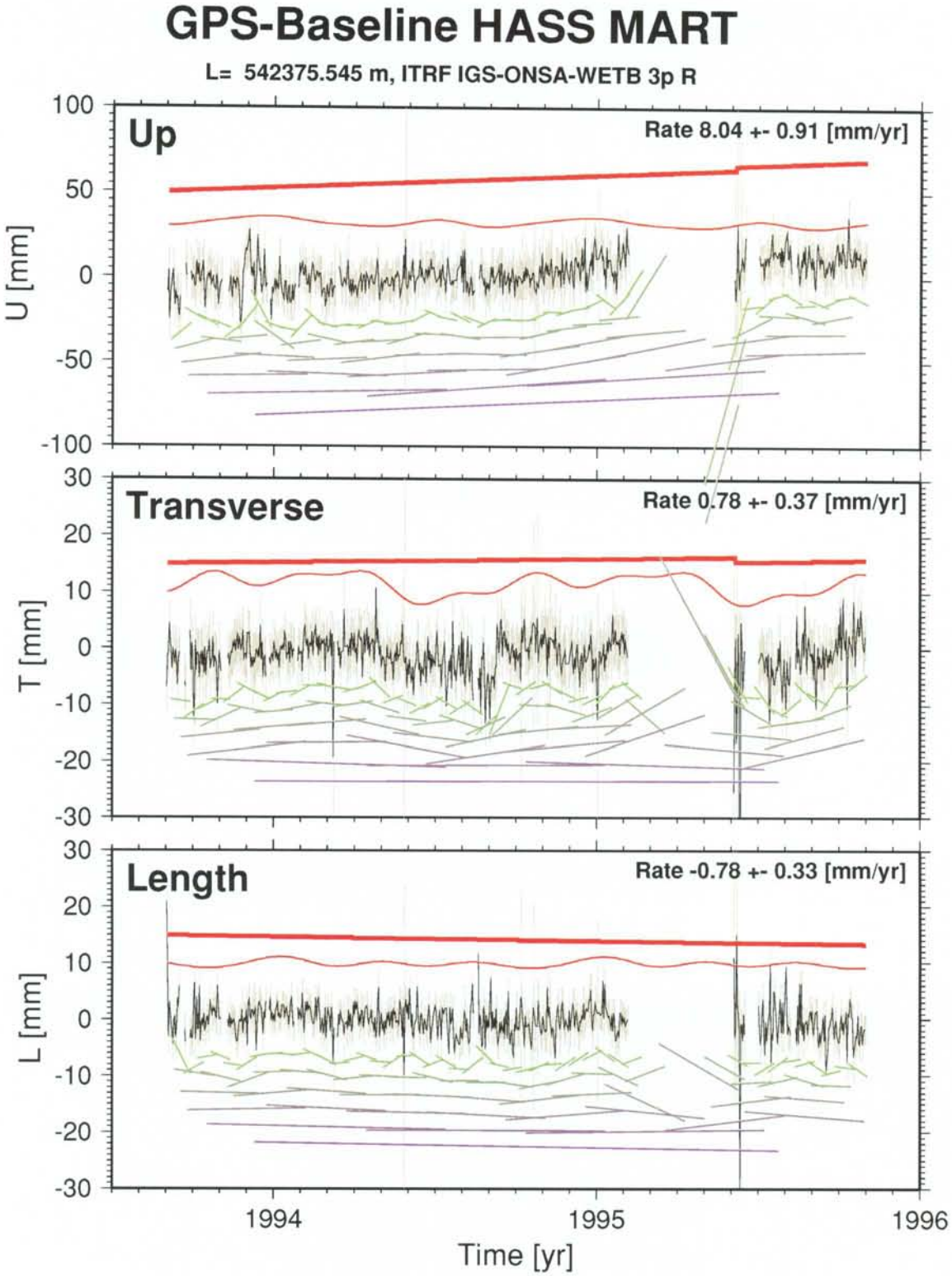

Figure 5-9. *Baseline Hässleholm–Mårtsbo, 720 km, like Fig. 5-3.*

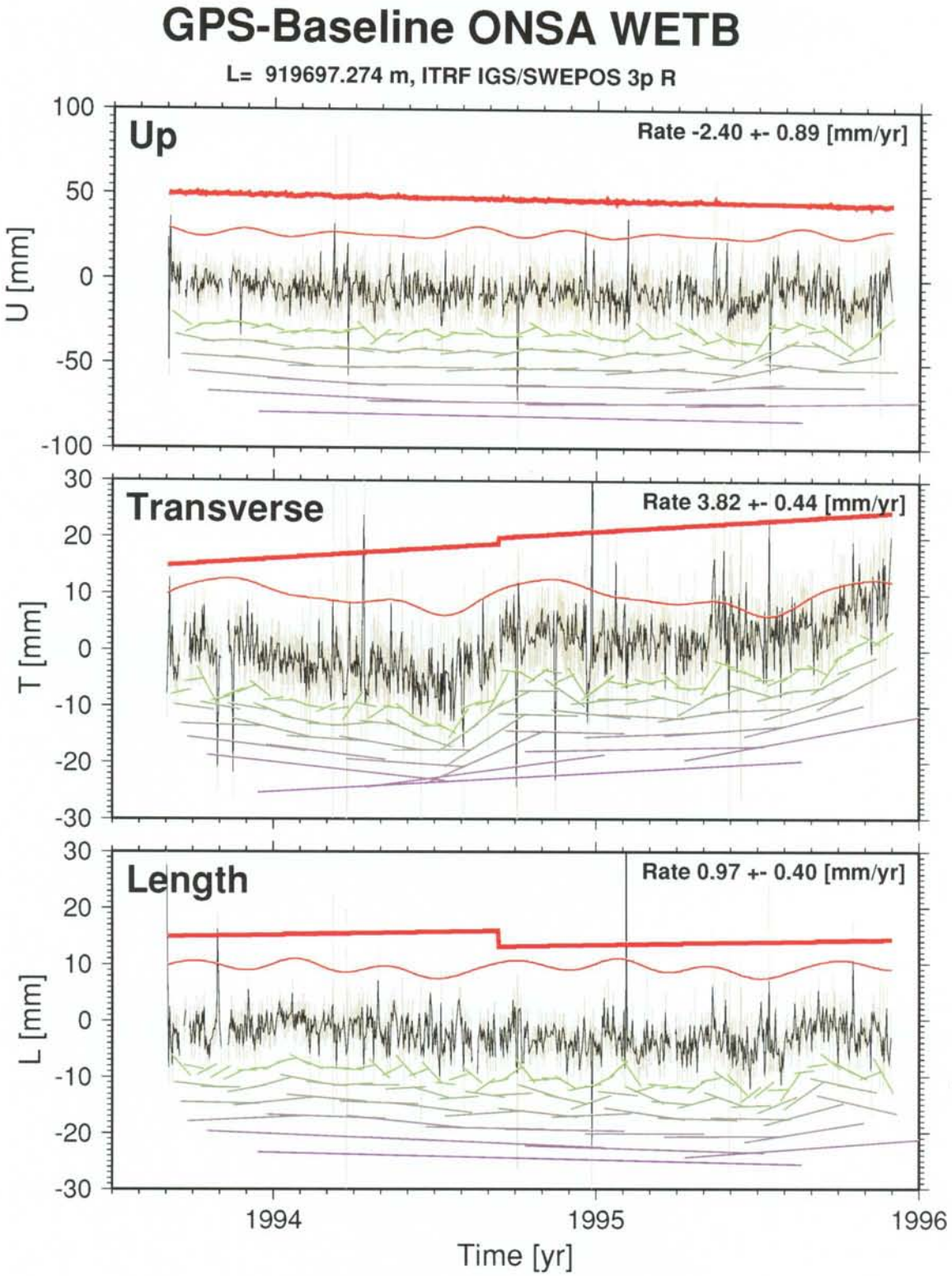

Figure 5-10. *Baseline Onsala–Wettzell, 920 km, like Fig. 5-3. No radome changes occurred. A horizontal bias term allows for a re-orientation of the Onsala antenna in Sep. 1994. The top curve of the Up-component includes an admittance for barometric pressure loading at each end point.*

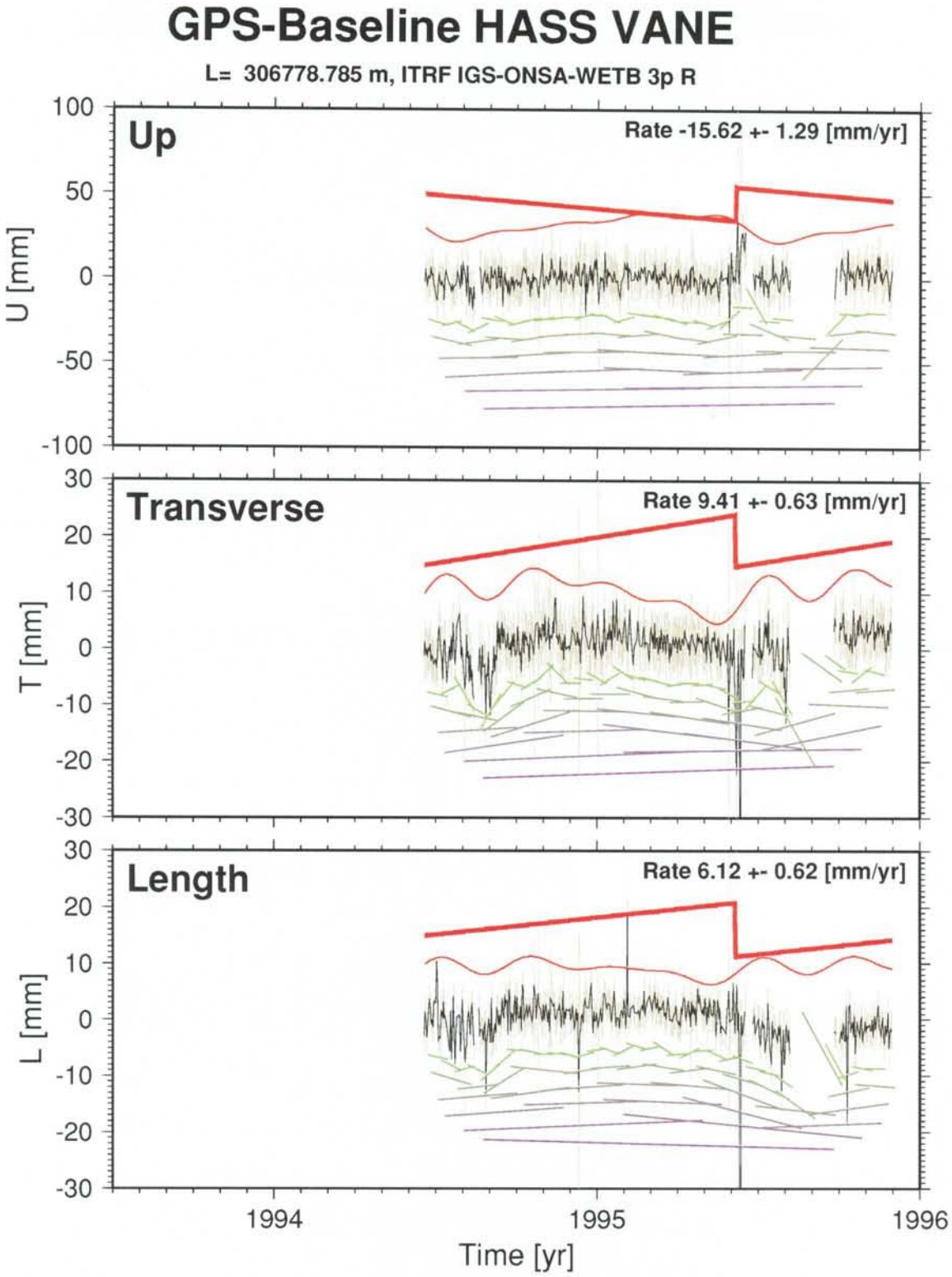

Figure 5-11. *Baseline Hässleholm–Vänersborg, 307 km, like Fig. 5-3. Radome changes occurred at both sites around the same date. This analysis includes seasonal cycles, yielding unrealistically high Up rate due to the limited length of data.*

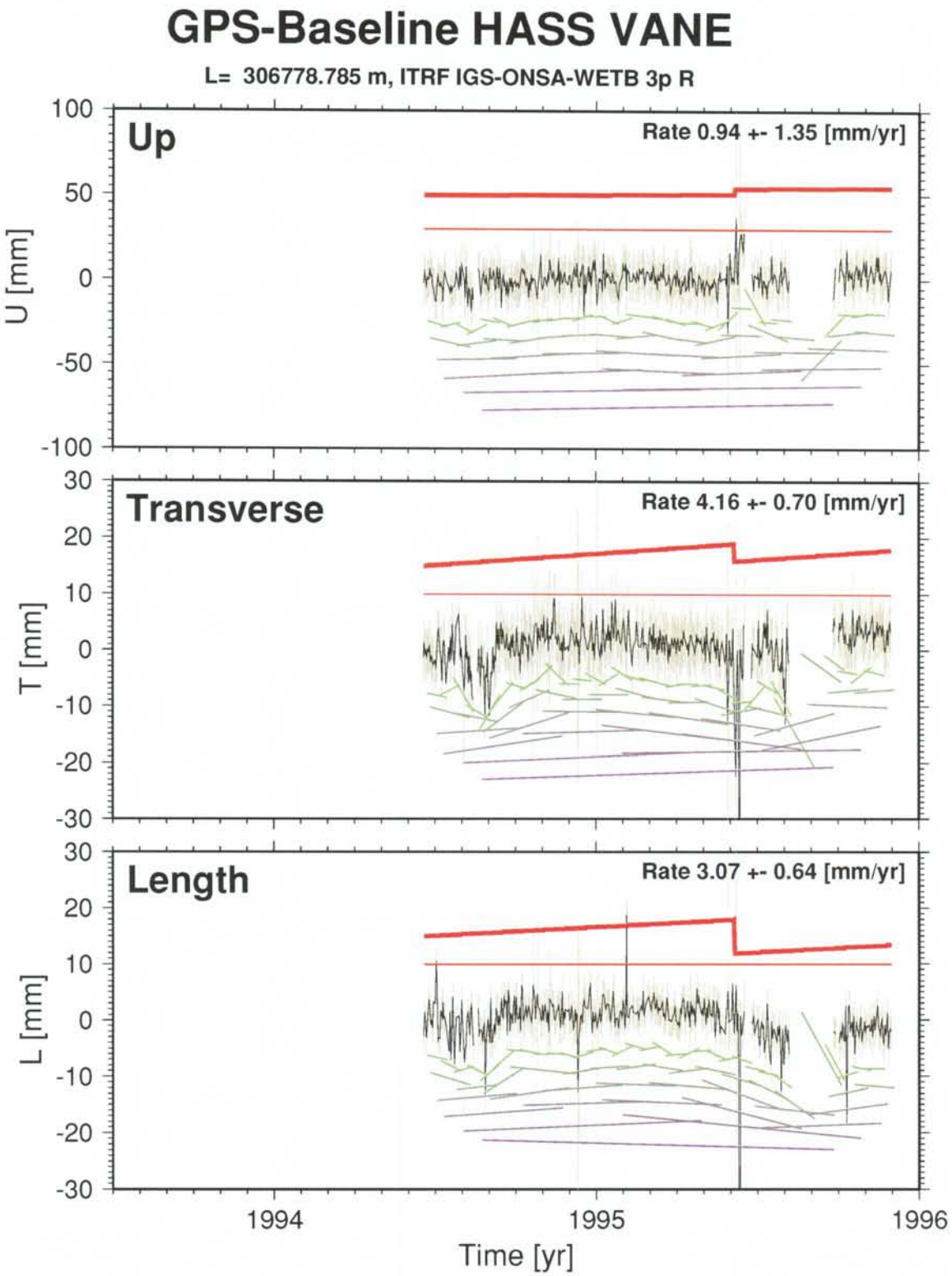

Figure 5-12. *Baseline Hässleholm–Vänersborg, like Fig. 5-11. This analysis does not admit seasonal cycles.*

6 FUTURE

We expect the number of available systems for precise geodetic positioning to increase and the availability of the individual components to improve during the years to come. GPS will continue to be available at least until 2010. The European Space Agency plans to deploy a positioning system for wide civil use with capabilites and performance equivalent or exceeding the GPS but without some of the limitations (free availability of codes and no artificial degradation). This system is actually a development of the Russian (former Soviet Union GLONASS) system which was a late cold-war answer of the Eastern Block to GPS.

Experience from VLBI as the first high-precision global method suggests that after five years of network operation results start to become safe and statistically robust, and problems which are inevitable in the initial phases of such complex systems have come under control. A similar conjecture applies to the building-out of the European VLBI network, which occurred when the method already had gained maturity. Still, five years of observation were needed to separate individual perturbations and conclude motions that extended prior knowledge.

We will be careful to maintain SWEPOS, replacing equipment after careful consideration. Experience shows that too frequently occurring replacements and rearrangements can render segments of recorded data and processed results quite useless. However, many types of replacements are needed, especially those that make the system more homogeneous. The balance is delicate.

Currently BIFROST daily analysis with the GIPSY/OASIS-II software can process ~45 sites within reasonable time. As data processing power is developing, utilizing distributed processing and subnetting techniques, the processing of ~100 stations in one merged solution appears feasible. We prioritize new stations in Sweden in areas where crustal stability appears to be lower. Data from new stations outside Sweden will be included, commencing this year, in the course of cooperating projects, goaded to within the Nordic Geodetic Commission and including the three Baltic states.

Data processing parameters and options are converging. After more than three years of operation it will be difficult for reasons of computation work load to reprocess. Thus, the studies on which optimum elevation cutoff, sampling rate, editing procedures etc. were decided, occurred in the first operational phase. The future will see studies rather on the interpreting side, for which homogeneity of the analysis is a major prerequisit. Being able after 2.5 years to conclude baseline rates at the 0.3 to 1.0 mm/yr level suggests a promising future.

7 ACKNOWLEDGMENTS

Without the help and advice of great number of persons this report would not have been possible. We thank our doctorands Ragne Carlsson and Per Jarlemark, and the recent PhD Kenneth Jaldehag for their commitment to the progress of the geogroup as a basis for knowledge, development and experience. We also thank our group advisor Prof Bernt Rönnäng for his efforts in coordinating our projects and encouraging us to seek for new routes and solutions.

We thank Jim Davis and Jerry Mitrovica for their tough discussions. We are also obliged to Herbert Henkel and Detlef Wolf for their inspiring seminar lectures on tectonics and isostatic rebound. Herbert Henkel has also originally suggested to establish a contact SKB.

We are grateful to Biörn Nilsson who maintains our computer systems healthy and in a Sysiphos role sees to that there is always enough disk space. Roger Hammargren has spent some of his free time to fix two nasty postscript pages so that finally all pages could be handled with only virtual scissors and glue.

We have used GMT graphics software due to Wessel and Smith (1995). Air pressure data from Wettzell was kindly provided by Dr. R. Dassing at IfAG.

REFERENCES

Adams J, 1989. Crustal stresses in eastern Canada, in Gregersen S, Basham P W (eds): Earthquakes at North-Atlantic Passive Margins: Neotectonics and Postglacial Rebound, pp. 289–297. Kluwer, Dordrecht.

Ahjos T, Uski M, 1992. Earthquakes in northern Europe in 1375–1989, Tectonophysics, Vol 207, 1–23.

Bakkelid S, 1986. The determination of the rate of land uplift in Norway, Tectonophysics, Vol 130, 307–326.

Balling N, Banda E, 1992. Europe's lithosphere - recent activity, in Blundell D, Freeman R, Mueller S (eds): A Continent Revealed. The European Geotraverse, pp. 111–137. Cambridge University Press, Cambridge.

Beutler G, Gurtner W, Bauersima I, Rothacher M, 1986. Efficient computation of the inverse of the covariance matrix of simultaneous GPS carrier phase difference observations, manuscripta geodaetica, Vol 11, 249–255.

Beutler G, Bauersima I, Gurtner W, Rothacher M, Schildknecht T, 1987. Evaluation of the 1984 Alaska Global Positioning System campaign with the Bearnese GPS software, J. Geophys. Res., Vol 92, 1295–1303.

BIFROST project members[1] , 1996. First results from a continuously operation GPS network in Fennoscandia, EOS Trans. Am. Geophys. Union, (subm.)

Blewitt G, 1993. Advances in Global Positioning System technology for geodynamics investigations: 1978–1992. In: Smith D E, Turcotte D L (eds), Contributions of Space Geodesy to Geodynamics: Techniques, pp

---

[1]BIFROST project members:

T. R. Carlsson, T. M. Carlsson, G. Elgered, R. T. K. Jaldehag, P. O. J. Jarlemark, J. M. Johansson, B. I. Nilsson, B. O. Rönnäng, H.-G. Scherneck—Onsala Space Observatory, Chalmers University of Technology, Göteborg, Sweden.

J. L. Davis, P. Elòsegui, I. I. Shapiro—Harvard-Smithsonian Center for Astrophysics, Cambridge, MA, USA.

M. Ekman, G. Hedling, B. Jonsson—National Land Survey, Division of Geodetic Research, Gävle, Sweden.

G. A. Milne, J. X. Mitrovica, R. N. Pysklywec—Department of Physics, University of Toronto, Ontario, Canada.

R Chen, J. Kakkuri, H. Koivula, M. Ollikainen, M. Pounonen, M. Poutanen, M. Vermeer—Finnish Geodetic Institute, Helsinki, Finland.

195–213. Crustal Dynamics Series. Vol 25. American Geophysical Union. Washington.

Bock Y, Agnew D C, Fang P, Genrich J F, Hager B H, Herring T A, Hudnut K W, King R W, Larsen S, Minster J-B, Stark K, Wdowinski S, Wyatt F K, 1993. Detection of crustal deformation from the Landers earthquake sequence using continuous geodetic measurements. Nature, Vol 361, 327–340.

Bock Y, et al. 1995. Permanent GPS Geodetic Array in Southern California: Continuous Monitoring of the Crustal Deformation Cycle, J. Geophys. Res., in preparation, 1995.

Bossler J D, Goad C C, Bender P L, 1980. Using the Global Positioning System (GPS) for geodetic positioning, Bull. Géodésique, Vol 54, 553–563.

Bosworth J M, Coates R J, Fischetti T L, 1993. The development of NASA's Crustal Dynamics Project. In: Smith D E, Turcotte D L (eds), Contributions of Space Geodesy to Geodynamics: Techniques, pp 1–20. Crustal Dynamics Series, Vol 25, American Geophysical Union, Washington.

Boucher, C, Altamimi Z, Duhem L, 1994. Results and analysis of the ITRF93. IERS Technical Note 18, Observatoire de Paris, 313 pp.

Breuer D, Wolf D, 1995. Deglacial land emergence and lateral upper-mantle heterogeneity in the Svalbard archipelago—I. First results for simple load models, Geophys. J. Int., Vol 121, 775–788.

Bungum H, 1989. Earthquake occurrence and seismotectonic in Norway and surrounding areas, in Gregersen S, Basham P W (eds): Earthquakes at North-Atlantic Passive Margins: Neotectonics and Postglacial Rebound, pp. 501–519. Kluwer, Dordrecht.

Bürki B, Elgered G, 1993. A Study of Wet Path Delay Variations Using Three Microwave Radiometers, Trans. AGU Eos Suppl., Vol 74, 105.

Carlsson T R, 1996. Site dependent error sources in geodetic Very-Long-Baseline Interferometry, Techn. Rep. No. 224L, School of Electrical and Computer Engineering, Chalmers University of Technology, Göteborg, Sweden, 52 pp.

Carter W (ed.), 1994. Report of the Surrey Workshop of the IAPSO Tide Gauge Bench Mark Fixing Committee, NOAA Techn. Rep., NOSO ES0006, NOAA Geosciences Laboratory, Silver Spring, MD, 81 pp.

Cartwright D E, Tayler R J, 1971. New Computations of the Tide-Generating Potential. Geophys. J. R. Astron. Soc., Vol 23, 45–74.

Chao B F, Eanes R, 1995. Global gravitational changes due to atmospheric mass redistribution as observed by the Lageos nodal residual, Geophys. J. Int, Vol 122, 755–764.

Chao B F, Gross R S, 1995. Changes in the Earth's rotational energy induced by earthquakes, Geophys. J. Int, Vol 122, 776–783.

Clark T A, Corey B E, Davis J L, Elgered G, Herring T A, Hinteregger H F, Knight C A, Levine J I, Lundqvist G, Ma C, Nesman E F, Phillips R B, Rogers A E E, Rönnäng B O, Ryan J W, Schupler B R, Shaffer D B, Shapiro I I, Vandenberg N R, Webber J C, Whitney A R, 1985. Precision geodesy using the Mark-III very-long-baseline interferometer system. IEEE Trans. Geosci. Remote Sens., Vol GE-23, 438–449.

Clark T A, Gordon D, Himwich W E, Ma C, Mallama A, Ryan J W, 1987. Determination of relative site motions in the western United States using MarkIII VLBI, J. Geophys. Res., Vol 92, 12,741–12,750.

Clark T A, Ma C, Sauber J M, Ryan J W, Gordon D, Shaffer D B, Carprette D S, Vandenberg N, 1990. Geodetic measurements in the Loma Prieta, California earthquake with Very Long Baseline Interferometry, Geophys. Res. Lett., Vol 17, 1215-1218.

Cloetingh S, Banda E, 1992. Mechanical Structure, in Blundell D, Freeman R, Mueller S (eds): A Continent Revealed. The European Geotraverse, pp. 80–91. Cambridge University Press, Cambridge.

Coates R J, Frey H, Mead G D, Bosworth J M, 1985. Space age geodesy: The NASA Crustal Dynamics Project, IEEE Trans. Geosci. Remote Sens, Vol GE-23, 360–368.

Counselman C C, Shapiro I I, 1979. Miniature interferometer terminals for earth surveying, Bull. Géodésique, Vol 53, 139–163.

Davidson J M, Trask D W, 1985. Utilization of mobile VLBI for geodetic measurements, IEEE Trans. Geosci. Remote Sens., Vol GE-23, 426–437.

Davis J L, Elgered G, Niell A E, Kuehn C E, 1993. Ground-based measurement of gradients in the "wet" radio refractive index of air, Radio Sci., Vol 28, 1003–1018.

DeMets C, Gordon G G, Argus D F, Stein S, 1990. Current plate motions. Geophys. J. Int., Vol 101, 425–478

DeMets C, Gordon G G, Argus D F, Stein S, 1994. Effect of recent revisions to the geomagnetic reversal time scale on estimates of current plate motions. Geophys. Res. Lett.. Vol 21, 2191–2194.

Dickey J O, Feissel M (eds.), 1994. Results from the SEARCH'92 Campaign, IERS Technical Note 16, Observatoire de Paris, 187 pp.

Dixon T H, 1991. An introduction to the Global Positioning System and some geological applications, Rev. Geophys., Vol 29, 249–276.

Dixon T H, Bills B, 1992. What is DOSE ? EOS Trans. American Geophysical Society, Vol 73, 276–277.

Dong D, Bock Y, 1989. Global Positioning System network analysis with phase ambiguity resolution applied to crustal deformation studies in California, J. Geophys. Res., Vol 94, 3949–3966.

Donnellan A, Hager B H, King R W, Herring, T A, 1993. Geodetic measurements of deformation in the Ventura Basin region, Southern California. J. Geophys. Res., Vol 98, No B12, 21,727–21,739.

Dziewonski A, Anderson D L, 1981. Preliminary reference earth model, Phys. Earth Planet. Int., Vol. 25, 297–356.

Ekman M, 1995. A consistent map of the postglacial uplift of Fennoscandia, submitted, preprint available.

Ekman M, Mäkinen J 1995. Recent postglacial rebound, gravity change and mantle flow in Fennoscandia, Geophys. J. Int., submitted, preprint avail.

Elgered G, 1993. Tropospheric Radio Path Delay from Ground-Based Microwave Radiometry, in Janssen M (ed.): Atmospheric Remote Sensing by Microwave Radiometry, 215–258, Wiley & Sons, New York.

Elgered G, Davis J L, Herring T A, Shapiro I I, 1991. Geodesy by radio interferometry: Water vapour radiometry for the estimation of the wet delay, J. Geophys. Res., Vol 96, 6541-6555.

Elgered G, Davis J L, 1993. Microwave Radiometry for Correction of Atmospheric Path-Length Variations in VLBI: Recent Results. In: Campbell J, Nothnagel A (eds.): Proc. of the 9th Working Meeting on European VLBI for Geodesy and Astrometry, 98–108. Mitteilungen Geodetische Institute, Univ. Bonn, No. 81, Bonn, FRG.

Elósegui P, Davis J L, Jaldehag R T K, Johansson J M, Neill A E, Shapiro I I, 1995. Geodesy using the Global Positioning System: The effects of signal scattering on estimates of site position, J. Geophys.

Res., Vol 100, No B7, 9921–9934.

EOS, 1995. Kobe earthquake: An urban disaster. (Editorial) EOS Trans. American Geophysical Union, Vol 76, No 6, 49–51.

Eubanks T M, 1993. Variations in the orientation of the Earth. In: Smith D E, Turcotte D L (eds), Contributions of Space Geodesy to Geodynamics: Earth Dynamics, pp 1–54. Crustal Dynamics Series, Vol 24, American Geophysical Union, Washington.

Farrell W E, 1972. Deformation of the Earth by Surface Loads, Rev. Geophys. Space Phys., Vol 10, pp. 761–797.

Feigl K L, Agnew D C, Bock Y, Dong D, Donnellan A, Hager B H, Herring T A, Jackson D D, Jordan T H, King R W, Larsen S, Larson K M, Murray M H, Shen Z, Webb F H, 1993. Space geodetic measurements of crustal deformation in Central and Southern California, J. Geophys. Res., Vol 98, 21,677–21,712.

Feissel M, Bourquard D, Charlot P, Eisop E, Essaifi N, Lestrade J-F, Arias E F, Boucher C, Altamimi Z, 1993. Earth orientation and related reference frames. In: Smith D E, Turcotte D L (eds), Contributions of Space Geodesy to Geodynamics: Earth Dynamics, pp 99–112. Crustal Dynamics Series, Vol 24, American Geophysical Union, Washington.

GPS World (n.n.), 1996. GPS World Receiver Survey. GPS World, Vol 7, No 1, 32–54.

Gasperini P, Yuen D A, Sabadini R, 1990. Effects of lateral viscosity variations on postglacial rebound: implications for recent sea-level trends, Geophys. Res. Lett., Vol 17, 5–8.

Geographical Survey Institute, 1995. Investigation of the South Hyogo Earthquake, Quick Review (update 9. Mar).
`http://graph.gsi-mc.go.jp:2000/www/kobe/info-e.html` WWW Internet.

Gordon R G, Stein S, 1992. Global tectonics and space geodesy. Science, Vol 256, 333–342.

Gregersen S, 1992. Crustal stress regime in Fennoscandia from focal mechanisms, J. Geophys. Res., Vol 97, 11,821–11,827.

Hasegawa H S, 1991. Four seismogenic environments in eastern Canada, Tectonophysics, Vol 186, 3–17.

Hasegawa H S, Basham P W, 1989. Spatial correlation between

seismicity and postglacial rebound in eastern Canada. in Gregersen S. Basham P W (eds): Earthquakes at North-Atlantic Passive Margins: Neotectonics and Postglacial Rebound, pp. 483–500. Kluwer. Dordrecht.

Heflin M, Bertiger W, Blewitt G, Freedman A, Hurst K, Lichten S, Lindqwister U, Vigue Y, Webb F, Yunck T, Zumberge J, 1992. Global geodesy using GPS without fiducial sites, Geophys. Res. Lett., Vol 19. 131-134.

Herring T A, 1986. Precision of vertical position estimates from very long baseline interferometry, J. Geophys. Res., Vol 91, 9177–9182.

Herring T A, 1996. The Global Positioning System, Scientific American, Vol 274, No 2, 32–38.

Herring T A, Gwinn C R, Shapiro I I, 1986. Geodesy by radio interferometry: Studies of the forced nutations of the earth, part I: Data analysis, J. Geophys. Res., Vol 91, 4745–4755; Q ibid. Vol 91, 14,165.

Herring T A, Shapiro I I, Clark T A, Ma C, Ryan J W, Schupler B R, Knight C A, Schaffer D B, Vandenberg N R, Hinteregger H F, Rogers A E E, Webber J C, Whitney A R, Elgered G, Lundqvist G, Rönnäng B O, Corey B E, and Davis J L, 1986a. Geodesy by Radio Interferometry: Evidence for Contemporary Plate Motion, J. Geophys. Res., Vol 91, 8341–8347.

Himwich W E, Watkins M M, Ma C, MacMillan D S, Clark T A, Eanes R J, Ryan J W, Schutz B E, Tapley B D, 1993. The consistency and scale of the terrestrial reference frames estimated from SLR and VLBI data. In: Smith D E, Turcotte D L (eds), Contributions of Space Geodesy to Geodynamics: Earth Dynamics, pp 113–120. Crustal Dynamics Series, Vol 24, American Geophysical Union, Washington.

Hudnut K, Shen Z, Murray M, McClusky S, King R, Herring T, Hager B, Feng Y, Fang P, Donnellan A, Bock Y, 1995. Coseismic displacements of the 1994 Northridge, California, earthquake, In press, Bulletin of the Seismological Society of America (Special Issue on the Northridge Earthquake).

IERS, 1995. 1994 IERS Annual Report. Observatoire de Paris, 146 pp.

Jaldehag R T K, 1992. Studies of Reflector Antenna Systems for Geodetic Very-Long-Baseline Interferometry, Tech. Rept. No. 120L, School of Electrical and Computer Engineering, Chalmers Univ. Tech.

Jaldehag R T K, Johansson J M, Rönnäng B O, Elósegui P, Davis J L, Shapiro I I, Neill A E, 1995. Geodesy using the Swedish Permanent GPS Network: Effects of signal scattering on estimates of rel-

ative site positions. J. Geophys. Res. (in print). Also in: Space Geodesy Techniques: An Experimental and Theoretical Study of Antenna Related Error Sources, PhD Thesis. Paper D. 43 pp. Chalmers University of Technology. School of Electrical and Computer Engineering, Techn. Rep. No. 276. Göteborg. 127 pp.

Jaldehag R T K, Kildal P-S, Rönnäng B O, 1993. Dual Band Reflector Feed Systems for Classical Cassegrain Radio Telescopes. IEEE Trans. Ant. Propagat., Vol AP-41, 325–332.

Jaldehag R T K, Ying Z, 1995. A preliminary study of GPS choke-ring antennas optimized for low side- and back-lobe scatter, in: Jaldehag K, Space Geodesy Techniques: An Experimental and Theoretical Study of Antenna Related Error Sources, PhD Thesis, Paper E, 16 pp, Chalmers University of Technology, School of Electrical and Computer Engineering, Techn. Rep. No. 276, Göteborg, 127 pp.

Jarlemark P O J, 1994. Microwave radiometry for studies of variations in atmospheric water vapor and cloud liquid content, Techn. Rep. No. 181L, School of Electrical and Computer Engineering, Chalmers University of Technology, Göteborg, Sweden, 99 pp.

Johansson J M, 1992. A Study of Precise Position Measurements Using Space Geodetic Systems, PhD Thesis, Chalmers University of Technology, School of Electrical and Computer Engineering, Techn. Rep. No. 229, Göteborg, 145 pp.

Johansson J M, Elgered G, Rönnäng B O, 1992. The space geodetic laboratory at the Onsala Observatory: Site information, in: Johansson J M, A Study of Precise Position Measurements Using Space Geodetic Systems, PhD Thesis, Paper A, 16 pp, Chalmers University of Technology, School of Electrical and Computer Engineering, Techn. Rep. No. 229, Göteborg, 145 pp.

Kakkuri J, 1986. Newest results obtained in studying the Fennoscandian land uplift phenomenon, Tectonophysics, Vol 130, 327–331.

Kakkuri J, 1988., Neotectonic movements in Finland, in Mörner N-A (ed): Present Processes and Properties of the Lithosphere, Proc. Lejondal Symp. on Neotectonics, Stockholm.

Kakkuri J, Chen R, 1992. On horizonal crustal strain in Finland, Bull. Géodésique, Vol 66, 12–20.

Kakkuri J, Vermeer M, 1985. The study of land uplift using the third levelling of Finland, Rep. Finn. Geod. Inst., Vol 85:1, Helsinki.

Kellermann K I, Thompson A R, 1985. The very long baseline

array, Science, Vol 229, 123–130.

Kellogg J N, Dixon T H, 1990. Central and South America GPS geodesy— CASA UNO, Geophys. Res. Lett., Vol. 17, 195–198.

Kuehn C E, Elgered G, Johansson J M, Clark T A, Rönnäng B O, 1993. A Microwave Radiometer Comparison and Its Implication for the Accuracy of Wet Delays, In: Smith D E, Turcotte D L (eds), Contributions of Space Geodesy to Geodynamics: Technology, pp 99–114. Crustal Dynamics Series, Vol 23, American Geophysical Union, Washington.

Lambeck K, 1993. Glacial rebound of the British Isles—I: Preliminary model results, Geophys. J. Int., Vol 115, 941–959.

Lambeck K, 1993a. Glacial rebound of the British Isles—II: A high-resolution high-precision model, Geophys. J. Int., Vol 115, 960-990.

Lichten S M, 1990. Estimation and filtering for high-precision GPS positioning applications, manuscripta geodaetica, 159–176.

Lichten S M, Border J S, 1987. Strategies for high precision Global Positioning System orbit determination, J. Geophys. Res., Vol 92, 12,751–12,762.

Lundqvist G, 1984. Radio interferometry as a probe of tectonic plate motion, PhD Thesis, Chalmers University of Technology, School of Electrical and Computer Engineering, Techn. Rep. No. 150, Göteborg, 83pp.

Ma C, Sauber C M, Bell L J, Clark T A, Gordon D, Himwich W E, Ryan J W, 1990. Measurement of horizontal motions in Alaska using VLBI, J. Geophys. Res., Vol 95, 21,991–22,011.

MacDoran P, 1979. Satellite emission radio interferometric Earth surveying: SERIES GPS geodetic systems, Bull. Géodésique, Vol. 53, 117–138.

MacMillan D S, Ma C, 1994. Evaluation of very long baseline interferometry atmospheric modeling improvements, J. Geophys. Res., Vol 99, 637–651.

Mäkinen J, Ekman M, Mitsundstad Å, Remmer O, 1986. The Fennoscandian Land Uplift Gravity Lines 1966–1984, Rep. Finn. Geod. Inst., Vol 85:4, 238 pp.

McCarthy, D. D. (ed), 1992. IERS Technical Note 13, IERS Standards (1992). Observatoire de Paris.

Melbourne, W G, 1985. The case for ranging in GSP based geodetic systems. In: Proceedings of the First Symposium on Precise Positioning with the Global Positioning System, pp 373–386. US Dept. of Commerce, Rockville. MD.

Mitrovica J X, Davis J L, Shapiro I I, 1994. A spectral formalism for computing
three-dimensional deformations due to surface loads, 2. Present-day glacial isostatic adjustment, J. Geophys. Res., Vol 99, 7075–7101.

Mitrovica J X, Davis J L, 1995. Some comments on the 3-D impulse response of a Maxwell earth. Geophys. J. Int., Vol 120, 227–234.

Mitrovica J X, Peltier W R, 1991. On postglacial geoid relaxation over the equatorial oceans, J. Geophys. Res., Vol 96, 20,053–20,071.

Mitrovica J X, Peltier W R, 1993. The inference of mantle viscosity from an inversion of the Fennsoscandian relaxation spectrum. Geophys. J. Int., Vol 114, 45-62.

Muir Wood R, 1993. A review of the seismotectonics of Sweden, SKB Techn. Rep. 93-13, Swedish Nuclear Fuel and Waste Management Co., Stockholm, 225 pp.

Müller G, 1986. Generalized Maxwell bodies and estimates of mantle viscosity, Geophys. J. R. Astr. Soc., Vol 87, 1113–1141.

Müller B, Zoback M L, Fuchs K, Mastin L, Gregersen S, Pavoni N, Stephansson O, Ljunggren C, 1992. Regionl patterns of tectonic stress in Europe, J. Geophys. Res., Vol 92, 11,783–11,803.

Nerem R S, 1995. Measuring global mean sea level variations using TOPEX/POSEIDON altimeter data, J. Geophys. Res., Vol 100, 25,135–25,151.

Oral M B, Reilinger R E, Toksöz M N, Barka A A, Kinik I, 1993. Preliminary results of 1988 and 1990 GPS measurements in Western Turkey and their tectonic implications. In: Smith D E, Turcotte D L (eds), Contributions of Space Geodesy to Geodynamics: Crustal Dynamics, pp 407–416. Crustal Dynamics Series, Vol 23, American Geophysical Union, Washington.

Peltier W R, 1974. The impuls response of a Maxwell earth, Rev. Geophys., Vol 12, 649–669.

Peltier W R, 1995. VLBI baseline variations from the ICE-4G model of postglacial rebound, Geophys. Res. Lett., Vol 22, 465–468.

Potash R, 1992. Accurate VLBI Geodetic Tie from Onsala VLBI Reference Point to Ground. Report. Interferometrics/GSFC Nov. 31.

Riis F, Fjeldskaar W, 1992. On the magnitude of the late tertiary and quaternary erosion and its significance of the uplift of Scandinavia and the Barents Sea., in Larsen R M, Brekke H, Larsen B T, Talleraas E (eds): Structural and Tectonic Modelling and its Application to Petroleum Geology. NPF Special Publication 1, pp.163–185, Elsevier, Amsterdam.

Rius A, Zarraoa N, Sardón E, Ma C, 1992. Centimeter repeatabilities of the VLBI estimates of European baselines, Bull. Géodésique, Vol 66, 21–26.

Robbins J W, Smith D E, Ma C, 1993. Horizontal crustal deformation and large scale plate motions inferred from space geodetic technique. In: Smith D E, Turcotte D L (eds), Contributions of Space Geodesy to Geodynamics: Crustal Dynamics, pp 21–36. Crustal Dynamics Series, Vol 23, American Geophysical Union, Washington.

Rogers A E E. 1970. Very-long-baseline interferometry with large bandwidth for phase-delay measurements, Radio Sci., Vol 5, 1239–1248.

Rogers A E E, Cappallo R J, Corey B E, Hinteregger H F, Neill A E, Phillips R B, Smythe D L, Whitney A R, Herring T A, Bosworth J M, Clark T A, Ma C, Ryan J W, Davis J L, Shapiro I I, Elgered G E, Jaldehag K, Johansson J M, Rönnäng B O, Carter W E, Ray J R, Robertson D S, Eubanks T M, Kingham K A, Walker R C, Himwich W E, Kuehn C E, MacMillan D S, Potash R I, Shaffer D B, Vandenberg N A, Webber J C, Allshouse R L, Shupler B R, Gordon D, 1993. Improvements in the accuracy of geodetic VLBI. In: Smith D E, Turcotte D L (eds), Contributions of Space Geodesy to Geodynamics: Techniques, pp 47–63. Crustal Dynamics Series, Vol 25, American Geophysical Union, Washington.

Rothacher M, Beutler G, 1988. Iceland 1986 GPS campaign: A complete network solution with fixed ambiguities (abstr), EOS Trans. American Geophysical Union, Vol 69, 1151.

Rümpker G, Wolf D, 1996. Vicoelastic relaxation of a Burgers halfspace: implications for the interpretation of the Fennoscandian uplift, Geophys. J. Int., Vol 124, 541–555.

Ryan J W, Ma C, Caprette D S, 1993. NASA Space Geodesy Program, GSFC data analysis—1992. NASA Technical Memorandum 104572, Greenbelt, MD.

Ryan J W, Clark T A, Coates R J, Ma C, Wildes W T, Gwinn

C R, Herring T A, Shapiro I I, Corey B E, Counselman C C, Hinteregger H F, Rogers A E E, Whitney A R, Knight C A, Vandenberg N R, Pigg J C, Schupler B R, Robertson D S, and Rönnäng B O, 1986. Geodesy by Radio Interferometry: Determinations of Baseline-Vector, Earth-Rotation, and Solid-Earth-Tide Parameters With the Mark I Very Long Baseline Radio Interferometry System, J. Geophys. Res., Vol 91, 1935–1946.

Sardon E, Rius A, Zarraoa N, 1994. Ionospheric calibration of single frequency VLBI and GPS observations using dual GPS data, Bull. Géodésique, Vol 68, 230–235.

Sauber J M, Clark T A, Bell L J, Lisowski M, Ma C, Carprette D S, 1993. Geodetic measurement of static displacement associated with the 1987-1988 Gulf of Alaska earthquakes. In: Smith D E, Turcotte D L (eds), Contributions of Space Geodesy to Geodynamics: Crustal Dynamics, pp 233–248. Crustal Dynamics Series, Vol 25, American Geophysical Union, Washington.

Sagiya T, Yoshimura A, Iwata E, Abe K, Kimura I, Uemura K, Tada T, 1995. Establishment of Permanent GPS Observation Network and Crustal Deformation Monitoring in the Southern Kanto and Tokai Areas, Bull. Geographical Survey Institute, Vol 41, and `http://www.gsi-mc.go.jp/BULLETIN/vol-41/gps.html` WWW Internet.

Savage J C, Lisowski M, 1995. Geodetic monitoring of the southern San Andreas fault, California, 1980–1991. J. Geophys. Res., Vol 100, No. B5, 8185–8192.

Scherneck H-G, 1983. Crustal Loading Affecting VLBI Sites, University of Uppsala, Institute of Geophysics, Dept. of Geodesy, Report No. 20, Uppsala, Sweden.

Scherneck H-G, 1990. Loading Green's functions for a continental shield with a Q-structure for the mantle and density constraints from the geoid, Bull. d'Inform. Marées Terr., Vol 108, pp. 7757–7792.

Scherneck H-G, 1991. A Parameterized Solid Earth Tide Model and Ocean Tide Loading Effects for Global Geodetic Baseline Measurements, Geophys. J. Int., Vol 106, pp. 677–694.

Scherneck H-G, 1993. Ocean Tide Loading: Propagation of Errors from the Ocean Tide into Loading Coefficients, Manuscripta Geodetica, Vol 18, pp. 59–71.

Schupler B R, Clark T A, 1991. How different antennas affect the GPS observable, GPS World, Nov/Dec 1991, 32-36.

Schupler B R, Allshouse R L, Clark T A, 1994. Signal characteristics of GPS user antennas. Navigation. Vol 41, 277-295.

Shapiro I I, 1976. Estimation of astrometric and geodetic parameters from VLBI observations. In: Meeks M L (ed.) Methods of Experimental Physics. pp 261–276. Academic Press. New York.

Shimada S, Bock Y, 1992. Crustal deformation measurements in central Japan determined by a Global Positioning System fixed-point network. J. Geophys. Res., Vol 97, 12,437–12,455.

Slunga R, 1991. The Baltic shield earthquakes, Tectonophysics, Vol 189, 323-331.

Smith D E, Turcotte D L, 1993a. Contributions of Space Geodesy to Geodynamics: Crustal Dynamics. Crustal Dynamics Series, Vol 23, American Geophysical Union, Washington, 429 pp.

Smith D E, Turcotte D L, 1993b. Contributions of Space Geodesy to Geodynamics: Earth Dynamics. Crustal Dynamics Series, Vol 24, American Geophysical Union, Washington, 219 pp.

Smith D E, Turcotte D L, 1993c. Contributions of Space Geodesy to Geodynamics: Techniques. Crustal Dynamics Series, Vol 25, American Geophysical Union, Washington, 213 pp.

Smith D E, Kolenkiewicz R, Nerem R S, Dunn P J, Torrence M H, Robbins J W, Klosko S M, Williamson R G, Pavlis E C, 1994. Contemporary global horizontal crustal motion. Geophys. J. Int., Vol 119, 511–520.

Smith D E, Kolenkiewicz R, Robbins J W, Dunn P J, Torrence M H, 1994a. Horizontal crustal motion in the Central and Eastern Mediterranean inferred from Satellite Laser Ranging measurements. Geophys. Res. Lett., Vol 21, 1979–1982.

Soudarin L, Cazenave A, 1995. Large-scale tectonic plate motions measured with the DORIS space geodesy system, Geophys. Res. Lett., Vol 22, 469–472.

Sovers O J, Border J, 1990. Observation model and parameters partials for the JPL GPS geodetic modeling software "GPSOMC", JPL Public. No. 87-21 Rev. 2, Jet Propulsion Laboratory, Pasadena, Cal., 37pp.

Stein S, Cloetingh S, S, Sleep N H, Wortel R, 1989. Passive margin earthquakes, stresses and rheology, in Gregersen S, Basham P W (eds): Earthquakes at North-Atlantic Passive Margins: Neotectonics and

Postglacial Rebound, pp. 231–259. Kluwer, Dordrecht.

Spada G, Sabadini R, Yuen D A, Ricard Y, 1992. Effects on postglacial rebound from the hard rheology in the transition zone. Geophys. J. Int., Vol 109, 683–700.

Stephansson O, Ljunggren C, Jing L, 1991. Stress measurements and tectonic implications for Fennoscandia. Tectonophysics, Vol 189, 317–322.

Straub C, Kahle H-G, 1995. Active crustal deformation in the Marmara Sea region, NW Anatolia, inferred from GPS measurements. Geophys. Res. Lett., Vol 22, 2534–2536.

Talbot C J, Slunga R, 1989. Patterns of active shear in Fennoscandia, in Gregersen S, Basham P W (eds): Earthquakes at North-Atlantic Passive Margins: Neotectonics and Postglacial Rebound, pp. 441–466. Kluwer, Dordrecht.

Talwani P, 1989. Characteristic features of intraplate earthquakes and the models proposed to explain them, in Gregersen S, Basham P W (eds): Earthquakes at North-Atlantic Passive Margins: Neotectonics and Postglacial Rebound, pp. 563–579. Kluwer, Dordrecht.

Tsuji H, Hatanaka Y, Sagiya T, Hashimoto M, 1995. Coseismic crustal deformation from the 1994 Hokkaido-Toho-Oki earthquake monitored by a nationwide continuous GPS array in Japan, Geophys. Res. Lett., Vol 22, 1669–1672.

Tushingham A M, Peltier W R, 1991. ICE-3G: A new global model of late Pleistocene deglaciation based upon geophysical predictions of postglacial relative sea level change. J. Geophys. Res., Vol 96, 4497–4523.

Vermeer M, 1994. The Finnish National Permanent GPS Network: Current status. In: Proc. 12^{th} NKG General Assembly, Ullensvang. Nordic Geodetic Commission. Statens Kartverk, Hönefoss, Norway. In print.

Wahlström, R, 1989. Seismodynamics and postglacial faulting in the Baltic Shield, in Gregersen S, Basham P W (eds): Earthquakes at North-Atlantic Passive Margins: Neotectonics and Postglacial Rebound, pp. 467–482. Kluwer, Dordrecht.

Webb F H, Zumberge J F, 1993. An Introduction to GIPSY/OASIS-II Precision Software for the Analysis of Data from the Global Positioning System, JPL Publ. No. D-11088, Jet Propulsion Laboratory, Pasadena, Cal.

Wessel P, Smith W H F, 1995. New version of the Generic Mapping Tools released. EOS Trans. AGU. Vol 76. 329.

Wolf D, 1991. Viscoelastodynamics of a stratified. compressible planet: incremental field equations and short- and long-time asymptotes. Geophys. J. Int., Vol 104. 401–417.

Whitney A R, 1974. Precision Geodesy and Astrometry via Very Long Baseline Interferometry, Ph.D. thesis, Dept. of Electrical Engineering, MIT, Cambridge, MA.

Wilson P, 1987. Kinematics of the Eastern Mediterranean region and the WEGENER–MEDLAS project. Geojournal, Vol 14, 143–161.

Wübbena G, 1985. Software developments for geodetic positioning with GPS using TI-4100 code and carrier measurements. In: Proceedings of the First Symposium on Precise Positioning with the Global Positioning System, pp 403–412, US Dept. of Commerce, Rockville, MD.

Zarraoa N, Rius A, Sardón E, Ryan J W, 1994. Relative motions in Europe studied with a geodetic VLBI network, Geophys. J. Int., Vol 117, 763-768.

Zarraoa N, Rekkedal S, Kristiansen O, Engen B, 1995. The mobile VLBI campaigns in Norway (1989-1993), Bull. Géodésique, Vol 69, 274–282.

APPENDIX

A INTERNET ADDRESSES

Maintenance of precedures and fundamental units, and data services are provided under the superintendence of a number of international organisations, notably the IAG (International Association of Geodesy), the IAU (International Astronomical Union), and the IERS (International Earth Rotation Service). Many universities and governmental or public service institutes cooperate in joint efforts. The following list shows locations where valuable information is available for computer access through Internet.

- *IGS - International GPS Service* - contains site descriptions ("log" files), coordinates, tracking site data (RINEX files), precise orbits, electronic mail archive. The central bureau is located at NASA Jet Propulsion Laboratory.
  `http://igscb.jpl.nasa.gov/cbis.html` provides access to the central information system.
  Documents describing the contributing centres (analysis, data, operating) can be received under
  `http://igscb.jpl.nasa.gov/igscb/center/`. The collection of electronic mail correspondence can be accessed under
  `http://igscb.jpl.nasa.gov/igscb/mail/igsmail`.

- *CDDIS - Crustal Dynamics Data Information System* - contains a wealth of documentation, results, and processing data archives for all space geodetic techniques. The site is maintained by NASA Goddard Space Flight Center, Greenbelt, Md. Glossy home pages inform about the programs (including CDP and DOSE) and guide through the archives, with
  `http://cddis.gsfc.nasa.gov/cddis.html` at the front end.
  The NASA publication series can be searched on-line through
  `http://techreports.larc.nasa.gov/cgi-bin/NTRS`, the NASA Technical Report Server.

- *IGN - Institut Géographique National*, Saint-Mandé, France, maintains the International Terrestrial Reference Frame. It provides the official ITRF coordinates and transformation parameters for different epochs in
  `ftp://schubert.ign.fr/pub/itrf/`

- *Computational procedures in Astronomy.*
  The `STARLINK` library, astronomical procedures in `SLALIB` pre-

sented by Rutherford Appleton Laboratory UK.
`http://star-www.rl.ac.uk/software.html`

- *Earth rotation bulletins and services* provided by the U.S. Naval Observatory, National Earth Orientation Service (NEOS)
`http://maia.usno.navy.mil/`
including the IERS Standards.

- *Canadian Space Science Forum, CANSPACE* keeps an archive for geophysics, geodesy, and astronomy, containing working group circulars, resolutions, and memorandums; GPS information; meeting programs incl. AGU (Americal Geophycal Union), located at the university of New Brunswick, Fredericton, Canada
`http://degaulle.hil.unb.ca/Geodesy/CANSPACE.html`
`gopher://unbmvs1.csd.unb.ca:1570/1EXEC%3aCANSPACE`
The site contains also the Circulars of the IAU Working Group on Astronomical Constants, ended Dec. 1994 (Toshio Fukuskima, Chairman). Subgroup reports contain informative documents, e.g. Circular 90 on issues of time, Circular 93 on definitions of time scales (IAU resolution C7, 1994), Circular 94 on current best estimates of important astronomical constants.

- *SLR, DORIS, and PRARE* information
`http://cddis.gsfc.nasa.gov/920_1/sgapo.html`
at NASA GSFC,
`http://192.134.216.41/English/TOPEX_POSEIDON/More_On_Payload.html` at CNES (French Space Agency) accessible via
`http://www.cnes.fr`, and
`http://www.gfz-potsdam.de/pb1/PRARE/PRARE-2way.html` at GeoForschungsZentrum Potsdam.

- Onsala Space Observatory
`http://www.oso.chalmers.se` Links to general pages on space geodesy exist. Appearing soon: SWEPOS information service.

List of SKB reports

Annual Reports

1977-78
TR 121
KBS Technical Reports 1 – 120
Summaries
Stockholm, May 1979

1979
TR 79-28
The KBS Annual Report 1979
KBS Technical Reports 79-01 – 79-27
Summaries
Stockholm, March 1980

1980
TR 80-26
The KBS Annual Report 1980
KBS Technical Reports 80-01 – 80-25
Summaries
Stockholm, March 1981

1981
TR 81-17
The KBS Annual Report 1981
KBS Technical Reports 81-01 – 81-16
Summaries
Stockholm, April 1982

1982
TR 82-28
The KBS Annual Report 1982
KBS Technical Reports 82-01 – 82-27
Summaries
Stockholm, July 1983

1983
TR 83-77
The KBS Annual Report 1983
KBS Technical Reports 83-01 – 83-76
Summaries
Stockholm, June 1984

1984
TR 85-01
Annual Research and Development Report 1984
Including Summaries of Technical Reports Issued during 1984. (Technical Reports 84-01 – 84-19)
Stockholm, June 1985

1985
TR 85-20
Annual Research and Development Report 1985
Including Summaries of Technical Reports Issued during 1985. (Technical Reports 85-01 – 85-19)
Stockholm, May 1986

1986
TR 86-31
SKB Annual Report 1986
Including Summaries of Technical Reports Issued during 1986
Stockholm, May 1987

1987
TR 87-33
SKB Annual Report 1987
Including Summaries of Technical Reports Issued during 1987
Stockholm, May 1988

1988
TR 88-32
SKB Annual Report 1988
Including Summaries of Technical Reports Issued during 1988
Stockholm, May 1989

1989
TR 89-40
SKB Annual Report 1989
Including Summaries of Technical Reports Issued during 1989
Stockholm, May 1990

1990
TR 90-46
SKB Annual Report 1990
Including Summaries of Technical Reports Issued during 1990
Stockholm, May 1991

1991
TR 91-64
SKB Annual Report 1991
Including Summaries of Technical Reports Issued during 1991
Stockholm, April 1992

1992
TR 92-46
SKB Annual Report 1992
Including Summaries of Technical Reports Issued during 1992
Stockholm, May 1993

1993
TR 93-34
SKB Annual Report 1993
Including Summaries of Technical Reports Issued during 1993
Stockholm, May 1994

1994

TR 94-33

SKB Annual Report 1994

Including Summaries of Technical Reports Issued during 1994.
Stockholm, May 1995

1995

TR 95-37

SKB Annual Report 1995

Including Summaries of Technical Reports Issued during 1995.
Stockholm, May 1996

List of SKB Technical Reports 1996

TR 96-01

Bacteria, colloids and organic carbon in groundwater at the Bangombé site in the Oklo area

Karsten Pedersen (editor)
Department of General and Marine Microbiology,
The Lundberg Institute, Göteborg University,
Göteborg, Sweden
February 1996

TR 96-02

Microbial analysis of the buffer/container experiment at AECL´s Underground Research Laboratory

S Stroes-Gascoyne[1], K Pedersen[2], S Daumas[3],
C J Hamon[1], S A Haveman[1], T L Delaney[1],
S Ekendahl[2], N Jahromi[2], J Arlinger[2], L Hallbeck[2],
K Dekeyser[3]
[1] AECL, Whiteshell Laboratories, Pinawa, Manitoba, Canada
[2] University of Göteborg, Department of General and Marine Microbiology, Göteborg, Sweden
[3] Guigues Recherche Appliquée en Microbiologie (GRAM), Aix-en-Provence, France
1996

TR 96-03

Reduction of Tc (VII) and Np (V) in solution by ferrous iron. A laboratory study of homogeneous and heterogeneous redox processes

Daqing Cui, Trygve E Eriksen
Department of Chemistry, Nuclear Chemistry,
Royal Institute of Technology, Stockholm, Sweden
March 1996

TR 96-04

Revisiting Poços de Caldas. Application of the co-precipitation approach to establish realistic solubility limits for performance assessment

Jordi Bruno, Lara Duro, Salvador Jordana,
Esther Cera
QuantiSci, Barcelona, Spain
February 1996

TR 96-05

SR 95

Template for safety reports with descriptive example
SKB
December 1995

TR 96-06

Äspö Hard Rock Laboratory Annual Report 1995

SKB
April 1996

TR 96-07

Criticality in a high level waste repository. A review of some important factors and an assessment of the lessons that can be learned from the Oklo reactors

Virginia M Oversby
VMO Konsult
June 1996

TR 96-08

A reappraisal of some Cigar Lake issues of importance to performance assessment

John Smellie[1], Fred Karlsson[2]
[1] Conterra AB
[2] SKB
July 1996

TR 96-09

The long-term stability of cement. Leaching tests

Ingemar Engkvist, Yngve Albinsson,
Wanda Johansson Engkvist
Chalmers University of Technology,
Göteborg, Sweden
June 1996

TR 96-10

Lake-tilting investigations in southern Sweden

Tore Påsse
Sveriges geologiska undersökning,
Göteborg, Sweden
April 1996

TR 96-11
Thermoelastic stress due to an instantaneous finite line heat source in an infinite medium
Johan Claesson, Göran Hellström
Depts. of Building Physics and Mathematical Physics, Lund University, Lund, Sweden
September 1995

TR 96-12
Temperature field due to time-dependent heat sources in a large rectangular grid
– Derivation of analytical solution
Johan Claesson, Thomas Probert
Depts. of Building Physics and Mathematical Physics, Lund University, Lund, Sweden
January 1996

TR 96-13
Thermoelastic stress due to a rectangular heat source in a semi-infinite medium
– Derivation of an analytical solution
Johan Claesson, Thomas Probert
Depts. of Building Physics and Mathematical Physics, Lund University, Lund, Sweden
May 1996

TR 96-14
Oklo: Des reacteurs nucleaires fossiles (Oklo: The fossil nuclear reactors). Physics study (R Naudet, CEA)
– Translation of chapters 6, 13, and conclusions
V O Oversby
VMO Konsult
September 1996

TR 96-15
PLAN 96
Costs for management of the radioactive waste from nuclear power production
Swedish Nuclear Fuel and Waste Management Co
June 1996

TR 96-16
Diffusion of I^-, Cs^+ and Sr^{2+} in compacted bentonite
– Anion exclusion and surface diffusion
Trygve E Eriksen, Mats Jansson
Royal Institute of Technology, Department of Chemistry, Nuclear Chemistry, Stockholm
November 1996

TR 96-17
Hydrophilic actinide complexation studied by solvent extraction radiotracer technique
Jan Rydberg
Department of Nuclear Chemistry, Chalmers University of Technology, Gothenburg, Sweden
and Radiochemistry Consultant Group AB,
V. Frölunda, Sweden
October 1996

TR 96-18
Information, conservation and retrieval
Torsten Eng[1], Erik Norberg[2], Jarl Torbacke[3], Mikael Jensen[4]
[1] Swedish Nuclear Fuel and Waste Management Co (SKB)
[2] National Swedish Archives
[3] Department of History, Stockholm University
[4] Swedish Radiation Protection Institute (SSI)
December 1996